OKINAWA INSTITUTE OF SCIENCE AND TECHNOLOGY
GRADUATE UNIVERSITY

Thesis submitted for the degree

Doctor of Philosophy

Control of Cold Atomic Systems for Quantum Heat Engines

by

Mohamed Boubakour

Supervisor: **Thomas Busch**

April 2024
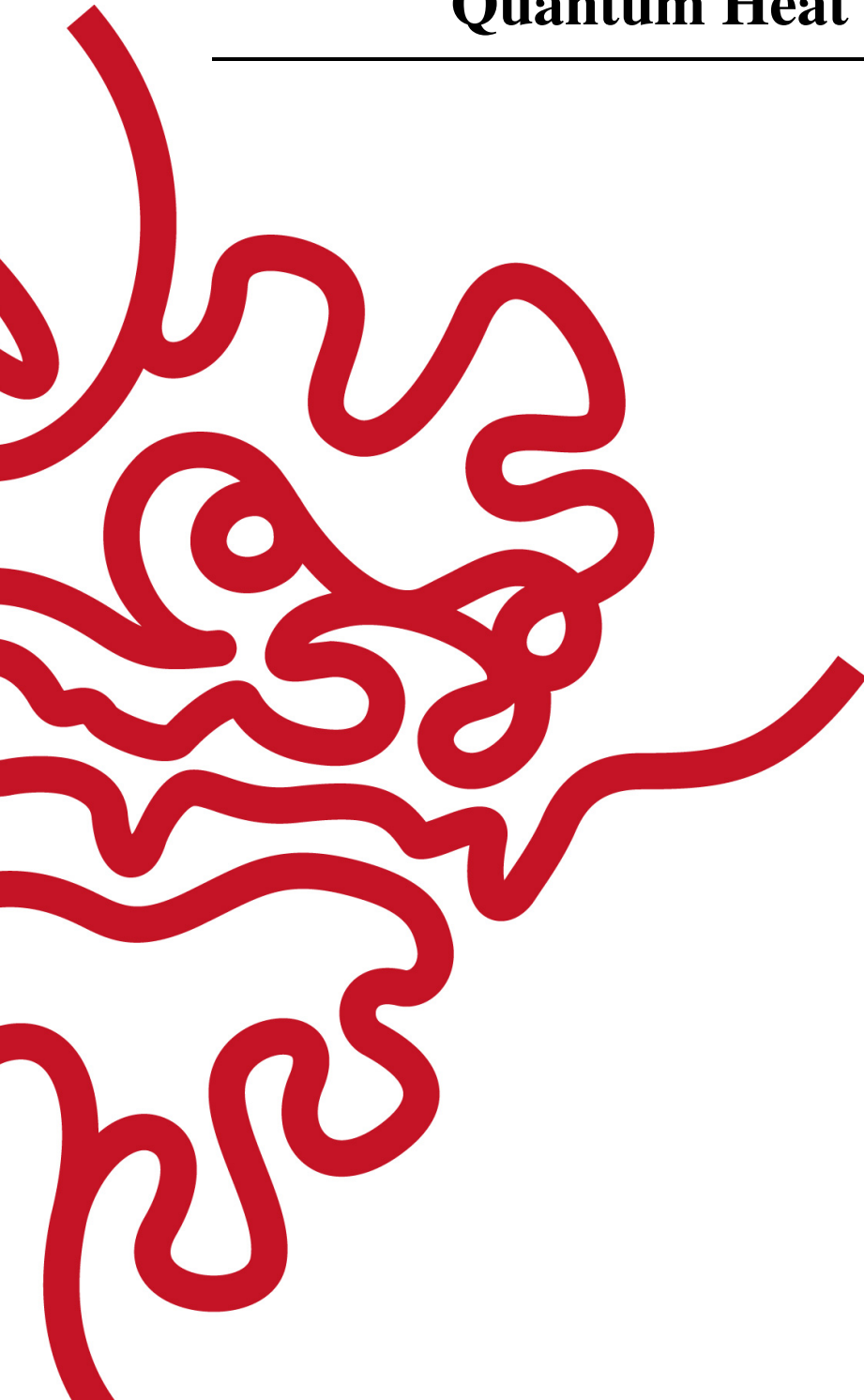
Declaration of Original and Sole Authorship

I, Mohamed Boubakour, declare that this thesis entitled *Control of Cold Atomic Systems for Quantum Heat Engines* and the data presented in it are original and my own work.

I confirm that:

- No part of this work has previously been submitted for a degree at this or any other university.

- References to the work of others have been clearly acknowledged. Quotations from the work of others have been clearly indicated, and attributed to them.

- In cases where others have contributed to part of this work, such contribution has been clearly acknowledged and distinguished from my own work.

- None of this work has been previously published elsewhere, with the exception of the followings:

  -the work presented in Section 2.2 is based on the publication:

  M. Boubakour, T. Fogarty, and T. Busch, *Interaction-enhanced quantum heat engine*, Phys. Rev. Res. **5**, 013088 (2023).

  I initiated the project, derived all of the presented results, and performed all of the numerical calculations. I wrote a first draft of the manuscript, and all the authors contributed to the discussion and interpretation of the results and to the writing of the final version.

  -The work presented in Section 3.2 is based from the preprint manuscript:

  M. Boubakour, S. Endo, T. Fogarty, and T. Busch, *Dynamical invariant based shortcut to equilibration*, arXiv **2401.11659** (2024).

  I initiated the project, derived all of the presented results, and performed all of the numerical calculations. I wrote a first draft of the manuscript, and all the authors contributed to the discussion and interpretation of the results and to the writing of the final version.

Date: April 2024

Signature:

Abstract

In this thesis, I present the work I did in my PhD in the field of quantum thermodynamics. The aim of this work is to explore quantum engines that can exploit the great tunability of cold atomic systems as the working medium. The thesis is divided into two parts. In the first part, I study the thermodynamics of one-dimensional interacting systems to use them for designing quantum engines. It consists of two research projects. In the first project, I explore anomalous heat flows between two strongly correlated particles and discuss the perspective of using it to realize a quantum fridge. In the second project, I study a quantum heat engine where the work extraction is assisted by changing the interaction within the working medium. In the second part of my thesis, I focus on controlling open quantum systems for optimizing the performance of quantum engines. The quantum Brownian motion has been used to test the different methods. This part consists of two projects, where in the first one, I realize a shortcut to equilibration protocol in a driven open quantum system. For that I propose two different methods. The first one consists of mapping the dynamics of the quantum Brownian motion to an effective stochastic dynamics of an isolated particle. The second methods consists of doing the shortcut protocol by reverse engineering a time-dependent master equation, which was derived by using the Lewis-Riesenfeld invariant. Finally in the second project, I use optimal control methods to speed up the thermalization in isochoric strokes. I also derive a speed limit that predicts the timescale at which the optimal control fails. All projects significantly contribute to the understanding and control of quantum engines.

Acknowledgment

I want to thank first my parents Ahmed and Meriem for supporting me for so long. Even though you were not enjoyed by the idea of me going so far away in a small island, and you have no idea about the content of my work, you accepted my decision and I really appreciate that. I know mom, a long time ago you wanted me to become a doctor in medicine, and I was not interested by this choice of career. But I hope becoming a doctor in physics still makes you happy. Also thank you for asking for news regularly. I also want to thank my brother and sisters for staying in touch, in particular Aya with who I really enjoyed the weekly calls.

I sincerely thank Thomas Busch for being my supervisor during my PhD. When I arrived at OIST I was not planning to do a PhD related to quantum mechanics and you were also not planning to hire me. But in the end you let me join your group after I suddenly started to have an interest in quantum thermodynamics. You gave me a complete freedom in my research and I really appreciate it, and I am very thankful to you for your trust and support. I also learned a lot from you, especially that research is also about how to present my results, and making nicer plots can indeed significantly improve the quality of a manuscript. I also really appreciated the kindness you have for all the members of the group.

A special thank goes for Thomás Fogarty alias Mossy who had a big impact in my choice of career and influenced the researcher that I became. Indeed you introduced me to the world of quantum thermodynamics and you are the reason why I started to be very interested by the field. I really enjoyed the time spent with you at the office, also in the lunch room during the tea breaks talking about the last Nicolas Cage movie or podcasts and youtube videos that you would be the only person to watch. I also enjoyed the times when we went out to try the last trendy fried chicken restaurant with Hasan, and the melodious sounds coming out of your body at the desk. But more importantly I really enjoyed all the discussions we had about physics during the past years. I really learned a lot from your skills and expertise. I was really impressed by your sharp intuition and really enjoyed your enthusiasm for physics. Thank you for working with me during my PhD and thank you for making me realize that I really like physics.

I want to thank Denis Konstantinov who has been my main training partner in kickboxing for the past years but also my instructor in quantum mechanics. The quality of your class was really outstanding and allowed me to have a solid background to start learning advanced concepts for my PhD. You are also an inspiring model and wish to be in the future a person like you: a skillful professor in physics who finds the time to do sports regularly and still in a great shape even after 50 years old. Spending time with you has been really beneficial for me and helped me to have a more disciplined and healthy lifestyle. I also really enjoyed talking with you about the last boxing fight of the weekend and the times we have been watching the UFC in the room C700.

Abbreviations

AHF	Anomalous heat flow
CL	Caldeira-Leggett
CK	Caldirola-Kanai
CRAB	Chopped random basis
DHO	Damped harmonic oscillator
DI	Dynamical invariant
EMP	Efficiceny at maximum power
EMW	Efficiency at maximum work output
EP	Effective power
KMS	Kubo-Martin-Schwinger
QBM	Quantum Brownian motion
QHE	Quantum heat engine
QSL	quantum speed limit
STA	Shortcut to adiabaticity
STE	Shortcut to equilibration
WM	Working medium

Nomenclature

$\hbar$ Planck constant ($1.054\,572\,66 \times 10^{-34}$ Js)

k_B Boltzmann constant ($1.380\,658 \times 10^{-23}$ JK^{-1})

I think I did pretty well, considering I started out with nothing but a bunch of blank paper.
Steve Martin

Contents

List of Figures

Introduction

Thermodynamics is one of the most fundamental and powerful theories in physics. This field has the particularity to be born and motivated by the technological progress made during the industrial revolution. Originally the theory was developed to understand heat transfers in machines, however its scope kept growing over time. For example, thermodynamics became able to generalize the concept of equilibrium, to describe and understand phase transitions in classical matter and their stability, or to describe non-equilibrium dynamics and relaxation process [3]. It also contributed to highlight the physical nature of information [4, 5]. Originally a macroscopic theory, it has been successfully extended to microscopic systems, where thermal fluctuations are important, to give birth to the field of stochastic thermodynamics [6].

In the past two decades, many physicists from various expertises started to study and formalize thermodynamics in the framework of quantum mechanics. Quantum thermodynamics became very recently a recognized field in the physics community whose aim is to extend standard thermodynamics to systems where quantum effect are strongly present [7, 8].

Interestingly, similar to the beginning of classical thermodynamics, the study of quantum engines is a central part of quantum thermodynamics [7, 9, 10]. They can be used to understand the role that quantum effects play compared to classical settings, while at the same time they have implications for the development of quantum technologies. Usually a quantum engine consists of a quantum system as the working medium to which a conventional thermodynamic cycle (Carnot, Otto etc.) is applied in order to extract work from the heat exchanged with a cold and a hot bath, or to transfer heat between the different baths by doing work on the working medium.

Technical progress allowed to realize the first successful engine cycle with a quantum working medium in 2016, by using a single-ion in a Paul trap [11, 12]. However after this accomplishment, few experimental realizations of quantum heat engines were reported [13] showing the difficulty to have good control for realizing a quantum engine cycle.

On the other hand, the first experimental realizations of a Bose-Einstein condensate in 1995 marked the boom of the field of cold atom physics [14, 15]. With great progress achieved in confining and laser cooling of atoms, cold atomic systems open the door to experimental realization of quantum systems that were only theoretical models so far. A great advantage of cold atomic systems is certainly the existence of Feschbach resonances [16] that allows to arbitrarily change the scattering length of the particles to explore many different types of interaction regimes [17, 18].

Combined with the confinement techniques that have been developed, experimental physicists in the community reached the stage where they have almost complete control over the spatial arrangement of atomic systems [19]. Recently the advantages of those systems have

been used to experimentally realize quantum engines, such as single particle engines driven by controlled collisions [20, 21, 22] but also engines with interacting quantum gases [23, 24], showing the important role of cold atomic systems in the understanding and development of quantum machines.

During my PhD, I studied and explored thermodynamics in cold atomic systems in order to realize quantum engines with properties that are unique to quantum systems and figure out how advantageous and different they can be compared to classical engines. In order to reach this aim, I proposed different ways to improve the performance of quantum heat engines. Possible ways to do that can be cast into two main approaches. The first one usually consists of exploiting non-trivial properties that can emerge from a quantum working medium during the operation of the engine while the second approach consists of controlling the working medium during the cycle in an appropriate way to make the strokes faster and more efficient. Therefore my work is divided into two parts. The first part focuses on few-body interacting cold atomic systems in one-dimension and their potential applications for quantum engines.

It consists of two research projects where in the first one, I study anomalous heat transports between two particles as a potential new way to implement cooling processes based on quantum correlations. In the second project I study a quantum heat engine realized with interacting particles in a harmonic potential where the work extraction is assisted by the manipulation of the interaction strength in the system. I show that an appropriate change of the interaction can enhance the performance of the engine compared to the non-interacting case. This work has been published in a peer reviewed journal [1].

The second part of my work focuses on the development of techniques for controlling open quantum systems in order to boost the performance of quantum heat engines by accelerating thermal strokes. This part is divided into two projects, where in the first one I realize a shortcut to equilibration protocol for driven open quantum systems. For this I work on two different approaches where in the first one, I propose to map the dynamics of a driven open quantum system to that of an isolated system where the effect of the environment is contained in a stochastic force.

The mapping is realized by using the Heisenberg equations of motion. Once the mapping is achieved, the control scheme is found by using techniques from shortcuts to adiabaticity [25] with a focus on the dynamical invariant method also known as the Lewis-Riesenfeld invariant [26]. The proposed method is applied to the quantum Brownian motion described by the Caldeira-Legget model [27, 28].

In the second approach, I propose to design shortcuts to equilibration in a driven open quantum system by deriving a time-dependent master equation based on the dynamical invariant. The proposed method is applied to the damped harmonic oscillator [29]. This work has been recently posted on arXiv and is now under review [2].

Finally in the last project, I used well known techniques from optimal control theory to speed-up the thermalization of an open quantum system by manipulating the interaction strength with the bath. I focus again on the quantum Brownian motion and use the advantageous properties of Gaussian states to solve exactly the dynamics of the particle [30]. This allows me to explore any interaction strength for a given set of bath parameters (number of particle in the bath, spectral density function...).

This thesis is structured as follows: in Chapter 1, I present the basic background and knowledge necessary for following the rest of the contents. In Section 1.1, I introduce the basics of cold atoms physics. In Section 1.2, I introduce the basics of classical and quan-

tum thermodynamics, how quantum engines are described and some of their fundamental properties. In Section 1.3, I discuss the basic theory of open quantum systems, where I first show the derivation of the master equation, and then examine Gaussian states and how one can exactly solve for the dynamics of open quantum systems made of harmonic oscillators. In Chapter 2, I present the results of the first part of my PhD where Section 2.1 is about the anomalous heat exchanges between two cold atoms and Section 2.2 concerns the quantum heat engine enhanced by the presence of interaction. Finally Chapter 3 focuses on the second part of my PhD where Section 3.1 describes the mapping of a driven quantum Brownian motion to the dynamics of an isolated quantum system for designing shortcuts to equilibration. Section 3.2 focuses on the same shortcut to equilibration realized this time with a time-dependent master equation based on the dynamical invariant, and Section 3.3 describes how I use optimal control theory to speed up the thermalization of the quantum Brownian motion.

Chapter 1

Background

1.1 One dimensional cold atomic systems

Indistinguishable particles

In quantum mechanics, it is not possible to label and distinguish identical particles due to the non-local nature of the wavefuntion. Indeed when the wavefunctions of the particles spread out and overlap, an exchange of particles cannot be detected. They are identical and nothing sets them apart.

Let us consider a system of two indistinguishable particles with the single particle wavefunctions $\psi_1(x_1)$ and $\psi_2(x_2)$. The state of the system is described by the wavefunction $\Psi(x_1, x_2)$ and the corresponding density has to be symmetric i.e $|\Psi(x_1, x_2)|^2 = |\Psi(x_2, x_1)|^2$. For that the wavefunction of the system has to be written as

$$\Psi(x_1, x_2) = P(x_1, x_2)\psi_1(x_1)\psi_2(x_2) + P(x_2, x_1)\psi_1(x_2)\psi_2(x_1), \tag{1.1}$$

where $P(x_1, x_2)$ is the permutation operator in coordinate representation. If the wavefunction is symmetric under permutation i.e $P(x_1, x_2) = P(x_2, x_1)$, the particles are bosons. They obey Bose-Einstein statistics [31]

$$n_i = \frac{1}{\exp\left(\frac{\epsilon_i - \mu}{k_B T}\right) - 1}, \tag{1.2}$$

where n_i is the expected number of particles with energy ϵ_i and μ is the chemical potential. With the Bose-Einstein distribution one can predict a phase transition where a macroscopic number of non interacting bosons can occupy the ground state which is Bose-Einstein condensation. Experimental realization of Bose-Einstein condensates at finite temperature is well known since 1995 [14, 15] and these systems offer a highly tunable and clean platform to investigate interesting physics like superfluidity [32, 33], wave-particle duality [34], condensed matter behaviour [35] and much more.

If the wavefunction is antisymmetric under permutation i.e $P(x_1, x_2) = -P(x_2, x_1)$, the particles are fermions. As a consequence of the antisymmetry of the wavefunction, the two-particle wavefunction vanishes when the two particles are in the same state. This is known as the Pauli exclusion principle. Fermions obey the Fermi-Dirac statistics [36]

$$n_i = \frac{1}{\exp\left(\frac{\epsilon_i - \mu}{k_B T}\right) + 1}. \tag{1.3}$$

As a consequence of the Pauli exclusion principle one has $0 \leq n_i \leq 1$. Moreover, for non-interacting and spin-polarized fermions at a temperature below the so-called Fermi temperature, each energy level is occupied by one fermion up to the highest excited occupied state (the so called Fermi level). This phenomenon is called the Fermi sea and can explain the behaviour of electrons in metals [37] or the formation of white dwarfs [38]. First experimental realizations of Fermi seas with ultracold atoms have been reported in 1999 [39] and 2001 [40]

Ultracold gases in one dimension

One-dimensional (1D) quantum many-body systems have rich history. Indeed, a few years after quantum mechanics was formalized, an analytical solution of the 1D Heisenberg model was found by Bethe by using an ansatz that now bears his name [41]. Subsequently more models have been exactly solved, but also computational methods have been developed to solve complicated integrable and non-integrable systems [42, 43, 44]. Initially the study of 1D systems was motivated by them being mathematically easier to treat, since in higher dimensions the task is more challenging. However with technological progress, it became possible to experimentally realize 1D systems whose physical properties are well described by these models.

Let us briefly explain how 1D systems can be experimentally realized in ultracold atom systems. To have a 1D system one needs to restrict the degrees of freedom of the particles in two directions. For example let us consider particles of mass m trapped in a 3D harmonic potential,

$$V(x, y, z) = \frac{1}{2}m(\omega_x^2 x^2 + \omega_y^2 y^2 + \omega_z^2 z^2). \tag{1.4}$$

In this case, one needs to freeze the degrees of freedom in two directions, for example along the y-axis and z-axis. One way to accomplish this is to tighten the trap along these directions such that $\omega_x \ll \omega_y, \omega_z$. The energy level spacing in the transverses directions then become sufficiently high so that the particles will not be able to occupy excited states. The atoms will remain in the ground state in these directions as long as $k_B T \ll \hbar \omega_y - \mu$, $\hbar \omega_z - \mu$ with μ the chemical potential, and can only have dynamics along the x-axis. Using very anisotropic traps therefore leads to quasi-1D systems [45, 40, 46].

The different interaction regimes in a Bose gas can be characterized by the Lieb-Liniger parameter, defined as [47]

$$\gamma = \frac{I}{K}, \tag{1.5}$$

where I is the interaction energy in the system and K quantifies the kinetic energy. In the case of a one-dimensional and homogeneous gas, the Lieb-Liniger parameter is given by

$$\gamma = \frac{mg_{1D}}{\hbar^2 n}, \tag{1.6}$$

where g_{1D} is the 1D interaction strength, m the mass of one atom and n is the density of the gas. When γ is small, the interaction in the system is weak while strong interaction regimes are characterized by a large value of the Lieb-Liniger parameter $\gamma \gg 1$. Let us also remark that the interaction strength can also be manipulated by changing the density of the gas and thus the chemical potential. Indeed based on the expression of the Lieb-Liniger parameter Eq. (1.6), increasing (decreasing) the density of the gas will reduce (increase) the effect of the interaction compared to the kinetic energy.

In the following I will focus on 1D bosonic systems. I will introduce continuous systems and briefly explain how the interaction in such systems is described. Then I will discuss two exactly solvable models that are relevant in my work: the two-particle problem and the 1D gas in the infinite interaction strength limit.

1.1.1 One dimensional continuous bosons models

Let us start by considering a 3D system of N bosons described by the wavefunction $\Psi(\vec{r}_1, ..., \vec{r}_N)$. The particles can freely move along the x-axis while their motion is confined in the transverse directions (y, z). Assuming that the particles are in the ground state $\psi_0(y, z)$ in the transverse directions, and the dynamics in these directions decouples, the wavefunction can be written as

$$\Phi(\vec{r}_1, ..., \vec{r}_N) = \Psi(x_1, ..., x_N) \prod_{i=0}^{N} \psi_0(y_i, z_i). \tag{1.7}$$

This approximation is valid as long as a very strong confinement is applied in the transverse direction, which leads to having a large gap between the ground state and the first excited state in the transverse direction compared to the excitation in the x-axis. It also allows us to describe the system in terms of the 1D wavefunction $\Psi(x_1, ..., x_N)$ only. The Hamiltonian of a one-dimensional interacting Bose gas can be written as

$$H = \sum_{i=1}^{N} \left(\frac{p_i^2}{2m} + V_{\text{ext}}(x_i) \right) + \sum_{i<j} V_{\text{int}}(x_i - x_j), \tag{1.8}$$

where m is the mass, p_i and x_i are respectively the momentum operator and the position operator of the ith particle, V_{ext} is the external potential and V_{int} is the interaction potential. Due to the low energy of the system and the fact that the gas is dilute, two-body interactions are dominating. Also at low energies, the pairwise interaction is mostly dominated by s-wave scatterings and can be effectively described by a point-like interaction in three dimensions [48, 49]

$$V_{\text{int}}(\vec{r}_i - \vec{r}_j) = g_{3D} \delta^{(3)}_{\text{reg}}(\vec{r}_i - \vec{r}_j), \tag{1.9}$$

where g_{3D} corresponds to the interaction strength in three dimensions and $\delta^{(3)}_{\text{reg}}(\vec{r})$ is the regularized delta function. The s-wave scattering process is characterized by only one number; the scattering length a_s that can be calculated in the Born approximation [49]

$$a_s = \frac{m}{4\pi\hbar^2} \int V_{\text{int}}(\vec{r}) d\vec{r}, \tag{1.10}$$

thus the interaction strength and the scattering length are related by

$$g_{3D} = \frac{4\pi\hbar^2 a_s}{m}. \tag{1.11}$$

With this result in mind, the cold atom community was able to take advantage of a powerful technique to experimentally tune the interaction strength between two particles: the Feshbach resonance [16]. With the Feshbach resonance, one can modify the scattering length a_s and so the interaction strength, by using Zeeman splitting with an external magnetic field [50, 51, 52]. The scattering length is modified by the magnetic field with respect to the formula [52]

$$a_s(B) = a_{bg}\left(1 + \frac{\Delta}{B - B_0}\right), \tag{1.12}$$

where a_{bg} is the off-resonant value of the scattering length, Δ is the resonance width, and B_0 is the resonant magnetic field at the point where the scattering length diverges.

So far we discussed an effective description of the interaction in three dimensions. However the same arguments are valid in the 1D case. The interaction can be effectively described as $V_{\text{int}}(x_i - x_j) = g_{1D}\delta(x_i - x_j)$ and now the 1D scattering length a_{1D} is related to the 1D interaction strength as [53]

$$g_{1D} = -\frac{2\hbar^2}{ma_{1D}}. \tag{1.13}$$

The 1D scattering length is related to the three dimensional scattering length a_s as [53]

$$a_{1D} = -\frac{a_\perp^2}{2a_s}\left(1 - C\frac{a_s}{a_\perp}\right), \tag{1.14}$$

where $C \approx 1.4603$ is a dimensionless value, and $a_\perp = \sqrt{2\hbar/m\omega_\perp}$ (with $\omega_\perp = \sqrt{\omega_y^2 + \omega_z^2}$) is the typical length of the ground state $\psi_0(y, z)$ in the transverse direction. One can see from Eq. (1.14), that the interaction strength can also be tuned by changing the confinement in the transverse direction $\omega_\perp$. Also it is worth mentioning that $g_{1D} > 0$ ($g_{1D} < 0$) corresponds to a repulsive (attractive) interaction type. In the following, I will use g instead of g_{1D} to denote the 1D interaction strength, for ease of notation.

1.1.2 Some exactly solvable models

Two interacting particles in a harmonic trap

Let us consider the case of two interacting particles of equal mass in a harmonic oscillator

$$H = \sum_{i=1}^{2} -\frac{\hbar^2}{2m}\frac{\partial^2}{\partial x_i^2} + \frac{1}{2}m\omega^2 x_i^2 + g\delta(x_1 - x_2). \tag{1.15}$$

The Hamiltonian has been analytically solved [48], by introducing the center of mass coordinate $X = \frac{x_1+x_2}{\sqrt{2}}$ and the relative coordinate $x = \frac{x_1-x_2}{\sqrt{2}}$, which allows one to split the Hamiltonian (1.15) into two decoupled single particle Hamiltonians $H(\omega, g) = H_{CM} + H_r$

with

$$H_{CM} = -\frac{\hbar^2}{2m}\frac{\partial^2}{\partial X^2} + \frac{1}{2}m\omega^2 X^2, \tag{1.16}$$

$$H_r = -\frac{\hbar^2}{2m}\frac{\partial^2}{\partial x^2} + \frac{1}{2}m\omega^2 x^2 + \frac{g}{\sqrt{2}}\delta(x). \tag{1.17}$$

The eigenstates are thus given by the two particle states $|n, \nu\rangle$, where $|n\rangle$ is the eigenstate of the center of mass, and $|\nu\rangle$ the eigenstate of the relative coordinate. Since the center of mass is not affected by the interaction, the eigenstates of H_{CM} are simply the standard harmonic oscillator eigenfunctions $\langle X|n\rangle = \frac{1}{\sqrt{2^n n!}}\left(\frac{m\omega}{\pi\hbar}\right)^{\frac{1}{4}} e^{-\frac{X^2}{2a^2}} H_n(\frac{X}{a})$, where $a = \sqrt{\frac{\hbar}{m\omega}}$ and H_n are the Hermite polynomials, and the eigenenergies are given by $E_{CM}^n = \hbar\omega(n + \frac{1}{2})$. For the relative coordinate, only the even states are affected by the interaction and are given by $\langle x|2\nu\rangle = N_{2\nu}e^{-\frac{x^2}{2a^2}} U\left(\frac{1}{4} - \frac{E_r^{2\nu}}{2\hbar\omega}, \frac{1}{2}, \frac{x^2}{a^2}\right)$ where $N_{2\nu}$ is a normalization factor, $E_r^{2\nu}$ the eigenenergy and U is the Kummer function [48]. The eigenenergies are determined by the solutions of the transcendental equation

$$-\tilde{g} = 2\frac{\Gamma\left(-\frac{E_r^{2\nu}}{2\hbar\omega} + \frac{3}{4}\right)}{\Gamma\left(-\frac{E_r^{2\nu}}{2\hbar\omega} + \frac{1}{4}\right)}, \tag{1.18}$$

where $\tilde{g} = \frac{g}{\sqrt{2}\hbar\omega a}$ and $\Gamma(x)$ is the gamma function. The odd eigenstates are again just harmonic oscillator states with the eigenenergies $E_r^{2\nu+1} = \hbar\omega(2\nu + \frac{3}{2})$.

Tonks–Girardeau gas

Now we consider a system described by the general Hamiltonian (1.8) with the contact interaction $V_{\text{int}}(x_i - x_j) = g\delta(x_i - x_j)$. The Tonks–Girardeau (TG) gas corresponds to the limit of infinite and repulsive interaction regime i.e when the Lieb-Liniger parameter γ goes to infinity [54]. In this limit, the wavefunction of the system vanishes when two particles are at the same position, similarly to the Pauli exclusion principle for fermions. With this observation in mind, Girardeau proved that one can map the bosonic TG gas to a state of non-interacting fermions [55]. Thus the wavefunction is given by

$$\Psi(x_1, ..., x_2) = S(x_1, ..., x_N)\Psi_F(x_1, ..., x_N), \tag{1.19}$$

where $S(x_1, ..., x_N) = \prod_{i<j}^N \text{sign}(x_i - x_j)$ ensures that the wavefunction of the TG gas remains symmetric under permutations, and $\Psi_F(x_1, ..., x_N)$ is the many-body wavefunction of non-interacting fermions. The fermionic many body state can be calculated by using the Slater determinant

$$\Psi_F(x_1, ..., x_N) = \frac{1}{\sqrt{N!}}\det_{(n,i)=(0,1)}^{(N-1,N)}\psi_n(x_i), \tag{1.20}$$

where ψ_n are the single particle eigenstates of the system

$$-\frac{\hbar^2}{2m}\frac{\partial^2\psi_n(x)}{\partial x^2} + V_{\text{ext}}(x)\psi_n(x) = E_n\psi_n(x). \tag{1.21}$$

The first experimental realizations of the TG gas have been reported in 2004 with rubidium atoms trapped in a two-dimensional optical lattice [56]. Also during the same year, the TG gas has been realized in a one-dimensional lattice where the confinement has been increased in the transverse direction [57]. This forces the particles to spread in the longitudinal direction and thus reduces the density. The interaction becomes dominant (see the expression of the Lieb-Liniger parameter (1.6)), and the particles can localize.

1.2 Basics of thermodynamics in quantum systems

1.2.1 Thermodynamics in classical systems

First law of thermodynamics

Thermodynamics is by essence an axiomatic theory describing energy exchanges between a system and an environment. The theory is a set of four axioms, usually called the laws of thermodynamics and allows us to define the concept of thermal equilibrium, the different kind of energies that are exchanged and in which direction the energy exchange occurs. Here I briefly review the basic concepts of classical thermodynamics that are necessary to introduce my work. We start with the first law of thermodynamics. It can be summarized by the following sentence [58],

During a transformation of a closed system, the amount of energy exchanged with the environment is equal to energy exchanged by thermal transfer (heat) and by mechanical transfer (work).

In other words, let us call E the total energy of a closed system (in classical thermodynamics a closed system corresponds to a system that can exchange energy with the environment with no exchange of particles), then the infinitesimal variation of the energy is given by

$$dE = \delta Q + \delta W, \tag{1.22}$$

where Q is the heat and W the work. I use the letter δ to emphasize that δQ and δW are non-exact differentials that depend on the trajectory during the transformation. The variation of the work can be expressed as

$$\delta W = -PdV, \tag{1.23}$$

with P the pressure of the system and dV the infinitesimal variation of the volume of the system during the transformation. The work can be seen as a "useful" energy that can allow us, for example, to generate movement of the system, while the heat corresponds to energy dissipated to the environment that we cannot use. The second law of thermodynamics allows us to characterize this with the concept of entropy.

The second law of thermodynamics

The first law alone describes the energy exchanges and suggests that if a thermodynamic transformation from a state to another one is possible, then the opposite transformation is also possible. However from experiments we know that for any macroscopic isolated system, there exists only one equilibrium state depending on state variables like the energy, the

volume or the number of particles, and the system will spontaneously and irreversibly evolve to this state. The second law of thermodynamics characterizes this equilibrium state and the direction in which a thermodynamics transformation occurs by using the entropy function introduced by Clausius [59].

For any system the entropy S is defined at equilibrium. The entropy is a state function, which means it depends only on the state variables of the system (energy, volume...), and is maximum at equilibrium. The entropy is also additive, which means that for an isolated system divided in two subsystems, the entropy of the isolated system is equal to the sum of the entropy of the two subsystems. The main formulation of the second law of thermodynamics states that for an isolated system (a system that exchanges no energy and no particles with the environment), the variation of entropy is positive

$$\Delta S \geq 0. \tag{1.24}$$

However I will focus on the Clausius formulation, since I am interested in the heat transfer as part of my work. Let us consider an isolated system divided in two subsystems 1 and 2. The energy (entropy) of the system is E (S), and the subsystems 1 and 2 have respectively an energy (entropy) E_1 (S_1) and E_2 (S_2). From the conservation of energy one deduces $E_2 = E - E_1$. By using the additive property of the entropy, one gets

$$S(E) = S_1(E_1) + S_2(E - E_1). \tag{1.25}$$

Let us assume now that the energy of the subsystem 1 gets a infinitesimal variation of energy in the form of heat dE_1. The new entropy of the system is then $S_1(E_1 + dE_1) + S_2(E - E_1 - dE_1)$ and by doing a first order Taylor expansion, one gets

$$dS = \left(\frac{\partial S_1}{\partial E_1} - \frac{\partial S_2}{\partial E_2} \right) dE_1. \tag{1.26}$$

The second law tells us that $dS \geq 0$, so we deduce that if $\frac{\partial S_1}{\partial E_1} > \frac{\partial S_2}{\partial E_2}$ then $dE_1 \geq 0$ which means the heat flows from the subsystem 2 to the subsystem 1. On the contrary if $\frac{\partial S_1}{\partial E_1} < \frac{\partial S_2}{\partial E_2}$, then $dE_1 \leq 0$ and the heat flows from the subsystem 1 to the subsystem 2. Intuitively the quantity $\frac{\partial S}{\partial E}$ has to be a decreasing function of the temperature $f(T)$ and for a choice of f one gets a definition of the temperature. To make sure that the definition of the temperature coincides with the one from statistical mechanics, one needs to choose f as the inverse function and so the temperature is defined as [60]

$$\frac{1}{T} = \frac{\partial S}{\partial E}. \tag{1.27}$$

Now that the thermodynamic identity (1.27) has been derived, we can derive the Clausius inequality. Let us consider a system in contact with a thermal bath. A thermal bath is a system that can receive or release heat without changing its temperature

$$dT_B = 0 \ \forall \, \delta Q_B, \tag{1.28}$$

where T_B is the temperature of the bath and Q_B the heat. A thermal bath is an ideal system but it can be approximated with a system that is very big compared to the studied system so that the variations of temperature due to the variations of energy can be neglected. The

system and the bath are isolated. From the thermodynamic identity (1.27) and the definition of the thermal bath, one can write

$$dS_B = \frac{\delta Q_B}{T_B},$$ (1.29)

where S_B is the entropy of the bath. Let us call Q the heat of the system, from the conservation of energy one gets $\delta Q = -\delta Q_B$ and so the entropy of the thermal bath becomes

$$dS_B = -\frac{\delta Q}{T_B} \implies \Delta S_B = -\frac{Q}{T_B}.$$ (1.30)

Using the second law and the additive property of the entropy, one gets $\Delta S + \Delta S_B \geq 0$ where S is the entropy of the system. Combined with Eq. (1.30), one deduces the Clausius inequality [59]

$$\Delta S \geq \frac{Q}{T_B}.$$ (1.31)

The Clausius inequality can be extended to the case of N thermal baths [60]

$$\Delta S \geq \sum_{i=1}^{N} \frac{Q_i}{T_i},$$ (1.32)

where Q_i is the heat exchanged between the system and the ith thermal bath at temperature T_i. This is one of the formulations of the second law of the thermodynamics and it gives the "natural" direction of a heat transfer between the system and the environment. In other words the Clausius formulation says that

no process is possible whose sole result is the transfer of heat from a body of lower temperature to a body of higher temperature.

We will also see in the last part of this section that the Clausius inequality (and so the second law) leads to a fundamental bound on the efficiency of heat engines.

1.2.2 Formulation of thermodynamics for quantum systems

Quantum thermodynamics is an active and recently established field of research [61, 58, 8]. Indeed thermodynamics has been a very successful theory for classical systems and extending it to quantum systems became a natural continuation. One of the most interesting questions in the field is to understand how the laws of thermodynamics need to be modified when we consider quantum systems. Such a question is very important from a fundamental point of view but also has direct implications on the operating regime of quantum engines [62, 63, 64]. Therefore one needs to define the concepts of work, heat and entropy in the quantum framework. There were many works on this direction considering different ideas and approaches [65, 66, 67, 68, 69, 70, 71, 72, 73, 74, 75, 76].

Here I will use the main results of [77] where the expressions of the different thermodynamic quantities, that are relevant for my work, have been derived. First let us consider a quantum system interacting with a thermal environment. Let us call $H(\lambda)$ the Hamiltonian where λ is a control parameter that drives the system from one state to another one, and let

us assume the process is quasistatic. As we will see in more details in the next section of this chapter, the dynamics of the system is described by a Liouville type equation [29, 78],

$$\frac{d\rho}{dt} = L_\lambda(\rho). \tag{1.33}$$

Here ρ is the density matrix of the system and L_λ is an operator that describes the dynamics of the system due to the Hamiltonian H and the interaction with the thermal environment.

Thermodynamics for a Gibbs state

In the case where the coupling between a system and its surrounding environment is weak, equation (1.33) has a unique stationary solution which corresponds to an equilibrium state. It is given by the Gibbs state [29, 78]

$$\rho_{\text{eq}} = \frac{\exp(-\beta H)}{Z}, \tag{1.34}$$

where $\beta = \frac{1}{k_B T}$ is the inverse temperature, k_B is the Boltzmann constant and $Z = \text{Tr}(\exp(-\beta H))$ is the partition function, with Tr the trace operator. In this case the thermodynamic entropy is given by the von Neumann entropy

$$S = -\text{Tr}(\rho_{\text{eq}} \ln(\rho_{\text{eq}})) = \beta(E - F). \tag{1.35}$$

Here $E = \text{Tr}(\rho_{\text{eq}} H)$ is the internal energy of the system, and $F = -\frac{1}{\beta} \ln(Z)$ is the free energy. Therefore the infinitesimal variation of entropy can be expressed as

$$dS = \beta \text{Tr}(d\rho_{\text{eq}} H). \tag{1.36}$$

Based on Eq. (1.30) one can identify the variation of heat as $\delta Q = \frac{dS}{\beta}$, and the work can be identified as the variation of energy due to the change of the Hamiltonian. The first law can then be written as

$$dE = \delta Q + \delta W \equiv \text{Tr}(d\rho_{\text{eq}} H) + \text{Tr}(\rho_{\text{eq}} dH). \tag{1.37}$$

As one can notice, the formulation is basically the same as the classical case and the reason is because we assume that the equilibrium state is of Gibbs form due to the weak coupling between the system and the environment. However quantum systems can be correlated with their environment, and furthermore their interaction energy cannot be neglected [79, 80, 81].

First law in the presence of quantum correlations

In the presence of quantum correlations one needs to take account of the energetic cost of keeping correlations between the system and the environment [80, 82]. To do that an information-theoretic approach is needed [83, 5]. Let us assume the system is in a non-Gibbs equilibrium state ρ_*, for which the von Neumann entropy can be written as,

$$S = -\text{Tr}\left(\rho_* \ln\left(\rho_*\right)\right) + \left(\text{Tr}\left(\rho_* \ln\left(\rho_{\text{eq}}\right)\right) - \text{Tr}\left(\rho_* \ln\left(\rho_{\text{eq}}\right)\right)\right)$$
$$= \beta[E - \left(F + \beta^{-1}S(\rho_*||\rho_{\text{eq}})\right)] \quad (1.38)$$
$$= \beta(E - F_I),$$

where $E = \text{Tr}\left(\rho_* H\right)$ is the internal energy of the system, $S(\rho_*||\rho_{\text{eq}}) = \text{Tr}\left(\rho_* \left(\ln(\rho_*) - \ln(\rho_{\text{eq}})\right)\right)$ is the relative entropy and $F_I = F + \beta^{-1}S(\rho_*||\rho_{\text{eq}})$ is the information free energy [84]. So for a quasistatic process, the infinitesimal variation of entropy can be written as

$$dS = \beta\left(\text{Tr}\left(d\rho_* H\right) + \left(\text{Tr}[\,\rho_* dH\,] - dF_I\right)\right) = \beta(\delta Q_{tot} - \delta Q_c). \quad (1.39)$$

In this equation the variation of total heat is identified as $\delta Q_{tot} \equiv \text{Tr}\left(d\rho_* H\right)$ and the energetic cost to keep coherence and quantum correlations as $\delta Q_c = dF_I - \text{Tr}\left(\rho_* dH\right)$. Therefore one defines the excess heat $\delta Q_{ex} \equiv \delta Q_{tot} - \delta Q_c$ which is associated with the entropy production and the first law becomes

$$dE = \delta W_{ex} + \delta Q_{ex} \quad (1.40)$$

with $\delta W_{ex} \equiv \delta W + \delta Q_c$ the excess work.

Second law in the presence of quantum correlations and spontaneous reversed heat flow

As we saw, the first law has to be modified because maintaining the correlations implies an extra energy cost. This result can be related to the Landauer principle and the physical nature of information [85]. Indeed correlation is a synonym of information, so the more a system is correlated to an environment the more we can know about it. Based on Eq.(1.40), to learn about the system, an additional amount of work is needed. In addition we can see correlations as a potential work reservoir and use it to drive the system to some state, like in an engine. A consequence is that the Clausius formulation of the second law presented before is no longer valid.

The consequences of correlations on the second law have been explored extensively [83, 86, 87, 88, 89, 90, 91]. Let us consider two systems A and B in thermal contact and ρ_{AB} being the corresponding density matrix. We assume that initially A (B) has a temperature T_A (T_B) which means that the reduced density matrix of A (B) is initially a Gibbs state, i.e

$$\rho_{A(B)}(t = 0) = \text{Tr}_{B(A)}\left(\rho_{AB}(t = 0)\right) = \frac{\exp\left(-\beta_{A(B)}H_{A(B)}\right)}{Z_{A(B)}}, \quad (1.41)$$

where H_i and Z_i are respectively the Hamiltonian and the partition function of the system i $(i = A, B)$. Therefore in presence of correlations the initial state of the system AB can be written as

$$\rho_{AB}(0) = \rho_A \otimes \rho_B + \chi_{AB}, \quad (1.42)$$

where χ_{AB} represents the initial correlations. We also assume the system AB is isolated and it evolves during a time τ with a Hamiltonian H_{AB}. The relative entropy between the initial state and the final state of one of the subsystems is

$$S(\rho_i(\tau)||\rho_i(0)) = -S(\rho_i(\tau)) + \beta_i \mathrm{Tr}\,(\rho_i(\tau)H_i) + \ln(Z_i). \tag{1.43}$$

By noticing that $S(\rho_i(0)||\rho_i(0)) = 0$ and using the previous expression, one can derive

$$S(\rho_i(\tau)||\rho_i(0)) = S(\rho_i(\tau)||\rho_i(0)) - S(\rho_i(0)||\rho_i(0)) = -\Delta S_i + \beta \Delta E_i, \tag{1.44}$$

where $\Delta S_i = S(\rho_i(\tau)) - S(\rho_i(0))$ and $\Delta E_i = \mathrm{Tr}_i\,((\rho_i(\tau) - \rho_i(0))H_i)$ are respectively the variation of entropy and internal energy of the ith subsystem. By writing the previous expression for both subsystems, then summing and rearranging the terms one gets,

$$\beta_A \Delta E_A + \beta_B \Delta E_B = \Delta S_A + \Delta S_B + S(\rho_A(\tau)||\rho_A(0)) + S(\rho_B(\tau)||\rho_B(0)). \tag{1.45}$$

Let us introduce now the mutual information between A and B

$$I_{AB} = S(\rho_A) + S(\rho_B) - S(\rho_{AB}). \tag{1.46}$$

Since the system AB is isolated, the von Neumann entropy is preserved and thus the variation of mutual information is $\Delta I_{AB}(\tau) = \Delta S_A + \Delta S_B$. Moreover by using the conservation of energy for an isolated system and the first law, one can deduce $\Delta E_A = Q_A = -\Delta E_B = -Q_B$. Finally Eq. (1.45) becomes

$$Q_B(\beta_B - \beta_A) = \Delta I_{AB}(\tau) + S(\rho_A(\tau)||\rho_A(0)) + S(\rho_B(\tau)||\rho_B(0)). \tag{1.47}$$

Since the relative entropy is a positive function, one gets the generalized Clausius inequality [83]

$$Q_B(\beta_B - \beta_A) \geq \Delta I_{AB}(\tau). \tag{1.48}$$

If the correlations between A and B are initially weak then the mutual information is close to 0 and since I_{AB} is a positive function ($\Delta I_{AB}(\tau) \geq 0$) one recovers the usual Clausius inequality. However if the systems are initially correlated, then $I_{AB} > 0$ and one can imagine a dynamics where the correlations are decreasing such that $\Delta I_{AB}(\tau) < 0$ and $|\Delta I_{AB}(\tau)| > S(\rho_A(\tau)||\rho_A(0)) + S(\rho_B(\tau)||\rho_B(0))$. In this case, based on Eq. (1.48), a heat flow from the low temperature system to the high temperature is possible. Recently the study of this counter-intuitive phenomenon has become of interest and in Ref. [92], Micadei *et al.* experimentally realized a reversed heat flow between two quantum-correlated spins.

1.2.3 Thermodynamics of heat engines

General properties

A heat engine is a physical system that converts heat into work in order to generate a mechanical motion. The physical system is usually called the working medium or the working fluid since for classical engines, it consists of a gas that is most of the time described as an ideal one. Their functioning is modeled with cycles corresponding to strokes that describe the different steps of the work extraction i.e compression/expansion of the working medium and

heat transfers with external baths. At the end of the cycle, the working medium goes back to its initial state and operates repeatedly. Even thought cycles are usually ideal representations of a real engine functioning, they provide a good understanding of it.

An engine can only work if there is at least two thermal baths at different temperatures that are coupled with the working medium. This is a direct consequence of the 1st and 2nd law of thermodynamics. Indeed let us assume that we have a heat engine coupled to only one thermal bath. After a cycle the working medium goes back to the initial state. Since the internal energy is a state variable, the first law tells us

$$\Delta E = W + Q = 0. \tag{1.49}$$

At the end of the cycle, we want to extract work out of the engine. By convention, the variation of energy is negative when it is lost due to the work done, which means that the engine produces extractable work when $W < 0$. From the first law, we deduce then that the heat exchange between the working fluid and the bath has to be positive. However this result violates the 2nd law. Indeed the total change of entropy after a cycle is given by the change of entropy of the bath $\Delta S_B = -Q/T_B$ and has to be positive. It is therefore impossible to extract work with only a single bath. This result is also another formulation of the 2nd law formulated by Kelvin [93]. A heat engine needs to be coupled to at least two baths: a hot bath at the temperature T_h from which it receives energy Q_h , and a cold bath at the temperature T_c in which energy is dissipated from the working medium Q_c in order to extract work.

The performance of an engine can be characterized with the work output W and the efficiency η that tells the amount of useful energy output we get compared to the amount of energy we used. In the case of heat engines, the efficiency is defined as

$$\eta = -\frac{W}{Q_h}. \tag{1.50}$$

The efficiency is a positive number between 0 and 1. In fact, the efficiency is fundamentally bound due to the 2nd law. Indeed let us consider a cycle performed on a heat engine coupled to two baths. Again from the 1st law, we get

$$W + Q_c + Q_h = 0 \implies W = -(Q_c + Q_h). \tag{1.51}$$

The efficiency can thus be rewritten as

$$\eta = 1 + \frac{Q_c}{Q_h}. \tag{1.52}$$

The Clausius inequality Eq. (1.32) applied during the cycle gives an inequality between the ratio of heats and the ration of temperatures

$$\frac{Q_c}{T_c} + \frac{Q_h}{T_h} \leq 0 \implies \frac{Q_c}{Q_h} \leq -\frac{T_c}{T_h}. \tag{1.53}$$

As a consequence, the efficiency of a heat engine is universally bound as

$$\eta \leq 1 - \frac{T_c}{T_h} \equiv \eta_C, \tag{1.54}$$
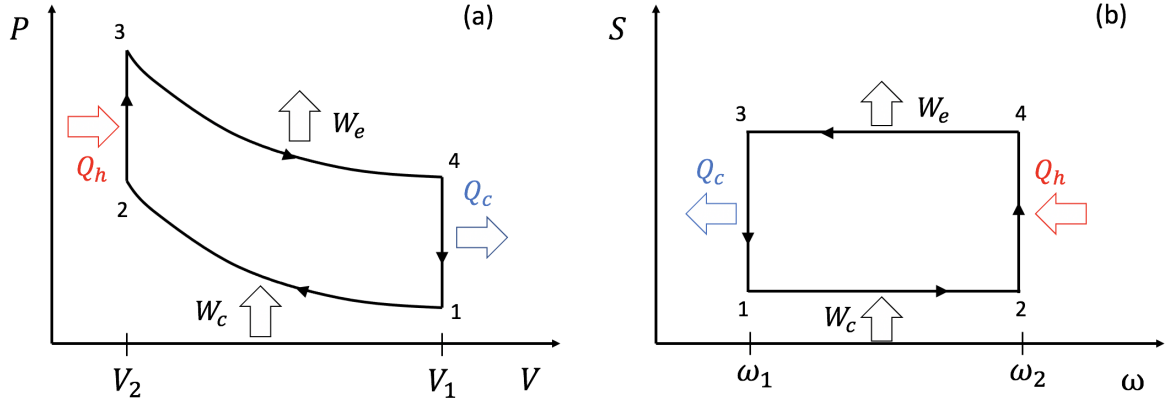
Figure 1.1: (a) P-V diagram of the classical Otto cycle, the x-axis represents the volume of the gas and the y-axis the pressure. (b) Diagram representation of the quantum Otto cycle for the harmonic oscillator. The x-axis represents the trap frequency and the y-axis the entropy of the particle.

where η_C is the Carnot efficiency named after Sadi Carnot who was the first to derive this result [94]. The Carnot efficiency can be reached by a heat engine realizing the Carnot cycle.

The Otto cycle: from the classical to quantum formulation

There are many cycles that have been proposed to model heat engines. In my work, I focuse on the Otto cycle named after the engineer Nicolaus Otto. The cycle is made of four strokes. I will first introduce the cycle in the classical case and then explain how the cycle can be extended to quantum working media. In the classical case, the different strokes are the following (see figure 1.1(a) representing the P-V diagram)

Adiabatic compression $(1 \rightarrow 2)$: the working medium undergoes an adiabatic reversible (isentropic) compression from a volume V_1 to V_2. During the stroke both pressure and temperature change, while the entropy remains constant.

Hot isochore $(2 \rightarrow 3)$: the volume of the working medium is kept constant and the temperature is increased by heating the working medium with the hot bath.

Adiabatic expansion $(3 \rightarrow 4)$: the working medium undergoes an isentropic expansion from the volume V_2 back to the volume V_1. This is when useful work is extracted.

Cold isochore $(4 \rightarrow 1)$: in the last stroke the working medium is cooled down by being coupled to the cold bath at constant volume. The working medium goes back to the initial state and then another consecutive cycle can be implemented.

In order to extend to the quantum case, we need to understand how these strokes should be realized when the working medium is a quantum system [95]. Indeed while carrying out an adiabatic stroke in a classical setting means that no heat exchange occurs during the process, for quantum systems it refers to the condition that the occupation populations of the eigenstates remain constant. This difference in the definition implies a stronger constraint on the timescale of the strokes.

In classical heat engines, the working medium will be driven quickly to prevent the system from relaxing and therefore exchanging heat with the environment, while for the quantum case, one needs to isolate the system to prevent heat exchanges but also to drive it quasistatically based on the adiabatic theorem. However the isochoric strokes are very similar both in the classical and the quantum cases. During the process, heat exchanges only occur between the working medium and the bath. The Hamiltonian thus remains fixed such that the eigenenergies are constant and only their occupations are changed (Eq. (1.37)).

To illustrate this, let us consider one of the simplest systems: a particle in a harmonic trap. The control parameter in this case is the trap frequency

$$H(\omega) = \frac{p^2}{2m} + \frac{1}{2}m\omega^2 x^2. \tag{1.55}$$

The trap frequency plays a role of the container size and accounts for compression or expansion of the wavefunction of the particle like a gas in a classical heat engine. The Otto cycle can then simply be formulated (see Fig. 1.1(b)). The adiabatic compression corresponds to a quantum adiabatic increase of the trap frequency from ω_1 to ω_2. During the hot isochore, the particle is heated by a hot bath and the trap frequency is fixed at the value ω_2. During the adiabatic expansion, the trap frequency goes back to the value ω_1. Finally during the cold isochore, the particle cools back down to the initial state.

The efficiency of the quantum Otto cycle with one particle can be simply calculated. Indeed since the work strokes are realized adiabatically and during the thermal stroke the Hamiltonian is fixed, we can just calculate the energy of the particle at the beginning/end of the different strokes (corners in the figure) in order to get the work and the heat exchanges. The heat exchange during the hot isochore Q_h is thus given by

$$Q_h = E_3 - E_2 = \text{Tr}((\rho_3 - \rho_2)H(\omega_2)) = \sum_n (p_n^h - p_n^c)E_n(\omega_2), \tag{1.56}$$

where p_n^h (p_n^c) are the occupations of the energy levels at the end (beginning) of the stroke and $E_n(\omega) = \hbar\omega(n + 1/2)$. At the end of the stroke, the particle is at equilibrium with the hot bath $p_n^h = Z_h^{-1}e^{-\beta_h\hbar\omega_2(n+1/2)}$. Also before the hot isochore, the particle was adibatically driven from the initial state where it was at equilibrium with the cold bath. We deduce then $p_n^c = Z_c^{-1}e^{-\beta_c\hbar\omega_1(n+1/2)}$. Thus the heat is given by

$$Q_h = \frac{\hbar\omega_2}{2}\left(\coth\left(\frac{\beta_h\hbar\omega_2}{2}\right) - \coth\left(\frac{\beta_c\hbar\omega_1}{2}\right)\right). \tag{1.57}$$

With the same reasoning, we can easily deduce the heat exchange during the cold isochore

$$Q_c = \frac{\hbar\omega_1}{2}\left(\coth\left(\frac{\beta_c\hbar\omega_1}{2}\right) - \coth\left(\frac{\beta_h\hbar\omega_2}{2}\right)\right), \tag{1.58}$$

and we deduce the efficiency of the quantum Otto cycle

$$\eta_O = 1 - \frac{\omega_1}{\omega_2}. \tag{1.59}$$

The Otto efficiency can be rewritten as $\eta_O = 1 - \kappa$ where $\kappa = \omega_1/\omega_2$ is the compression ratio, which is given by the ratio of the trap frequencies for the harmonic oscillator case. Since we know the efficiency is bound by the Carnot one, we deduce $\frac{\omega_1}{\omega_2} \geq \frac{T_c}{T_h}$. If this inequality is violated then the system can not operate as a heat engine.

Efficiency at maximum power/work

In practice the power output of an engine modeled by an ideal cycle like the Otto cycle or the Carnot one goes to zero. This is because the different strokes in the cycle require long times to be realized (in principle an infinite amount of time). To evaluate the performance of heat engines at finite time, the efficiency at maximum power (EMP) becomes a more relevant quantity than the ideal efficiency.

The EMP was introduced first by Curzon and Ahlborn who evaluated the efficiency of a Carnot engine operating at finite time. They showed that the efficiency of the engine while maximizing the power of it is given by [96, 97]

$$\eta_{CA} = 1 - \sqrt{\frac{T_c}{T_h}}. \tag{1.60}$$

This efficiency is commonly called the Curzon-Ahlborn (CA) bound and actually this quantity is more fundamental and universal than it looks [98]. Indeed, let us go back to the quantum Otto cycle of a particle in a harmonic potential. The work output is

$$W = -Q_c - Q_h = \frac{\hbar}{2}(\omega_2 - \omega_1)\left(\coth\left(\frac{\beta_c \hbar \omega_1}{2}\right) - \coth\left(\frac{\beta_h \hbar \omega_2}{2}\right)\right). \tag{1.61}$$

In the high temperature limit $\beta_c \hbar \omega_1 \ll 1$ and $\beta_h \hbar \omega_2 \ll 1$, the work output can be approximated by

$$W \approx (\omega_2 - \omega_1)\left(\frac{1}{\beta_c \omega_1} - \frac{1}{\beta_h \omega_2}\right) = (1 - \kappa)\left(\frac{1}{\kappa \beta_c} - \frac{1}{\beta_h}\right). \tag{1.62}$$

The work is maximum when $\kappa = \sqrt{\beta_h/\beta_c} = \sqrt{T_c/T_h}$ and so the efficiency at maximum work output (EMW) of the Otto cycle is given by the CA bound. The EMP became a paradigmatic quantity to study in order to characterize heat engines at finite time and has been extensively studied in classical thermodynamics [98, 99, 100, 101]. In the linear response regime, it is bound by η_{CA} [98], however cases where the EMP goes beyond the CA bound have been reported and also the universal behavior of it up to quadratic order for any cycle [99, 102, 103, 104].

The EMP has also been widely studied in the quantum case where universal features have been observed and cases where, beyond the linear response regime, the EMP goes above the CA bound [105, 106, 107, 108]. Other works have shown that the EMP can go beyond the CA bound due to purely quantum effects like entanglement between the working medium and the baths [109] or coherence [110, 111]. Also a quantum Otto cycle operating at finite time can go above the bound [112, 113, 114].

Quantum control for boosting quantum heat engines performance

As already mentioned, realistic engines operate at finite time and this is required to get non-zero power output. However, while reducing the duration of the strokes increases the power, it will inevitably lead to the decrease of the efficiency from the ideal one. Indeed, during the compression and expansion strokes, non-adiabatic excitations due to coherence between the energy levels will be created. This will cost additional work that causes a reduction of the net work that can be extracted. This is why coherence is also sometimes called "quantum friction" [115, 116, 117, 118, 119, 120, 121, 122, 123, 124, 125].

A way to reduce the work lost from non-adiabatic driving during the compression and expansion strokes is to use shortcut to adiabaticity (STA) techniques. Shortcuts to adiabaticity refers to strategies that allow to mimic adiabatic dynamics in finite times. Many different approaches in the last two decades have been developed to realize such protocols, making STA techniques a powerful framework for controlling isolated quantum systems [25]. They have been successfully applied to quantum heat engines with many different systems and proved to be an efficient method to boost the power while reducing the friction [126, 127, 128, 129, 130, 131, 132, 133, 134, 135, 136, 137, 138, 139].

Protocols to realize fast thermalization strokes have only recently been explored. One of the main reason the thermal strokes case has been less fruitful than the adiabatic strokes case is because the challenge of accelerating the thermalization of an open quantum system comes with the challenge of describing its dynamics in a practical way for control. However in the last few years some groups were able to come up with interesting approaches to solve the problem such as optimal control [140, 141, 142, 143], linear response theory [144], techniques inspired by STA [145, 146] and reverse engineering [147, 148, 149]. Some of these approaches have been successfully applied to design an optimized quantum Carnot engine [150] or an optimized quantum Otto engine [151, 139], showing that a potential quantum advantage can be achieved. Indeed in [150] the acceleration of the isothermal strokes in the quantum Carnot cycle are guaranteed by the creation of coherence, while in [151] an anti-Zeno like effect was used to accelerate the isochoric strokes in the quantum Otto cycle, by periodically switching on and off the coupling between the system and the bath.

1.3   Dynamics of open quantum systems

1.3.1   Quantum Master Equation

To study a realistic quantum system, we need to take account of the interaction with the environment that can significantly influence the system's behaviour [152]. This is all the more true in the context of thermodynamics. Indeed thermodynamics originally aimed to understand the behavior of heat that is by definition an energy resulting from interacting with an external environment. Thus open quantum systems are the core model for studying quantum thermodynamics and in particular quantum heat engines [153].

A naive and straightforward way to study open quantum systems is to consider the system of interest and the environment as an isolated big system and solve for the dynamics. However in most cases one does not have access to the environment, it is too complicated to describe it, or it is simply irrelevant to get detailed information on it.

To overcome these difficulties, the framework of master equations has been developed [29]. The theory is now well established and has been used in different fields such as quantum optics [154] or condensed matter [155, 156, 157], but still a lot of questions and technical challenges remain like non-Markovian effects [158, 159] or the time-dependency of the system Hamiltonian [160, 161]. In this part I will briefly present and discuss how one can derive the master equation and the approximations needed to use this description.

The von Neumann equation

Let us consider a quantum system S and the environment B respectively described by the Hilbert spaces H_S and H_B, and the dynamics is given by an Hamiltonian H. The total system $S + B$ is then described by a state $|\Psi_{SB}\rangle$ in the Hilbert space $H_S \otimes H_B$. If the total system is in a mixed state, it is more convenient to characterize it with the density matrix

$$\rho_{SB} = |\Psi_{SB}\rangle \langle \Psi_{SB}| . \tag{1.63}$$

The state Ψ_{SB} can be expressed in the basis of the Hilbert space $H_S \otimes H_B$, where the vectors evolve according to the Schrödinger equation. As a consequence, the state of the total system at a time t is given by

$$\rho_{SB}(t) = U(t)\rho_{SB}(0)U^\dagger(t), \tag{1.64}$$

where $U(t)$ is the time evolution operator given by

$$U(t) = T_\leftarrow \exp\left(-\frac{i}{\hbar}\int_0^t H(s)ds\right), \tag{1.65}$$

with $T_\leftarrow$ the time-ordering operator. By differentiating the previous equation, one gets the von Neumann equation,

$$\frac{d}{dt}\rho_{SB}(t) = -\frac{i}{\hbar}[H(t), \rho_{SB}(t)], \tag{1.66}$$

where $[.,.]$ is the commutator between two operators. Sometimes the von Neumann equation is rewritten as,

$$\frac{d}{dt}\rho(t) = L(t)\rho(t), \tag{1.67}$$

where $L(t) = -\frac{i}{\hbar}[\hat{H}(t), .]$ is called a Liouville superoperator.

System-environment model

Now we assume the Hamiltonian of the total system can be written as

$$H = H_S + H_B + H_I, \tag{1.68}$$

where H_S is the Hamiltonian describing the system of interest, H_B describes the environment and H_I describes the interaction between the system and the environment. We usually assume that the interaction part can be written as a sum of products of operators acting re-

spectively on the system and the environment

$$H_I = g \sum_n A_n \otimes B_n, \tag{1.69}$$

where A_n acts on the system, B_n acts on the environment and g is a real number characterizing the strength of the interaction. To derive the master equation, we start from the von Neumann equation (1.67) that can describe the total system. We write the dynamics in the interaction picture

$$\frac{d\tilde{\rho}_{SB}(t)}{dt} = -\frac{i}{\hbar} \left[\tilde{H}_I(t), \tilde{\rho}_{SB}(t) \right], \tag{1.70}$$

where the tilde denotes the operator written in the interaction picture $\tilde{X}(t) = U_S^\dagger(t) U_B^\dagger(t) X U_S(t) U_B(t)$. The interaction picture is a convenient representation to deal with the influence of interaction on the dynamics of a given quantum system. The previous equation can be formally solved

$$\tilde{\rho}_{SB}(t) = \rho_{SB}(0) - \frac{i}{\hbar} \int_0^t \left[\tilde{H}_I(s), \tilde{\rho}_{SB}(s) \right] ds. \tag{1.71}$$

Substituting the solution back to the von Neumann equation and taking the partial trace over the environment gives

$$\frac{d\tilde{\rho}_S}{dt} = -\frac{i}{\hbar} \text{Tr}_B \left(\left[\tilde{H}_I(t), \rho_{SB}(0) \right] \right) - \frac{1}{\hbar^2} \text{Tr}_B \left(\left[\tilde{H}_I(t), \int_0^t \left[\tilde{H}_I(s), \tilde{\rho}_{SB}(s) \right] ds \right] \right), \tag{1.72}$$

where $\rho_S(t) = \text{Tr}_E(\rho_{SB}(t))$ is the density matrix of the system obtained by tracing out the environment. The first term in the right hand side is usually equal to zero or can be put equal to zero by shifting the environment operator B_n without changing the dynamics of the system [29]. After a change of variable $\tau = t - s$ we get

$$\frac{d\tilde{\rho}_S}{dt} = -\frac{1}{\hbar^2} \text{Tr}_B \left(\left[\tilde{H}_I(t), \int_0^t \left[\tilde{H}_I(t - \tau), \tilde{\rho}_{SB}(t - \tau) \right] d\tau \right] \right). \tag{1.73}$$

The Born approximation

Now in order to have a solvable and manipulable master equation, we need to use approximations. The first approximation we use is the Born approximation. For a sufficiently large environment we can assume that its state remains unaffected and that the interaction between the system and the environment is sufficiently small to neglect correlations, so that the total state can be written as $\rho_{SB}(t) \approx \rho_S(t) \otimes \rho_B$. This allows to trace out the degrees of the freedom of the environment in the integral and to expand the commutators without difficulty. After few lines of algebra and assuming the operators A_n and B_n are hermitian we obtain the equation

$$\frac{d\tilde{\rho}_S(t)}{dt} = -\frac{g^2}{\hbar^2} \sum_{k,l} \int_0^t \left(B_{kl}(\tau) \left[\tilde{A}_k(t), \tilde{A}_l(t - \tau) \tilde{\rho}_S(t - \tau) \right] + h.c \right) d\tau, \tag{1.74}$$

where $B_{kl}(\tau) = \text{Tr}_B \left(\tilde{B}_k(\tau) B_l \rho_B \right)$ is the two-point correlation function of the bath.

Markov approximation and Redfield equation

The master equation we have remains difficult to solve because it is non-local in time and thus we need to know all past states of the system to obtain the state at a given time. To deal with this issue, we use the Markov approximation: we assume that the bath two-point correlation function decays rapidly (exponentially or algebraically) with a characteristic time τ_B. Thus this characteristic time has to be small compared to the other characteristic times involved in the dynamics. The other times are the time at which we track the state of the system t and the relaxation time τ_R. The relaxation time characterizes the time at which the transient effects of the interaction on the dynamics are over and is given by the interaction strength $\tau_R \sim g^{-1}$. Thus the Markov approximation can be written as

$$g^{-1} \gg \tau_B, \ \ t \gg \tau_B. \tag{1.75}$$

Since the integral is strongly dominated by the bath two-point correlation function, the Markov approximation allows us to replace $\tilde{\rho}_S(t - \tau)$ by $\tilde{\rho}_S(t)$ and we can extend the upper limit of the integral to infinity

$$\frac{d\tilde{\rho}_S(t)}{dt} = -\frac{g^2}{\hbar^2} \sum_{k,l} \int_0^\infty \left(B_{kl}(\tau) \left[\tilde{A}_k(t), \tilde{A}_l(t - \tau)\tilde{\rho}_S(t) \right] + h.c \right) d\tau. \tag{1.76}$$

This equation is known as the Redfield equation and has been extensively studied to describe relaxation phenomena in quantum systems [162, 163, 29]. While this equation can be solved, its dynamics can lead to states that do not preserve the positivity of the density matrix and which are therefore non-physical [164, 165].

Secular approximation and Lindblad master equation

The non-preserve of the positivity in the Redfield equation (1.76) can be mitigated by writing the master equation in the Lindblad form [166, 167, 168]. To do that we write the operators $\tilde{A}_k(t)$ in the frequency domain by expanding the Hamiltonian of the system in its basis $H_S = \sum_n \varepsilon_n |\epsilon_n\rangle \langle \epsilon_n|$

$$\tilde{A}_k(t) = U_S^\dagger(t) A_k U_S(t) = \sum_\omega A_k(\omega) e^{-i\omega t}, \tag{1.77}$$

where

$$A_k(\omega) = \sum_{\varepsilon_m - \varepsilon_n = \hbar\omega} \langle \varepsilon_n| A_k |\varepsilon_m\rangle |\varepsilon_n\rangle \langle \epsilon_m|. \tag{1.78}$$

By using the fact that the operators are hermitian, we can rewrite the Redfield equation in the frequency domain as

$$\frac{d\tilde{\rho}_S(t)}{dt} = -\frac{g^2}{\hbar^2} \sum_{k,l} \sum_{\omega,\omega'} \left(\Gamma_{kl}(\omega) e^{i(\omega' - \omega)t} \left[A_k^\dagger(\omega'), A_l(\omega)\tilde{\rho}_S(t) \right] + h.c \right), \tag{1.79}$$

where $\Gamma_{kl}(\omega) = \int_0^\infty B_{kl}(\tau)e^{i\omega\tau}d\tau$. Now we proceed to the last approximation: the secular approximation. We neglect the non-secular terms i.e the terms in the sum for which $\omega \neq \omega'$. We can use this approximation by assuming that those non-secular terms oscillate fast enough so that their contributions average to zero. In this case rapid oscillations means $t \gg \min_{\omega \neq \omega'} |\omega - \omega'|$. Since we have the Markov approximation, the secular approximation is consistent as long as $\min_{\omega \neq \omega'} |\omega - \omega'| > \tau_B^{-1}$.

We also introduce the Fourier transform of the correlation function, sometimes called the decay/dephasing rates

$$\gamma_{kl}(\omega) = \int_{-\infty}^\infty B_{kl}(\tau)e^{i\omega\tau}d\tau. \tag{1.80}$$

By using the well known identity $\int_0^\infty e^{i\omega\tau}d\tau = \pi\delta(\omega) + iP(1/\omega)$ where P denotes the Cauchy principal value, we can write

$$\Gamma_{kl}(\omega) = \frac{1}{2}\gamma_{kl}(\omega) + iS_{kl}(\omega), \tag{1.81}$$

where

$$S_{kl}(\omega) = \frac{1}{2\pi}\int_{-\infty}^\infty \gamma_{kl}(\omega')P\left(\frac{1}{\omega - \omega'}\right)d\omega'. \tag{1.82}$$

After using the secular approximation, rearranging the terms in the sum and going back to the Schrödinger picture, we get the Lindblad master equation

$$\frac{d\rho_S}{dt} = -\frac{i}{\hbar}[H_S + H_{LS}] + \frac{g^2}{\hbar^2}\sum_\omega\sum_{kl}\gamma_{kl}(\omega)\left(A_l(\omega)\rho_S(t)A_k - \frac{1}{2}\left\{A_k^\dagger A_l(\omega), \rho_S(t)\right\}\right), \tag{1.83}$$

where $\{.,.\}$ is the anticommutator and H_{LS} is the so called Lamb shift

$$H_{LS} = \frac{g^2}{\hbar}\sum_\omega\sum_{kl}S_{kl}(\omega)A_k^\dagger(\omega)A_l(\omega). \tag{1.84}$$

The Lindblad master equation ensures the positivity of the state as long as the matrix of elements $\gamma_{kl}(\omega)$ is positive [29]. We can see that the master equation is explicitely split into two parts. The first part corresponds to the unitary dynamics with a renormalization given by the Lamb shift, resulting from the coupling with the environment. The second part corresponds to the dissipative dynamics that involves transitions between the eigenstates of the system, characterized by the rates $\gamma_{kl}(\omega)$. Let us also remark that all the information we need to describe the influence of the environment on the system are contained in $\gamma_{kl}(\omega)$ and thus the two-point correlation function.

Kubo-Martin-Schwinger condition and the emergence of the Gibbs state

I finish this section with some remarks on the stationary behavior of the Lindblad master equation (1.83). One of the implicit assumptions we used to derive the master equation is that the environment is in a stationary state of its Hamiltonian and thus the two-point

correlation function satisfies the following invariant property

$$\mathrm{Tr}_B\left(\tilde{B}_k(t+\tau)\tilde{B}_l(t)\right) = \mathrm{Tr}_B\left(\tilde{B}_k(\tau)\tilde{B}_l(0)\right). \tag{1.85}$$

If on top of that, the state of the environment is a Gibbs state $\rho_B = e^{-\beta H_B}/Z_B$ with β the inverse temperature, the point-correlation function satisfies the Kubo-Martin-Schwinger (KMS) condition [29]

$$\mathrm{Tr}_B\left(\tilde{B}_k(\tau)\tilde{B}_l(0)\right) = \mathrm{Tr}_B\left(\tilde{B}_l(0)\tilde{B}_k(\tau+i\hbar\beta)\right). \tag{1.86}$$

We can rewrite it as

$$B_{kl}(\tau) = B_{lk}(-\tau - i\hbar\beta). \tag{1.87}$$

After we use the Fourier transform we get the the KMS condition in the frequency domain

$$\gamma(-\omega)_{kl} = e^{\beta\hbar\omega}\gamma_{lk}(\omega). \tag{1.88}$$

This relation is very similar to the detailed balance in classical stochastic processes. Indeed one can show that if the KMS condition (1.88) is satisfied, then the Gibbs state $\rho_G = e^{-\beta H_S}/Z_S$ is a stationary state of the Lindblad equation (1.83) and thus the system equilibrates. However the KMS condition only ensures that the Gibbs state is stationary but not unique. To be the unique stationary state we need also to introduce the concept of ergodicity (see Ref. [169] for more details).

1.3.2 Dissipative dynamics of harmonic oscillators and Gaussian states

Harmonic oscillator and Gaussian states

The master equation is a great operational framework to study open quantum systems and explore quantum thermodynamics. But as we saw, its derivation requires approximations that restrict the regime at which we can study a given system and dynamics. Also even if we can formulate the assumption in terms of inequalities between different characteristic times, they can be still vague for a given system and they can lack physical motivations.

However some models can be exactly solved due to their convenient and elegant mathematical properties, and allow to explore effects that can be hard to describe with the master equation such as non-Markovianity, strong coupling with the environment, small size of the environment or driving. Among those models, there are the dissipative harmonic oscillator models. In these cases the system consists of a harmonic oscillator coupled to an environment of N oscillators

$$
\begin{aligned}
H_S &= \frac{p^2}{2m} + \frac{1}{2}m\omega_S^2 x^2, \\
H_B &= \sum_{n=1}^{N} \frac{p_n^2}{2m} + \frac{1}{2}m\omega_n^2 x_n^2.
\end{aligned}
\tag{1.89}
$$

A convenient way to describe the total system is to introduce the vector of operators, also

called the symplectic vector [170]

$$X = (x, x_1, \ldots, x_N, p, p_1, \ldots, p_N)^\intercal. \tag{1.90}$$

The commutation relation between the canonical observables can be rewritten as

$$[X_i, X_j] = i\hbar\sigma_{ij}, \tag{1.91}$$

where σ is the symplectic matrix

$$\sigma = \begin{bmatrix} 0 & \mathbb{I}_{N+1} \\ -\mathbb{I}_{N+1} & 0 \end{bmatrix}. \tag{1.92}$$

So far we have described the state with the density matrix ρ. However other operators can be used to describe the state of a quantum system. Instead of considering unitary operators acting on a density matrix, we can represent the dynamics of a quantum system on a symplectic vector space. In that case the quantum state can be represented by a function defined in a phase space. One of those possible functions is the characteristic function defined as [170]

$$\chi_\rho(\xi) = \mathrm{Tr}\left(\rho W(\xi)\right), \tag{1.93}$$

where $\xi \in \mathbb{R}^{2(N+1)}$ and $W(\xi)$ is the Weyl operator

$$W(\xi) = e^{i\xi^\intercal \sigma X}. \tag{1.94}$$

The density matrix is related to the characteristic function through the Fourier-Weyl transform

$$\rho = \frac{1}{(2\pi)^{2(N+1)}} \int \chi_\rho(-\xi) W(\xi) d^{2(N+1)}\xi. \tag{1.95}$$

A convenient property of the harmonic oscillator is that its state is usually Gaussian [171, 170]. A Gaussian state can be simply defined with a Gaussian characteristic function

$$\chi_\rho(\xi) = \chi_\rho(0) e^{-\frac{1}{4}\xi^\intercal C\xi + D^\intercal \xi}, \tag{1.96}$$

where $D \in \mathbb{R}^{2(N+1)}$ is the displacement vector given by the expectation value of the canonical observables $D_i = \mathrm{Tr}(\rho X_i)$ and C is the covariance matrix defined as

$$C_{ij} = \mathrm{Tr}\left(\rho\{X_i, X_j\}\right) - 2\,\mathrm{Tr}\left(\rho X_i\right)\mathrm{Tr}\left(\rho X_j\right). \tag{1.97}$$

We see that a Gaussian state of a many-body system can be fully characterized by a $(2N + 2) * (2N + 2)$ matrix and a vector in $\mathbb{R}^{2*(N+1)}$. Most of the times the displacement vector will be zero and we just need to calculate the covariance matrix i.e. $2(N+1)^2 + N + 1$ real numbers.

An other great property of Gaussian states is that they remain Gaussian under unitary operators given by a quadratic Hamiltonian [170]. This implies that as long as we consider a dynamics described by a quadratic Hamiltonian, which is the case for dissipative harmonic oscillators, we can solve the full system exactly by only time-evolving the covariance matrix. This is a great advantage in terms of computational cost, since we do not need to span the

density matrix of the total system in the Hilbert space that grows exponentially with the number of particles.

Besides having convenient mathematical properties, dissipative harmonic oscillators can be used to describe a variety of physical phenomena. In my work, I focus on two specific models. The first one is the damped harmonic oscillator (DHO). The interaction with the environment is described in the rotating wave approximation [29]

$$H_I = \sum_{n=1}^{N} g_n \left(a b_n^\dagger + a^\dagger b_n \right), \tag{1.98}$$

where g_n is a constant coupling strength between the particle of interest and the n-th oscillator of the environment, a ($a^\dagger$) and b_n ($b_n^\dagger$) are respectively the annihilation (creation) operators of the particle and the n-th oscillator of the bath. This model can describe atomic and opto-mechanical systems, which are also used to explore quantum heat engines [11, 172, 136]. The second model I work with is the quantum Brownian motion (QBM) described by the so called Caldeira-Leggett model (CL) [27, 28]. In this model, the interaction between the particle and the environment is harmonic

$$H_I = -x \sum_{n=1}^{N} \kappa_n x_n. \tag{1.99}$$

Also a counter term is usually added in the total Hamiltonian to cancel out the divergent renormalization of the energy of the particle resulting from the interaction with the environment

$$H_c = x^2 \sum_{n=1}^{N} \frac{\kappa_n^2}{2 m_n \omega_n^2}. \tag{1.100}$$

The CL model is paradigmatic in open quantum systems theory and has been extensively studied to explore dissipation and decoherence in quantum systems [29, 152, 173]. Moreover recently the model attracted additional attention in the field of cold atoms, where it has been used as an interesting framework to describe Bose polaron systems (impurities in a Bosonic gas) [174, 175]. Those systems show to be promising platforms to explore quantum thermodynamics phenomena like heat transport between mesoscopic quantum gases [176] or thermometry [177, 178].

Exact dynamics of Gaussian states

Finally I present briefly how we can exactly track the dynamics of dissipative harmonic oscillators by time-evolving the covariance matrix of the system of interest. The method is based on Ref. [30]. I will consider the example of the quantum Brownian motion with a constant trap frequency but the method can be applied in the presence of driving. The QBM is described, as mentioned earlier, by the CL model

$$H = H_S + H_B + H_I + H_c, \tag{1.101}$$

To obtain the time-evolution of the covariance matrix and describe the dynamics of the system, we derive the Heisenberg equations of motion for the Brownian motion and the bath oscillators.

$$\dot{x}(t) = \frac{i}{\hbar}[H, x(t)] = \frac{p(t)}{m}, \tag{1.102}$$

$$\dot{p}(t) = \frac{i}{\hbar}[H, p(t)] = -m\omega_S^2 x(t) + \sum_{n=1}^{N} \kappa_n x_n(t) - x(t)\sum_{n=1}^{N} \frac{\kappa_n^2}{m_n\omega_n^2}, \tag{1.103}$$

$$\dot{x}_n(t) = \frac{i}{\hbar}[H, x_n(t)] = \frac{p_n(t)}{m_n}, \tag{1.104}$$

$$\dot{p}_n(t) = \frac{i}{\hbar}[H, p_n(t)] = -m_n\omega_n^2 x_n(t) + \kappa_n x(t). \tag{1.105}$$

The equations can be written in matrix form by introducing the symplectic vector

$$\frac{dX(t)}{dt} = MX(t), \tag{1.106}$$

where the matrix M can be defined by blocks

$$M = \begin{bmatrix} 0_{N+1} & \mu \\ \gamma & 0_{N+1} \end{bmatrix}, \tag{1.107}$$

where 0_{N+1} is the null matrix of size $(N+1)^2$, $\mu = \text{diag}(\frac{1}{m}, \frac{1}{m_1}, \ldots, \frac{1}{m_N})$, and the matrix γ reads

$$\gamma = \begin{bmatrix} -m\omega_s^2 - \sum_{n=1}^{N}\frac{\kappa_n^2}{m_n\omega_n^2} & \kappa_1 & \kappa_2 & \ldots & \kappa_N \\ \kappa_1 & -m_1\omega_1^2 & & & \\ \kappa_2 & & -m_2\omega_2^2 & & \\ \vdots & & & \ddots & \\ \kappa_N & & & & -m_N\omega_N^2 \end{bmatrix}. \tag{1.108}$$

The equation (1.106) can be formally solved $X(t) = U(t)X(0)$ with the time-evolution exponential matrix $U(t) = e^{Mt}$. It is then straightforward to show that the evolution of the elements of the covariance matrix are given by

$$C_{ij}(t) = \sum_{k,l=1}^{2N+2} U_{ik}(t)U_{jl}(t)C_{kl}(0). \tag{1.109}$$

In particular one can fully determine the dynamics of the Brownian particle with its corresponding covariances $C_{11}(t)$, $C_{1N+2}(t)$ and $C_{N+2N+2}(t)$. Their expression can be written as

a scalar product

$$C_{11}(t) = \left\langle \tilde{U}_1(t), C(0)\tilde{U}_1(t) \right\rangle, \tag{1.110}$$

$$C_{1N+2}(t) = C_{N+21}(t) = \left\langle \tilde{U}_1(t), C(0)\tilde{U}_{N+2}(t) \right\rangle, \tag{1.111}$$

$$C_{N+2N+2}(t) = \left\langle \tilde{U}_{N+2}(t), C(0)\tilde{U}_{N+2}(t) \right\rangle, \tag{1.112}$$

where $\langle ., . \rangle$ denotes the scalar product, $\tilde{U}_1(t) = (U_{11}(t), U_{12}(t), \dots, U_{12N+2}(t))^\mathsf{T}$ and $\tilde{U}_{N+2}(t) = (U_{N+21}(t), U_{N+22}(t), \dots, U_{N+22N+2}(t))^\mathsf{T}$.

Chapter 2

Quantum engines with few-body cold atomic systems

2.1 Anomalous heat flow between two correlated atoms

2.1.1 Motivation and introduction of the research project

As it has been previously mentioned in subsection 1.2.2, the presence of correlations between two systems at different temperatures can lead to a spontaneous reversal of the heat flow. This mechanism has been theoretically explored with physical systems such as a double two-level system coupled to a bath [179], trapped ions [180] and very recently in a quantum dot coupled to two heat reservoirs [181].

However so far cold atomic systems have not been considered for the study of this intriguing phenomenon, even though they are a promising platform for potential experimental realizations. Also its numerical investigation by the means of exact diagonalization is within reach for a reasonable number of particles [182]. In this research project, I investigate the anomalous heat flow (AHF) in the minimal model of two interacting atoms at different temperatures in a harmonic potential.

The AHF occurs by coupling the two atoms with the contact interaction. I characterize the dynamics by considering different interaction strengths and specific types of correlation. I also mention that the AHF can be adapted to design an atomic quantum fridge with correlation as the resource instead of using two thermal baths. This could pave the way for the exploration of purely quantum cooling devices working with only unitary processes.

2.1.2 Model and dynamics

I consider two particles of equal mass that are initially in a one-dimensional harmonic potential. The corresponding Hamiltonian is

$$H = \sum_{n=1}^{2} H_n = \sum_{n=1}^{2} -\frac{\hbar^2}{2m}\frac{\partial^2}{\partial x_n^2} + \frac{1}{2}m\omega^2 x_n^2. \qquad (2.1)$$

The state of the two particles is described with the density matrix that I denote as ρ. Initially both particles are at different temperatures and correlations between them exist. As

we already saw above, the initial state can be written as

$$\rho(0) = \rho_1(0) \otimes \rho_2(0) + \chi, \tag{2.2}$$

where the reduced density matrix of one particle is obtained by tracing out the other one

$$\rho_i(0) = \mathrm{Tr}_{j \neq i}\left(\rho(0)\right) = \frac{\exp(-\beta_i H_i)}{Z_i}, \tag{2.3}$$

with β_i the inverse temperature and Z_i the partition function, and the correlations have a null trace $\mathrm{Tr}(\chi) = 0$. The particles are put into thermal contact by doing a sudden quench of the Hamiltonian with an interaction term H_I, described by the contact interaction

$$H_I = g\delta(x_1 - x_2). \tag{2.4}$$

The Clausius inequality with the presence of correlations (Eq. (1.48)) was derived by assuming that the interaction preserves the energy of the total system. However the contact interaction does not satisfy this property and therefore the extra energy added by the quench needs to be taken account. This modifies the Clausius inequality as

$$Q_2(\beta_2 - \beta_1) \geq \Delta I + \beta_1 \mathrm{Tr}\left((\rho(t) - \rho(0)) H_I\right), \tag{2.5}$$

where the heat exchange for a single particle is defined as

$$Q_i(t) = \mathrm{Tr}\left((\rho_i(t) - \rho_i(0)) H_i\right), \tag{2.6}$$

and ΔI is the change of mutual information between the two particles during the dynamics. The contribution from the interaction (second term on the right hand side of the inequality (2.5)) gives a positive contribution and thus it can reduce the effect of the AHF. Therefore, one needs to be careful with the amount of energy added by H_I and so with the interaction strength g.

To calculate the quantities of interest, I time-evolve the density matrix of the two-particles $\rho(t)$ whose dynamics is formally given by

$$\rho(t) = \exp\left(-\frac{i}{\hbar}\left(H + H_I\right) t\right) \rho(0) \exp\left(\frac{i}{\hbar}\left(H + H_I\right) t\right). \tag{2.7}$$

The knowledge of the density matrix at any time can thus be obtained by simply calculating the overlaps between the eigenstates of the quench Hamiltonian $H + H_I$ and the vectors of the basis used for writing the initial state of the two particles $\rho(0)$ (in this case, it corresponds to the eigenbasis of the non-interacting Hamiltonian H).

For the initial correlations, I consider two different types. Those correlations are not necessarily possible to be experimentally prepared, however they allow to easily check that the initial state is physical. Indeed, the correlations cannot be arbitrarily chosen but they need to ensure that the density matrix of the two particles is definite positive and describes a
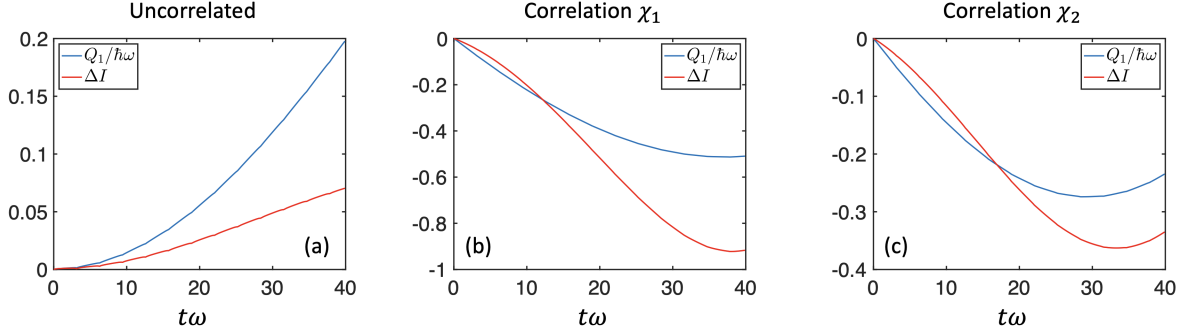
Figure 2.1: Heat of the particle 1, Q_1, and variation of the mutual information between the two particles ΔI as a function of time during the thermal contact. Panel (a) shows the case where the particles are initially uncorrelated. Panel (b) corresponds to the case where $\rho(0) = \rho_1 \otimes \rho_2 + \chi_1$ and the panel (c) shows the case where $\rho(0) = \rho_1 \otimes \rho_2 + \chi_2$.

physical state. The first type of correlations is defined as

$$\chi_1 = \sum_{n=1}^{\infty} \alpha_n \left|0, n\right\rangle \left\langle n, 0\right| + \alpha_n^* \left|n, 0\right\rangle \left\langle 0, n\right|, \tag{2.8}$$

where $\left|n, m\right\rangle$ is a two body state made of the product of single particle states. In this configuration, the ground state of one particle is correlated to the excited states of the other particles. To check the positivity of the density matrix, I calculate the determinant of the density matrix and find a condition on α_n. For this type of correlation, a sufficient condition for the density matrix to be positive is

$$\left|\alpha_n\right|^2 \leq \rho_{n,0}\rho_{0,n}, \tag{2.9}$$

where $\rho_{n,m} = \left\langle n, m\right| \rho_1(0) \otimes \rho_2(0) \left|n, m\right\rangle$. The second type of correlations that I consider is written as

$$\chi_2 = \sum_{n=0}^{\infty} \alpha_n \left|n, n+1\right\rangle \left\langle n+1, n\right| + \alpha_n^* \left|n+1, n\right\rangle \left\langle n, n+1\right|. \tag{2.10}$$

In this case, an eigenstate $\left|n\right\rangle$ of one particle is correlated to the next eigenstate $\left|n+1\right\rangle$ of the other particle. This can be seen as an extension of the Bell state to an infinite discrete spectrum. A sufficient condition for the density matrix to be positive is

$$\left|\alpha_n\right|^2 \leq \rho_{n+1,n}\rho_{n,n+1}. \tag{2.11}$$

From those conditions, we can see that the amount of correlations between the particles are limited by their temperatures. The higher the temperatures of the particles are, the less they can be correlated.

2.1.3 Results

For the simulation of the dynamics, I choose the temperatures of the two particles to be $\beta_1 \hbar\omega = 1$ and $\beta_2 \hbar\omega = 0.5$ and thus the particle 1 is colder than the particle 2. For the initial correlations, I set $\alpha_n = i0.9\rho_{n,0}\rho_{0,n}$ for χ_1 and $\alpha_n = i0.9\rho_{n,n+1}\rho_{n+1,n}$ for χ_2. The figure 2.1 shows the evolution of the heat of the particle 1, Q_1, and the variation of the mutual
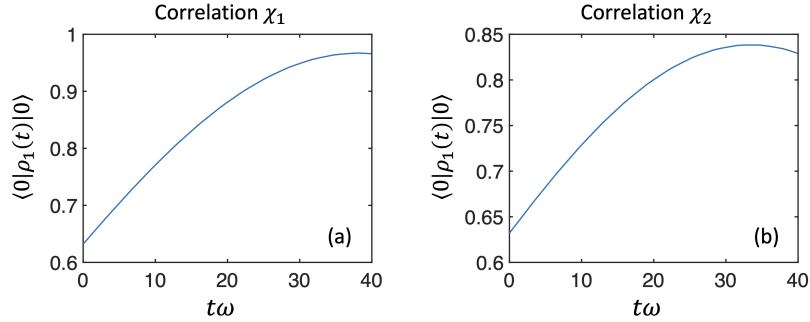
Figure 2.2: Probability of occupying the ground state for the particle 1 during the dynamics. The panel (a) shows the case where $\rho(0) = \rho_1 \otimes \rho_2 + \chi_1$ and panel (b) shows the case where $\rho(0) = \rho_1 \otimes \rho_2 + \chi_2$

information between the two particles as a function of time. For comparison, I also show the case where the two particles are initially uncorrelated (panel (a) in Fig. 2.1).

For the case where the particles are initially uncorrelated, we see that the heat is positive meaning the particle is receiving energy as expected in a conventional heat transport where the flow goes from the higher temperature system to the lowest temperature system. Also we see from the variation of the mutual information that the particles become correlated during the thermal contact.

However for the both cases where the two particles are initially correlated, the heat flow is spontaneously reversed. At the same time, the variation of mutual information is negative showing that both particles are decorrelated due to the thermal contact and this causes the AHF. The dynamics is characterized by an oscillatory behavior. We can see that after some time the heat Q_1 as well as ΔI reach a minimum and then increase.

This behavior is characteristic of the harmonic trap. Due to the equidistant distribution of the eigenenergies of the harmonic oscillator, the dynamical phase of the state of the particles will be pseudo-periodic in the presence of the interaction. The pseudo-period is related to the interaction strength used for the quench. The stronger the interaction is, the faster the oscillations occur. As a consequence, an observable of the system will evolve periodically and never reach a stationary limit. This effect is washed out if one increases the number of particles because the presence of the interaction breaks the integrability for larger systems [183].

Here the interaction strength I use is $g = 0.1\hbar\omega a$ (with $a = \sqrt{\frac{\hbar}{m\omega}}$). This corresponds to a small interaction strength and this explains why the oscillations have a large timescale compared to the typical timescale of the system ω^{-1}. We can also see that the dynamics is faster for the correlation χ_2. This is because the initial state is less correlated and therefore the decorrelation process happens faster. We can also notice that the amount of heat is lower in absolute value for the correlation χ_2 showing that the more correlation we have initially, the more AHF we get.

2.1.4 Proposal for an atomic fridge based on quantum correlations

Interestingly, the AHF can be related to the operation of the fridge (or a heat pump). Indeed in a conventional fridge, a working medium will absorb heat from the cold bath and restore it to the hot bath. In the presented configuration we have a very similar process where heat

is extracted from the cold particle and is restored to the hot particle. The difference is the working medium is replaced by the presence of correlations. Therefore the AHF can lead to the realization of purely quantum refrigerator (or heat pump) cycle at the atomic scale, based on correlations.

The figure 2.2 shows the probability for the particle 1 to occupy the ground state $\langle 0| \rho_1(t) |0\rangle$ as a function of time during the dynamics, for both types of correlations. We can see that in both cases it increases showing that the particle cools down due to the AHF and approaches the ground state. This suggests that a controlled engineering of the interaction strength and the correlations could lead to a quantum fridge that cools a system its ground state.

The cycle can be formulated as follows: we have two particles initially uncorrelated at different temperatures. Then we prepare them in a correlated state given by the density matrix (2.2). In the above presented results, I assume that the particles are already in such a state, and the correlations that I consider are chosen arbitrarily and do not originate from a physical process. However the preparation of the correlated state could be possible with the contact interaction. Indeed, we saw that the contact interaction can create correlations for the case of the conventional heat flow (Fig. 2.1(a)). Therefore an appropriate manipulation of the interaction strength could prepare the desired state.

In particular we could increase the interaction through a Feshbach resonance to the hard-core limit $\frac{g}{\hbar\omega a} \gg 1$ to have two hardcore particles at different temperatures which can give a highly entangled state due to the presence of large spatial correlations in this regime. However one needs to be careful to prevent heat exchanges during the process and for that, one needs to drive the interaction very fast. This is actually very similar to the adiabatic stroke in the classical sense. Once the state is prepared, we put them in thermal contact with a small interaction strength until they are completely decorrelated, then the interaction is turned off and that ends the quantum fridge cycle.

2.1.5 Conclusion and perspectives

In this project, I have studied the AHF in cold atomic systems by considering two particles in a harmonic trap and interacting via the contact interaction. I have shown that the AHF can be predicted in this type of configuration and therefore that cold atomic systems have a great potential to explore this non-intuitive phenomenon. I characterized the dynamics in the case where the two particles are put in thermal contact by quenching the interaction. However I plan to do further investigations in the future by considering more interaction strength regimes and time-dependent protocols such as linear ramps and periodic drivings for a complete analysis.

I have also mentioned that the AHF can be adapted to design a quantum fridge cycle based on correlations. The cycle involves no working medium and heat is absorbed from the cold particle and restored to the hot particle by using correlations as a resource. The proposed cycle can be realized with an appropriate manipulation of the interaction strength, allowing the preparation of the correlated state and the heat exchange to occur between the two particles.

In the future I plan to study the proposed atomic fridge. I will first consider the ideal cycle, where I assume the system is prepared to the desired state at the end of each stroke, and study its performance. In particular I will study how the performance of the fridge is degraded when the temperatures of the two particles increase. Another interesting question

is actually the choice of the appropriate quantity to evaluate the performance of the fridge. In classical fridges, this is evaluated with the coefficient of performance given by the ratio between the heat extracted from the cold bath and the work input. One can use a similar coefficient in the quantum fridge where the work input is the energy used to prepare the correlated state. However an alternate definition could be considered by using the mutual information as the input instead.

I will then study the fridge cycle for finite times. A shortcut to adiabaticity has been derived to prepare two initially non-interacting particles in the Tonks–Girardeau limit by using a variational approach [184]. This could be used to realize the cycle for finite times without reducing significantly the performance of the fridge.

Finally, I plan to extend the work to a larger number of particles to see how the AHF scales with larger systems. A first step will be to consider two particles correlated with two other particles. Also more complicated configurations can be studied by considering imbalanced systems like three cold particles correlated to one hot particle or inversely, one cold particle correlated to three hot particles. Also internal correlations within particles of the same temperature could play a role in the AHF [179], and therefore it could be interesting to also consider this case.

2.2 Interaction-enhanced quantum heat engine

2.2.1 Motivation and introduction of the research project

The study of quantum heat engines (QHEs) has in the past mostly addressed single particle systems [12, 185, 186, 187, 188, 189, 11, 136, 10, 190, 191, 192], however more recently QHEs that use interacting systems have attracted more attention [193, 194, 195, 196]. In particular, it is interesting to understand the effect of the interaction on the performance, and to identify parameter regimes in which cooperative effects due to these interactions allow to outperform single particle QHEs [197, 198, 199, 200, 201, 202]. However, care must be taken as interactions have also been shown to reduce engine performance [203], and the dynamical control of these systems can be more complex leading to the creation of irreversible excitations [197, 204, 137, 135, 138, 205, 184, 206].

In this work I show that a suitable tuning of the interactions can be used to improve the performance of QHEs when compared to systems with non-interacting working media. For this, I consider interacting bosons confined in a harmonic trapping potential and realize the adiabatic compression and expansion strokes of the Otto cycle through increasing and decreasing the trap frequency. However, the interaction is also driven between two distinct values during these strokes and I find that optimal interaction strengths exist that increase the work output and the efficiency when compared to a non-interacting engine.

I also show that the effect of the interaction strongly depends on if one considers distinguishable or indistinguishable particles, and I calculate the efficiency at maximum work output (EMW) showing that the interaction significantly improves this quantity in the low temperature regime. Finally I study the performance of the engine at finite-time and show that it can provide a great boost in the performance compared to the non-interacting case.

2.2.2 Quantum Otto heat engine with driven interaction

I consider a QHE cycle where the working medium (WM) is an interacting quantum gas confined to one dimension and trapped in a harmonic potential. The Hamiltonian is given by

$$H(\omega, g) = \sum_{n=1}^{N} -\frac{\hbar^2}{2m}\frac{\partial^2}{\partial x_n^2} + \frac{1}{2}m\omega^2 x_n^2 + g\sum_{n<p}\delta(x_n - x_p), \qquad (2.12)$$

where m is the mass of the particles and ω is the trap frequency. As mentioned in Sec. 1.1.2, this Hamiltonian can be analytically solved for $N = 2$ [48], however for $N \geq 3$ numerical methods are required to find the eigenstates [207, 182]. The engine cycle I explore is similar to a standard quantum Otto cycle except that the adiabatic strokes occur by changing two parameters: the trap frequency ω and the interaction strength g. A schematic is shown in Fig. 2.3 and the individual strokes are given by

Adiabatic compression $(1 \to 2)$: the WM is initially trapped in a harmonic potential with frequency ω_i and at equilibrium with inverse cold temperature β_c. The interaction strength is given by g_i. From there a compression stroke is carried out that performs work on the system by increasing the trap frequency to ω_f and changing the interaction strength to g_f. The work is given by $W_c = \langle H(\omega_f, g_f)\rangle_2 - \langle H(\omega_i, g_i)\rangle_1$.

Hot isochore $(2 \to 3)$: the next stroke increases the temperature of the WM by coupling it to an external hot bath at the inverse temperature β_h with the control parameters g_f and ω_f fixed. In equilibrium the heat exchanged during this stroke is given by $Q_h = \langle H(\omega_f, g_f)\rangle_3 - \langle H(\omega_f, g_f)\rangle_2$.

Adiabatic expansion $(3 \to 4)$: the system is then decoupled from the hot bath and work is extracted from the WM by adiabatically driving the trap frequency and interaction strength back to ω_i and g_i. The work is given by $W_e = \langle H(\omega_i, g_i)\rangle_4 - \langle H(\omega_f, g_f)\rangle_3$.

Cold isochore $(4 \to 1)$: in the last stroke the WM is cooled down by exchanging heat with a cold bath at the inverse temperature β_c. It returns to the initial state and the heat exchanged during this stroke is given by $Q_c = \langle H(\omega_i, g_i)\rangle_1 - \langle H(\omega_i, g_i)\rangle_4$.

By convention, I choose the variation of energy to be negative when the WM loses energy, which means that the engine produces extractable work when $W = W_c + W_e < 0$. Like in a conventional quantum heat engine, the trap frequency at the end of the compression is larger than the initial frequency, $\omega_f > \omega_i$, however g_f can be larger or smaller than g_i.

2.2.3 Engine performance in the adiabatic limit

Non-interacting limit and influence of the statistics on the performance

Before examining the effects of the interactions in the working medium, let us first consider the non-interacting limit ($g_i = g_f = 0$) in order to outline the influence of the quantum statistical properties on the engine performance. Below I consider distinguishable particles and indistinguishable bosons, where their respective statistics leads to a difference in the
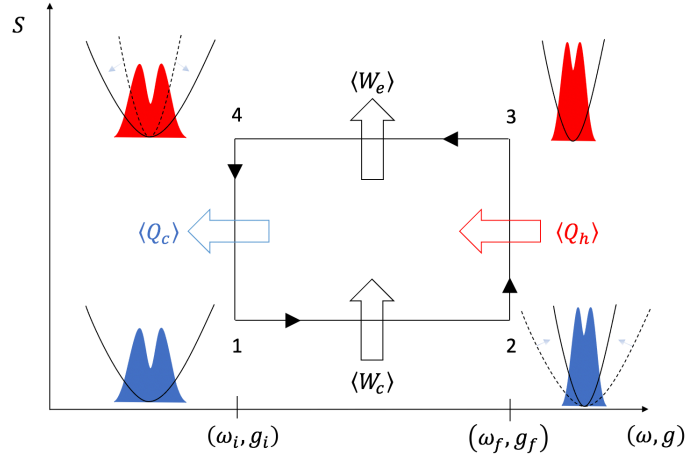
Figure 2.3: Schematic of the heat engine cycle. The y-axis represents the entropy of the WM and the x-axis represent the trap frequency and the interaction. While $\omega_f > \omega_i$, the final interaction strength g_f can be chosen to be lower or greater than g_i.

degeneracy of the energy levels given by

$$
d(E_n) = \sum_{n_1} ... \sum_{n_N} \delta_{E_n, \hbar\omega\left(\sum_{j=1}^N n_j + \frac{1}{2}\right)}, \tag{2.13}
$$

where $\delta_{a,b}$ is the Kronecker symbol. I illustrate this in Fig. 2.4(a)-(b) for two and three particles systems. Unsurprisingly the number of states for a given energy is higher for distinguishable particles. In fact, the difference between these two distributions increases exponentially with the number of particles. The probability for N indistinguishable bosons to be at the same energy is therefore higher than for N distinguishable particles and this increases with the number of particles. In particular, indistinguishable bosons will most likely stay in the ground state and the probability for a boson to transition to an excited state will be small for low temperatures.

As a consequence, the performance of an engine realized with non-interacting bosons will be limited in terms of work output in the temperature regimes of our interest (which corresponds, as we will see later, to the temperature regime where interactions lead to interesting behaviors). The respective work output of the Otto-cycle of non-interacting bosons and distinguishable particles as a function of the number of particles is shown in Fig. 2.4(c). As expected, the work output for distinguishable particles increases linearly and from physical arguments one can expect the work output for bosons to be sub-linear.

However in Fig. 2.4(c), one can see that the behaviour is more than sub-linear and it, in fact, reaches a plateau for $N \geq 3$. This means that the mean occupations of the energies for bosons at the hot and cold temperatures become so similar that adding particles only contributes negligibly to the work output. Given this drastically different behavior in the non-interacting limit, I study both distinguishable particles and indistinguishable bosons in the presence of interactions in the following.
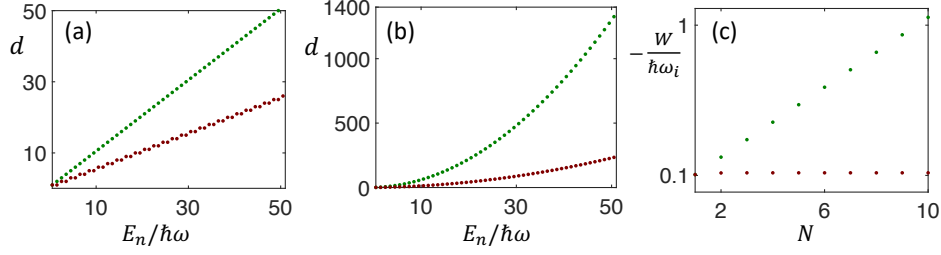
Figure 2.4: Degeneracy of the energy levels for a system of (a) two distinguishable particles (green dots) and two indistinguishable bosons (brown dots) and (b) three distinguishable particles (green dots) and three indistinguishable bosons (brown dots). (c) Work output of the Otto cycle of non-interacting distinguishable particles (green dots) and non-interacting indistinguishable bosons (brown dots) as a function of the number of particles. The compression ratio is $\kappa = \frac{\omega_i}{\omega_f} = \frac{1}{3}$, the cold inverse temperature is $\beta_c = \frac{10}{\hbar\omega_i}$ and the hot inverse temperature is $\beta_h = \frac{1}{\hbar\omega_i}$.

Two particles working medium

I take account of the interaction by first considering the two particle case ($N = 2$). The Hamiltonian is solved by using the analytical solution discussed in Sec.1.1.2. I introduce the center of mass coordinate $X = \frac{x_1 + x_2}{\sqrt{2}}$ and the relative coordinate $x = \frac{x_1 - x_2}{\sqrt{2}}$, which allows to split the Hamiltonian (2.12) into two decoupled single particle Hamiltonians $H(\omega, g) = H_{CM}(\omega) + H_r(\omega, g)$ with

$$H_{CM}(\omega) = -\frac{\hbar^2}{2m}\frac{\partial^2}{\partial X^2} + \frac{1}{2}m\omega^2 X^2, \qquad (2.14)$$

$$H_r(\omega, g) = -\frac{\hbar^2}{2m}\frac{\partial^2}{\partial x^2} + \frac{1}{2}m\omega^2 x^2 + \frac{g}{\sqrt{2}}\delta(x). \qquad (2.15)$$

The eigenenergy of the center of mass is given by $E_{CM}^n = \hbar\omega(n + \frac{1}{2})$. For the relative coordinate, only the even states are affected by the interaction and the corresponding eigenenergy $E_r^{2\nu}$ is obtained by solving the transcendental equation (1.18). The odd eigenstates are again just harmonic oscillator states with the eigenenergies $E_r^{2\nu+1} = \hbar\omega(2\nu + \frac{3}{2})$. To understand how the interaction affects the efficiency, I rewrite the eigenenergies of the relative coordinate as

$$E_r^\nu = \hbar\omega(\nu + 1/2 + \epsilon(\nu, \tilde{g})), \qquad (2.16)$$

where $\epsilon(\nu, \tilde{g})$ is an extra energy term due to the interaction, which depends on the quantum number ν and the rescaled interaction $\tilde{g} = \frac{g}{\sqrt{2}\hbar\omega a}$ (with $a = \sqrt{\frac{\hbar}{m\omega}}$). Since the interaction only affects the even states, we have $\epsilon(2\nu + 1, \tilde{g}) = 0 \,\forall\, \nu$. In the limit of repulsive infinite interactions, fermionization occurs [55] and the even eigenenergies asymptotically approach the next higher lying odd eigenenergies, which leads to $\epsilon(2\nu, +\infty) = 1 \,\forall\, \nu$. It is also worth noting that the contact interaction has the strongest effect on the ground state energy $\epsilon(0, \tilde{g}) \geq \epsilon(2\nu, \tilde{g}) \,\forall\, (\nu, \tilde{g})$.

Two indistinguishable bosons

Here I focus on the case of two indistinguishable bosons, where only the states that preserve even parity can be occupied in the relative coordinate. To calculate the efficiency of the engine, I first express the heat exchanged during the hot and cold isochores as

$$Q_h = \sum_{n,\nu} E^f_{n,2\nu} \left(p^f_{n,2\nu} - p^i_{n,2\nu} \right), \tag{2.17}$$

$$Q_c = \sum_{n,\nu} E^i_{n,2\nu} \left(p^i_{n,2\nu} - p^f_{n,2\nu} \right), \tag{2.18}$$

where $E^s_{n,2\nu} = \langle n, 2\nu | H(\omega_s, g_s) | n, 2\nu \rangle = \hbar\omega_s(n + 2\nu + 1 + \epsilon(2\nu, \tilde{g}_s))$ (with $s \in \{i, f\}$) and the occupation populations are given by $p^i_{n,2\nu} = \langle n, 2\nu | \frac{\exp(-\beta_c H(\omega_i, g_i))}{Z(\omega_i, g_i, \beta_c)} | n, 2\nu \rangle$ and $p^f_{n,2\nu} = \langle n, 2\nu | \frac{\exp(-\beta_h H(\omega_f, g_f))}{Z(\omega_f, g_f, \beta_h)} | n, 2\nu \rangle$ (where $Z(\omega, g, \beta) = \text{Tr}\left[\exp\left(-\beta H(\omega, g) \right) \right]$ is the partition function). From this, the efficiency can be expressed as

$$\eta = 1 + \frac{Q_c}{Q_h} = 1 - \frac{\sum_{n,\nu} \lambda_{n,2\nu} E^f_{n,2\nu} \left(p^f_{n,2\nu} - p^i_{n,2\nu} \right)}{\sum_{n,\nu} E^f_{n,2\nu} \left(p^f_{n,2\nu} - p^i_{n,2\nu} \right)}, \tag{2.19}$$

where I have introduced $\lambda_{n,2\nu}$ as the ratio between the eigenenergies before and after the compression [203]

$$\lambda_{n,2\nu} = \frac{E^i_{n,2\nu}}{E^f_{n,2\nu}} = \kappa \frac{n + 2\nu + 1 + \epsilon(2\nu, \tilde{g}_i)}{n + 2\nu + 1 + \epsilon(2\nu, \tilde{g}_f)}, \tag{2.20}$$

with $\kappa = \frac{\omega_i}{\omega_f}$ being the compression ratio. From Eq. (2.19) one can see that the efficiency is influenced by the interaction through the ratio $\lambda_{n,2\nu}$, and the change of population occupation $p^f_{n,2\nu} - p^i_{n,2\nu}$. Let us recall that the eigenstates of the harmonic oscillator for two different frequencies ω_i and ω_f are related by the scaling transformation $\langle x | n(\omega_f) \rangle = \kappa^{-\frac{1}{4}} \left\langle x\kappa^{-\frac{1}{2}} \middle| n(\omega_i) \right\rangle$. Also the contact interaction described by a delta function obeys the scaling law $g\delta(\lambda x) = \frac{g}{\lambda}\delta(x)$. As a consequence, if one chooses the final interaction to be $g_f = g_i\kappa^{-\frac{1}{2}}$ (and so $\tilde{g}_f = \tilde{g}_i$), then the system will remain scale-invariant, and all eigenenergies change by the same ratio given by κ, i. e.

$$E^i_{n,2\nu} = \kappa E^f_{n,2\nu} \; \forall(n, \nu). \tag{2.21}$$

In this case the efficiency is given by the Otto efficiency $\eta_O = 1 - \kappa$. This is illustrated in Fig. 2.5(a), where the ratio between η and η_O is plotted as a function of $\epsilon(0, \tilde{g}_i)$ and $\epsilon(0, \tilde{g}_f)$ and the diagonal corresponds to the case where the WM is scale-invariant. To obtain an efficiency that differs from η_O, one therefore needs to consider systems where the eigenenergies do not change uniformly during the adiabatic strokes [208]. To do that, I tune the initial and final interactions such that $g_f \neq g_i\kappa^{-\frac{1}{2}}$, which allows one to distinguish two possible cases.

The first case is when the interaction weakens during the compression stroke ($\tilde{g}_i > \tilde{g}_f$), which leads to $\epsilon(2\nu, \tilde{g}_f) < \epsilon(2\nu, \tilde{g}_i)$ and $\lambda_{n,2\nu} > \kappa$ (the region above the diagonal in Fig. 2.5(a)). One then needs to be careful with the sign of the change of the occupation
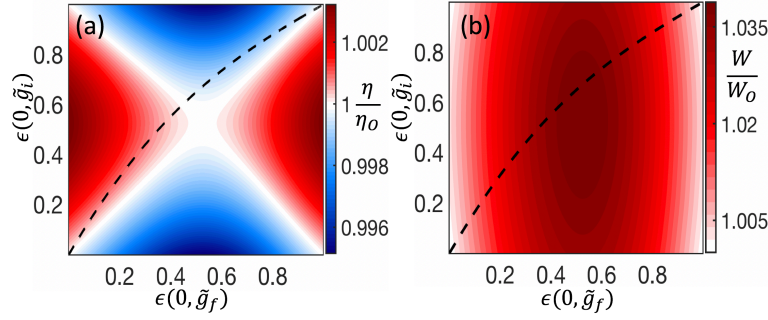
Figure 2.5: (a) Efficiency and (b) work output normalised to their respective Otto-cycle values for an engine with a WM made of two interacting bosons as a function of $\epsilon(0, \tilde{g}_i)$ and $\epsilon(0, \tilde{g}_f)$. The black dash line shows the situation where the interaction is fixed ($g_i = g_f$). Note that the efficiency converges to η_O in the limit of strong interactions due to the fermionization in the system. In both plots the compression ratio is $\kappa = \frac{1}{3}$ ($\eta_O = \frac{2}{3}$), the cold inverse temperature is $\beta_c = \frac{10}{\hbar\omega_i}$ and the hot inverse temperature is $\beta_h = \frac{1}{\hbar\omega_i}$.

population $p^f_{n,2\nu} - p^i_{n,2\nu}$. For the excited states, the sign will be positive since at higher temperatures, the occupation population in the excited states increases. However the change of population for the ground state will be negative since it decreases for higher temperatures. Thus, depending on which terms have the largest contribution, the efficiency can be higher or lower than η_O.

When the interactions affect the ground state more than the excited states, the change of the occupation population of the ground state is thus more important and we get $\eta > \eta_O$ (red area above the diagonal in Fig. 2.5(a)). However, when the interactions are such that the extra energy $\epsilon(2\nu, \tilde{g})$ affects significantly the excited states, the change of the occupation population for the excited states can be large enough that $\eta < \eta_O$ (blue area above the diagonal in Fig. 2.5(a)). The situation where the interaction is fixed $g_i = g_f$ is also indicated (black dashed line in Fig. 2.5(a)), which is similar to the situation studied in [203]. In their case the WM is an interacting gas trapped in a box and the efficiency only decreases in the presence of the interaction. For the harmonic oscillator, however, we observe that the interaction can enhance or hinder the performance of the engine.

The second case is when the interaction strength increases during the compression stroke ($\tilde{g}_f > \tilde{g}_i$). This implies that $\epsilon(2\nu, \tilde{g}_f) > \epsilon(2\nu, \tilde{g}_i)$ and $\lambda_{n,2\nu} < \kappa$. By doing the same analysis as above, the opposite conclusion to the first case can be reached: if the interactions affect the ground state more we get $\eta < \eta_O$ (blue area below the diagonal in Fig. 2.5(a)), and if the interactions affect the excited states sufficiently we find $\eta > \eta_O$ (red area below the diagonal in Fig. 2.5(a)). The area near the anti-diagonal is highlighted in Fig. 2.5(a), where the efficiency is equal to η_O. This area is not exactly the anti-diagonal and corresponds to a crossover between the regime where $\eta > \eta_O$ and $\eta < \eta_O$ in which the contribution from the ground state and the excited states are such that they compensate each other and one recovers the Otto efficiency.

The maximum efficiency shown in Fig. 2.5(a) is $\eta \approx 1.003\eta_0$ and achieved for $\tilde{g}_i = 1.6$ and $\tilde{g}_f = 50$ ($\epsilon(0, \tilde{g}_i) \approx 0.52$ and $\epsilon(0, \tilde{g}_f) \approx 0.98$). One can see from the work output shown in panel (b) that the engine outperforms the Otto cycle of two non-interacting bosons when the final interaction takes intermediate values, and the initial interaction does not seem to influence the work output significantly. This plot also shows that the work output always

exceeds W_O and becomes equal to it when the initial and final interaction are zero or go to infinity (the four corners in Fig. 2.5(b)). In the infinite interaction regime this is due to the system behaving like two non-interacting fermions. The maximum work output is $W \approx 1.039 W_O$ for $\tilde{g}_i = \tilde{g}_f = 1.6$.

Two distinguishable particles

While driving the interaction during the cycle can clearly modify the performance of the engine, the changes observed above for a working medium made from two identical bosons are not very significant and the performance of the engine stays relatively close to its non-interacting counterpart. Next I therefore consider the situation where the working medium consists of two distinguishable particles, for which two major differences come into play: first, as shown above, the degeneracy of the states is different in the non-interacting limit, and, second, for such a system the odd states of the energy spectrum of the relative coordinate need to be taken into account.

The efficiency and work output for this engine are shown as a function of the interaction energies in Figs. 2.6(a)-(b). Like for indistinguishable particles, the diagonal represents the scale-invariant cycle and therefore retains the Otto efficiency. The Otto efficiency is exceeded for $\epsilon(0, \tilde{g}_i) > \epsilon(0, \tilde{g}_f)$. Indeed, we note that interactions can noticeably improve the performance of the distinguishable cycle (note the difference in the colour scale) with the maximum efficiency $\eta \approx 1.124 \eta_O \approx 0.75$ for $\tilde{g}_i = 3$ and $\tilde{g}_f = 0.8$ ($\epsilon(0, \tilde{g}_i) \approx 0.69$ and $\epsilon(0, \tilde{g}_f) \approx 0.34$), and maximum work $W \approx 1.43 W_O$ for $\tilde{g}_i = 1.95$ and $\tilde{g}_f = 1.4$ ($\epsilon(0, \tilde{g}_i) \approx 0.58$ and $\epsilon(0, \tilde{g}_f) \approx 0.48$). In contrast to indistinguishable bosons the efficiency is always reduced when the final interaction is larger than the initial one, $\tilde{g}_f > \tilde{g}_i$. Furthermore, the work output can be significantly lower than for a cycle with non-interacting particles, and we note that the WM can act as a dissipator ($W > 0$) for combinations of strong and weak interactions, ($\tilde{g}_i \approx 0, \tilde{g}_f \to \infty$) and ($\tilde{g}_i \to \infty, \tilde{g}_f \approx 0$), indicated by the grey regions in Figs.2.6(a)-(b). I have also calculated the efficiency for higher temperatures and have observed the same general behavior, however, the variations of the efficiency and the work output become less pronounced.

To illustrate and better understand the behaviour of the QHE with distinguishable particles, I also calculate the efficiency as a function of the initial interaction $\tilde{g}_i$ while tuning the final interaction such that $\tilde{g}_f = \alpha \tilde{g}_i$, with α fixed. Fig. 2.6(c) shows the efficiency for three different values of α ($\alpha = 1, 3$ and $\frac{1}{3}$) and one can clearly see that the changes in the efficiency are more significant and also very different from the setting using indistinguishable particles. The efficiency can be enhanced when $\tilde{g}_f < \tilde{g}_i$, while it is significantly reduced when $\tilde{g}_f > \tilde{g}_i$.

To understand this, I consider the amount of heat exchanged with the hot and cold baths as shown in Fig. 2.6(d,e). In Fig. 2.6(d) we see that the presence of the interaction increases the amount of heat received by the hot bath in all three cases, for weak and intermediate values of $\tilde{g}_i$. However it decreases for large $\tilde{g}_i$ and reaches a limit that is approximately half of the non-interacting working medium. In this limit the even eigenstates in the relative coordinate approach the next higher-lying odd eigenstates and thus the spectrum becomes doubly degenerated for distinguishable particles which implies less heat is required for the WM to thermalize.

We observe similar behavior for Q_c in the large $\tilde{g}_i$ limit (Fig. 2.6(e)), however for weak
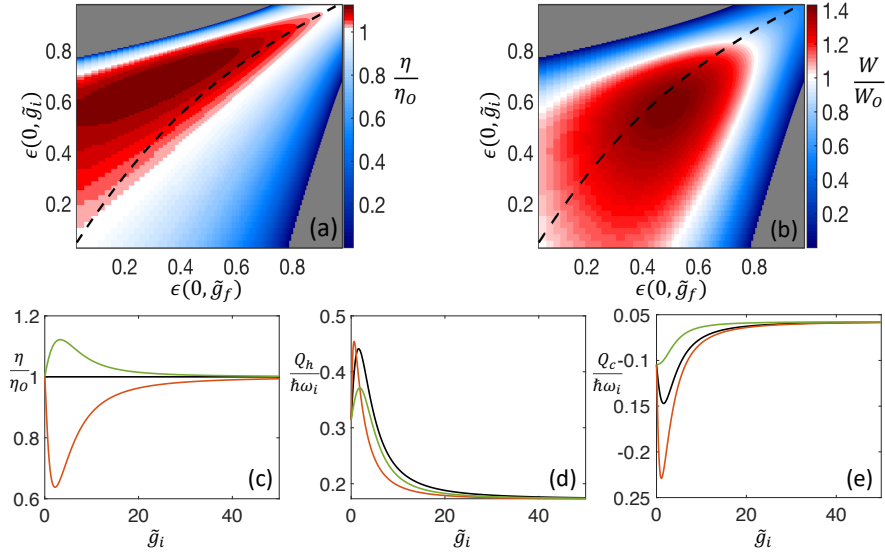
Figure 2.6: (a) Efficiency and (b) work output normalised to their respective Otto-cycle values for an engine with a WM made of two interacting distinguishable particles as a function of $\epsilon(0, \tilde{g}_i)$ and $\epsilon(0, \tilde{g}_f)$. The gray areas correspond to interaction regimes where the system does not work as a heat engine but rather like a dissipator with $W > 0$. The black dashed line shows the case where the interaction is fixed ($g_i = g_f$). (c) Efficiency normalized to the Otto efficiency and heat exchanged with the (d) hot bath and (e) cold bath as a function of the initial interaction $\tilde{g}_i$, with the final interaction given by $\tilde{g}_f = \tilde{g}_i$ (black line), $\tilde{g}_f = \frac{\tilde{g}_i}{3}$ (green line) and $\tilde{g}_f = 3\tilde{g}_i$ (orange line). The compression ratio for all plots is $\kappa = \frac{1}{3}$ ($\eta_O = \frac{2}{3}$), the cold inverse temperature is $\beta_c = \frac{10}{\hbar\omega_i}$ and the hot inverse temperature is $\beta_h = \frac{1}{\hbar\omega_i}$.

and intermediate values of $\tilde{g}_i$ the amount of heat dissipated in the cold bath is significantly larger when $\tilde{g}_f = 3\tilde{g}_i$, which is the reason for the decreasing efficiency. For the same initial interaction $\tilde{g}_i$ the best strategy to reduce energy loss in the cold bath is therefore to choose a weaker final interaction $\tilde{g}_f$. This allows the statistics at the inverse temperature β_h to be closer to the initial statistics of the WM and thus the change of the occupation population $p^i_{n,\nu} - p^f_{n,\nu}$ becomes smaller in magnitude such that less heat is released during the cold isochore. The changes in the performance of the QHE are more extreme when the baths are at low temperatures because the WM is more affected by finite interactions.

I also look at the efficiency at maximum work output (EMW). It was calculated by maximizing the work output over κ, $\tilde{g}_i$ and $\tilde{g}_f$ for two fixed cold bath temperatures $\beta_c\hbar\omega_i = 1$ and $\beta_c\hbar\omega_i = 10$ (see Fig. 2.7). I also compare the EMW of both engines, with distinguishable and indistinguishable interacting working media, with their non-interacting counterparts in the low temperature regime $\beta_c\hbar\omega_i = 10$ in Fig. 2.7(a). One can see that for the non-interacting engines, this quantity is far below the CA bound, which is due to the fact that at low temperature the WM dissipates a large amount of energy into the cold bath in order to close the cycle. At the same time the efficiency for non-interacting bosons is the lowest as its statistics makes low energy states more favorable than in the distinguishable case. The EMW of the interacting bosons is extremely close to that of non-interacting bosons, which is not surprising since the influence of the interaction on the engine performance is very small (as seen in Fig. 2.5).

However for the two distinguishable particles, it is vastly improved by the presence of the interaction and even coincides with the CA bound for $\beta_h/\beta_c \gtrsim 0.5$. One can see that

the gap between the efficiency of bosons and distinguishable particles decreases when the temperature of the hot bath is large, $\beta_h/\beta_c \to 0$, as their statistics become identical and are given by the classical Maxwell-Boltzmann distribution. Also the energy scales of the hot bath dwarf that of the cold bath and therefore the influence of the initial interaction $\tilde{g}_i$ becomes negligible.

This is highlighted in the inset of Fig. 2.7(a) where the corresponding extra energy $\epsilon(0, \tilde{g}_i)$ and $\epsilon(0, \tilde{g}_f)$ for the case of two distinguishable particles is shown. As expected from the previous analysis, the final interaction $\tilde{g}_f$ has to be smaller than $\tilde{g}_i$ in order to improve the performance of the engine. The optimal final interaction $\tilde{g}_f$ decreases when the temperature of the hot bath increases and becomes zero for $\beta_h/\beta_c \lesssim 0.08$. As already mentioned, the work output in the high temperature limit is mostly dictated by the energy of the WM at the inverse temperature β_h. Therefore the influence of the interaction becomes negligible since the particles behave like non-interacting classical particles with an energy approximately given by β_h^{-1}.

Moreover, from the preceding analysis, we know that the work output is significantly improved for non-zero and finite interaction strengths (Fig. 2.6(b)) and we can thus conclude that the interactions start to influence the performance of the engine for $\beta_h/\beta_c \gtrsim 0.08$. We can also observe this in the efficiencies of the different cycles which start to deviate from each other at around this temperature (see Fig. 2.7(a)).

When $\beta_h/\beta_c \to 1$ both $\tilde{g}_i$ and $\tilde{g}_f$ tend to the same limit in which the cycle is scale invariant. Let us note that slight irregularities can be seen for the behavior of $\epsilon(0, g_f)$ in the inset of Fig. 2.7(a) when $\beta_h/\beta_c \gtrsim 0.8$. This is due to numerical issues, as the optimization algorithm has difficulties in finding the maximum work output when the temperatures of both baths are close, and therefore the work output starts to vanish. Regardless, in this regime the efficiencies of each cycle converge to the Curzon-Ahlborn bound as expected. Finally, I show that for a larger temperature of the cold bath $\beta_c \hbar \omega_i = 1$, the EMW for both working media are exactly equal to η_{CA} (see Fig. 2.7(b)). In this temperature regime, the effect of the short-range interaction becomes negligible and the particles behave like a non-interacting ideal and classical gas.

Three particles working medium

In order to show how the influence of the interaction on the engine performance scales with the number of particles, I extend the analysis to a three particle system. In that case the Hamiltonian can no longer be analytically solved and a numerical method such as exact diagonalization is required to calculate the quantities of interest. To compare with the two particle engines, I consider equivalent temperatures and compression ratios, and also define the interaction energy $\epsilon_{3P}(n, \tilde{g})$ in a similar way. With n being the quantum index that characterizes the n-th three particle eigenstate, the ground state interaction energy term is given by

$$\epsilon_{3P}(0, \tilde{g}) = \frac{\langle 0 | H(\omega, g) | 0 \rangle}{\hbar \omega} - \frac{3}{2}. \tag{2.22}$$

This excess energy is such that $\epsilon_{3P}(0, 0) = 0$ and $\epsilon_{3P}(0, +\infty) = 3$ and again allows us to quantify the interaction strength in the system. In Fig. 2.8 the efficiency and work output for both indistinguishable and distinguishable particles is shown. We note that the optimal interactions needed for maximizing the performance do not significantly change
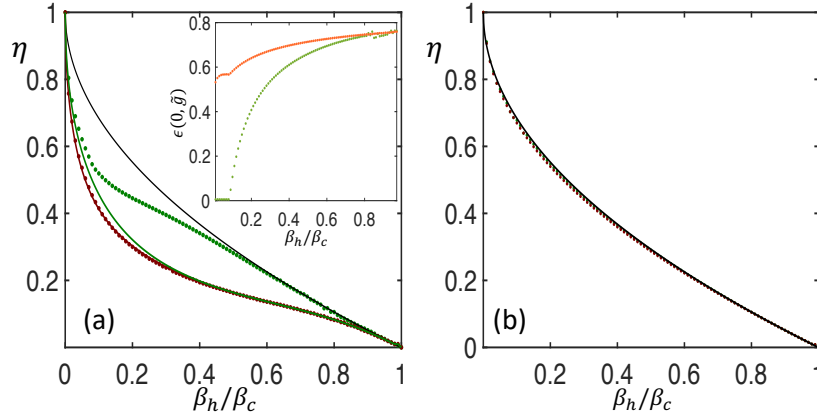
Figure 2.7: Efficiency at maximum work output (EMW) for the engine using two interacting bosons (brown dots) and two interacting distinguishable particles (green dots) for two different temperature regimes. Panel (a) shows the efficiency calculated in the low temperature regime with $\beta_c \hbar \omega_i = 10$ and panel (b) in the intermediate temperature regime with $\beta_c \hbar \omega_i = 1$. In both panels the back line corresponds to the Curzon-Ahlborn bound η_{CA}. The inset in panel (a) shows the corresponding extra energies $\epsilon(0, \tilde{g}_i)$ (orange dots) and $\epsilon(0, \tilde{g}_f)$ (green dots) for the case of two distinguishable particles. The values of $\epsilon(0, g_f)$ we obtained for $\beta_h/\beta_c \gtrsim 0.8$ become less accurate because the work output starts to vanish in this regime. We also show the efficiency at maximum work output of two non-interacting distinguishable particles (green line) and two non-interacting bosons (brown line) at the low temperature regime (a). Note the EMW for two interacting bosons is extremely close to that of the two non-interacting bosons.

compared to the two particle case, however, the degree of enhancement is marginally increased, with a gain of 0.1% for the maximum efficiency ($\eta \approx 1.004\eta_O \approx 0.668$ for $\epsilon_{3P}(0, \tilde{g}_i) \approx 1.64$ and $\epsilon_{3P}(0, \tilde{g}_f) \approx 2.96$) and 1.1% for the work output ($W \approx 1.05W_O$ for $\epsilon_{3P}(0, \tilde{g}_i) = \epsilon_{3P}(0, \tilde{g}_f) \approx 1.64$).

However, the engine using a WM of distinguishable particles shows a more significant enhancement of the performance as the number of states that are not affected by the interaction is much larger than in the two particle case (see Fig. 2.4(a)-(b)) allowing for a more efficient work extraction process. The resulting maximum efficiency and work output, $\eta \approx 1.21\eta_O \approx 0.807$ for $\epsilon_{3P}(0, \tilde{g}_i) \approx 2.48$ and $\epsilon_{3P}(0, \tilde{g}_f = 0.8) \approx 1.49$ and $W \approx 1.59W_O$ for $\epsilon_{3P}(0, \tilde{g}_i) \approx 1.73$ and $\epsilon_{3P}(0, \tilde{g}_f) \approx 1.49$, allowing for gains of 8.6% and 16% respectively over the distinguishable two particle engine. This highlights the important role the density of states plays in the performance.

Finally, the EMW is shown in in Fig. 2.9, together with the case of two distinguishable particles. While the EMWs for the engines with indistinguishable particles are very similar, one can note a slight enhancement of the efficiency for the WM made from indistinguishable particles in the intermediate temperature regime.

2.2.4 Finite time dynamics

So far the performance of the engine has been studied in the adiabatic limit which results, as discussed in Sec. 1.2.3, in a vanishing power output due to the long time-scale of the strokes. Also decreasing the duration of the strokes will decrease the efficiency due irreversibility and inner friction [115, 116, 117, 118, 119, 120, 121, 122, 123, 124, 125]. In order to understand the trade-off between the power and the efficiency of the engine, I next study the compression
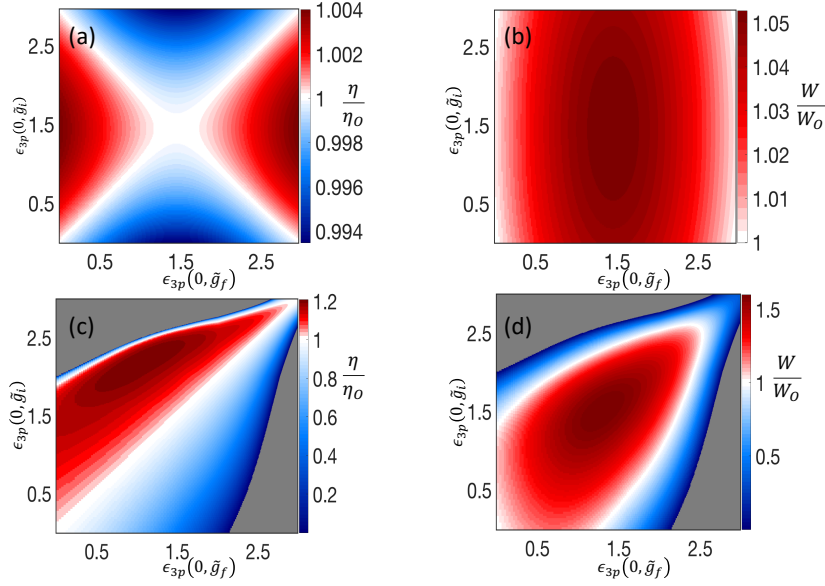
Figure 2.8: Efficiency and work output normalised to their respective Otto values as a function of $\epsilon_{3P}(0, \tilde{g}_i)$ and $\epsilon_{3P}(0, \tilde{g}_f)$ for a WM consisting of (a)-(b) three indistinguishable bosons and (c)-(d) three distinguishable particles.

and expansion strokes at finite-time for an engine made from two distinguishable particles.

For this I consider three cases. First, the interaction is changed between two values that are known to give a boost to the efficiency and work output in the adiabatic limit (the optimal case), and second the interaction is driven in such a way that the WM remains scale-invariant, for which the efficiency in the adiabatic limit is given by η_O. As a third case, I consider two non-interacting particles in order to benchmark my results.

As the focus is on the non-adiabatic excitation during the compression and expansion strokes, I do not consider the dynamics of the isochoric strokes. The duration τ of the compression and expansion stokes are taken to be same and for the optimal case the ramps for the time-dependent protocols for the trap and interaction strengths are given by

$$ f(t) = f(0) + 10\Delta f \left(\frac{t}{\tau}\right)^3 - 15\Delta f \left(\frac{t}{\tau}\right)^4 + 6\Delta f \left(\frac{t}{\tau}\right)^5, \qquad (2.23) $$

where $\Delta f = f(\tau) - f(0)$ for $f = \{g, \omega\}$. In the case of scale-invariant dynamics the interaction strength is connected to the trap frequency through $g(t) = g(0)\sqrt{\frac{\omega(t)}{\omega(0)}}$ and we choose $\omega(t)$ to be given by Eq. (2.23). To quantify the performance of the engine at finite-time, I calculate the efficiency η and also a quantity that I call the effective power (EP) of the engine defined as

$$ P(\tau) = -\frac{W(\tau)}{2\tau}. \qquad (2.24) $$

While, the latter does not strictly correspond to the power of the engine since I only consider the total duration of the compression and expansion strokes 2τ, I always assume that the WM fully thermalizes during the isochoric stokes for a short fixed time. The EP then tells us how the power of the engine is affected by non-adiabatic excitations created during the work strokes, and if the duration of the isochoric stokes is short enough, it corresponds to the first
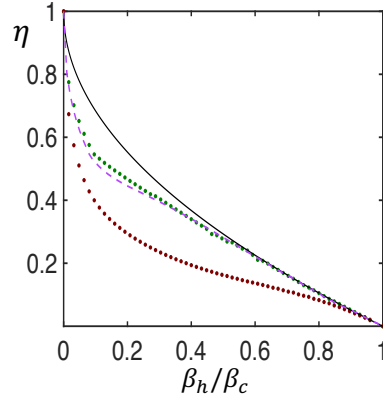
Figure 2.9: Efficiency at maximum work output for three interacting bosons (brown dots) and three distinguishable particles (green dots) in the low temperature regime $\beta_c \hbar \omega_i = 10$. The black line corresponds to the Curzon-Ahlborn bound η_{CA} and the purple dashed line shows the two distinguishable interacting particles case.

approximation of the engine power. Finally I also quantify the irreversibility of the cycle by calculating the irreversible work

$$W_{irr}(\tau) = W(\tau) - W_{ad}, \tag{2.25}$$

where W_{ad} is the work output of the engine in the adiabatic limit. The irreversible work allows to quantify the excess energy generated by non-adiabatic excitations in the WM that leads to an additional cost in the work extraction process. The irreversibility generated during the process can also be related to the relative entropy between the state of the WM and the adiabatic state [209, 210]

$$W_{irr}(\tau) = \beta^{-1} S(\rho(\tau) || \rho_{ad}), \tag{2.26}$$

where β denotes the inverse temperature of the initial state of the WM.

The EP, the irreversible work and the efficiency as functions of τ are shown in Fig. 2.10. Compared to the non-interacting case, using an interacting system in a cycle of finite duration provides a significant boost to the power in both the optimal case and the scale-invariant case. Moreover, one can see that the EP in the optimal case is larger than in the scale-invariant case for longer stroke durations, which is due to the work output being larger in the adiabatic limit. However for fast strokes the EP for the scale-invariant case becomes larger and the maximum value is reached at a shorter time than in the optimal case.

While this is a small effect, it is consistent with the greater amount of irreversible work being generated in the optimal case (see Fig. 2.10(b)). This can also be seen from the fact that even if the efficiency in the adiabatic limit in the optimal case is greater, it decreases faster for shorter times than in the scale-invariant case (see Fig. 2.10(c)). Finally, one can note that the irreversible work generated by driving the interaction in the scale-invariant case is not very significant and therefore the efficiency in this case stays relatively close to the efficiency of the non-interacting case, even for short times.
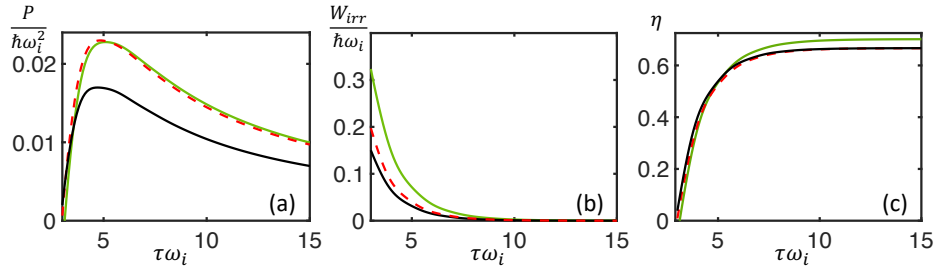
Figure 2.10: (a) Effective power output (EP), (b) irreversible work and (c) efficiency as a function of τ. The green line corresponds to the optimal case, the red dashed line corresponds to the scale-invariant case and the black line to the non-interacting case. The compression ratio is $\kappa = \frac{1}{3}$, the cold inverse temperature is $\beta_c = \frac{10}{\hbar \omega_i}$ and the hot inverse temperature is $\beta_h = \frac{1}{\hbar \omega_f}$. For the optimal case the interactions are $\tilde{g}_i = 1.95$ and $\tilde{g}_f = 1.4$ such that the efficiency in the adiabatic limit is $\eta \approx 0.7$, and for the scale-invariant case the interactions are $\tilde{g}_i = \tilde{g}_f = 1.95$.

2.2.5 Conclusion and perspectives

I have proposed and studied a quantum Otto engine where the interaction is driven with the trapping parameter of the system (here the trap frequency). I have shown that the presence of interactions can modify the performance of the engine compared to the non-interacting case. This change can be explained by two reasons: the first is that the interaction does not have the same effect on all eigenstates and therefore the eigenenergies do not change uniformly during the adiabatic strokes. This is in contrast to models where the energy shift due to the interactions is the same for all states, such as the Calogero-Sutherland model, and which do not diverge from the Otto efficiency in the adiabatic limit [196, 193]. The second reason is that the interaction affects the energy distribution which allows, for example, to lose less energy during the cold isochore.

The interaction has however only a very small effect in the case of indistinguishable bosons, while it can significantly modify the engine performance for distinguishable particles due to the presence of odd eigenstates that are not affected by the interaction. While the tiny influence of the interaction in the indistinguishable case would be extremely difficult to experimentally observe, the significant improvement obtained in the distinguishable case can be expected to be experimentally measurable. Furthermore, the interactions mostly matter at low temperatures, and increasing the number of particles does not seem to modify the influence of the interaction on the engine performance. In fact, the latter continues to enhance the work output and the efficiency in the case of distinguishable particles.

I have also shown that using an interacting system in a finite time cycle is advantageous in terms of power. The irreversibility generated by driving the interaction stays marginal and the advantageous properties of the interaction in the adibatic limit remain at finite-time. Therefore this research project shows the potential for developing QHEs that possess multiple control parameters which can be changed during the work strokes.

A number of interesting questions immediately emerge from this work. While I have only considered repulsive interactions, attractive interactions could potentially also lead to even higher efficiencies. Considering long range interactions within the working medium [211] could lead to engines that show different behaviour at higher temperatures. Finding a shortcut to adiabaticity to optimize the performance of the engine at finite-time could also be an interesting follow up to this project in the future.

Chapter 3

Controlling open quantum systems for boosting engines

3.1 An effective closed dynamics description of the quantum Brownian motion and shortcuts to equilibration

3.1.1 Motivation and introduction of the research project

As it has been mentioned in Sec. 1.2.3, getting control over the dynamics of open quantum systems is extremely relevant to accelerate the thermal strokes during a cycle and therefore, to improve both efficiency and power of quantum heat engines. Even beyond the scope of quantum thermodynamics and quantum engines, understanding and controlling open quantum systems is a major challenge for the exploration of quantum phenomena in the presence of dissipative effects, the deterministic preparation of quantum states, and the development of quantum devices [212, 213, 214, 215].

While recently some interesting works have been reported in that direction, the acceleration of the adiabatic strokes has been very fruitful thanks to the large toolbox provided by shortcuts to adiabaticity (STA) [25]. Such a powerful framework could be also effective in the case of thermal strokes if one can find a way to apply it to open quantum systems.

A shortcut to equilibration (STE) for an open quantum system has been realized by using the counter-diabatic driving, a well known method for STAs, in Ref. [146]. The counter-diabatic driving consists of adding an auxiliary time-dependent Hamiltonian $H_1(t)$ to the reference Hamiltonian of the system $H_0(t)$. The method assumes that the eigenstates of the Hamiltonian $H_0(t)$ can be controlled with the auxiliary Hamiltonian. The dynamics is given by $H_0(t) + H_1(t)$ and $H_1(t)$ is defined such that the system remains in the instantaneous eigenstates of $H_0(t)$ (see Ref. [216] for more details).

In Ref. [146] the same principle is used, the difference is that the auxiliary Hamiltonian is designed such that the system remains in the instantaneous Gibbs state of the reference Hamiltonian i.e $\rho(t) = \exp\left(-\beta H_0(t)\right)/Z(t)$. By doing so, they obtained an effective time-dependent Lindblad master equation where the dissipative part of the dynamics is related to the reference Hamiltonian $H_0(t)$.

The proposed method allows to realize STE protocols by reverse-engineering the master equation they obtained, however it has two strong limitations. The first limitation is that the

method lacks physical motivations. Indeed they do not actually consider an open quantum system model and thus a physical bath in their approach. The dissipative part of the dynamics is a pure mathematical construction since it is derived only from the reference Hamiltonian $H_0(t)$. The second limitation is that the shortcut is obtained by finding a specific time-dependent profile of the decay rates in their master equation, which can be extremely difficult to experimentally realize.

In this section, I propose to also use STA techniques to design STE protocols in driven open quantum systems. For that, I consider a driven open quantum system model and propose a mapping of its dynamics to the dynamics of an effective isolated system. The model to which I apply the approach is the Caldeira-Leggett (CL) model that describes the dynamics of the quantum Brownian motion (QBM). This model has the advantage to have been extensively studied with various mathematical techniques to solve its dynamics [29, 152, 217].

The mapping is inspired from the classical Brownian motion: it is obtained by deriving the Langevin equation of the quantum Brownian particle and from it, I construct a Lagrangian for the effective isolated particle. The information about the effect of the environment on the system are contained in a stochastic force acting on the particle, and also in the position and momentum operators of the effective particle with a rescaling factor.

The Hamiltonian that I obtain is very similar to the Caldirola-Kanai model, which is a toy model to describe dissipative dynamics of the quantum harmonic oscillator [218]. Once the mapping is obtained I can design a STE protocol by using STA techniques that are specifically defined for closed systems. The technique that I use is the dynamical invariant (DI). Also known as the Lewis-Riesenfeld invariant, it was originally introduced by the latter to solve the time-dependent dynamics of closed quantum systems [26], and has also been used to do STAs for the harmonic oscillator [219, 220].

I derive the DI for the effective Hamiltonian and propose to use reverse-engineering to design the shortcut protocol. Unfortunately, I will show that the reverse-engineering leads to non consistent boundary conditions for the profile of the trap frequency, and therefore the method does not work. However the mathematical derivations and the idea in itself are worth to mention and also strongly motivate the exploration of STA techniques in quantum stochastic dynamics for the future, and the work presented in the later section.

3.1.2 Effective description of the quantum Brownian motion

Time-dependent Caldeira-Legget model and Langevin equation

I consider the CL model where the Brownian particle is in a trap with time-dependent frequency

$$H(t) = H_S(t) + H_B + H_I + H_c, \tag{3.1}$$

where $H_S(t)$ is the Hamiltonian of the particle

$$H_S(t) = \frac{p^2}{2m} + \frac{1}{2}m\omega^2(t)x^2, \tag{3.2}$$

H_B is the Hamiltoninan of the bath

$$H_B = \sum_n \frac{p_n^2}{2m_n} + \frac{1}{2} m_n \omega_n^2 x_n^2, \tag{3.3}$$

and H_I describes the interaction between the particle and the bath

$$H_I = -x \sum_n \kappa_n x_n. \tag{3.4}$$

Here κ_n is the constant coupling strength between the particle and the n-th oscillator. Finally the last term is the counter term

$$H_c = x^2 \sum_n \frac{\kappa_n^2}{2m_n \omega_n^2}. \tag{3.5}$$

In order to do the mapping, I derive first the quantum Langevin equation. The derivation of the quantum Langevin equation for the CL model is well known, but I briefly describe it here for completeness. The Langevin equation is obtained from the Heisenberg equations of motion written for the Brownian particle and the oscillators of the bath

$$\dot{x}(t) = \frac{i}{\hbar} [H(t), x(t)] = \frac{p(t)}{m}, \tag{3.6}$$

$$\dot{p}(t) = \frac{i}{\hbar} [H(t), p(t)] = -m\omega^2(t)x(t) + \sum_n \kappa_n x_n - x(t) \sum_n \frac{\kappa_n^2}{m_n \omega_n^2}, \tag{3.7}$$

$$\dot{x}_n(t) = \frac{i}{\hbar} [H(t), x_n(t)] = \frac{p_n(t)}{m_n}, \tag{3.8}$$

$$\dot{p}_n(t) = \frac{i}{\hbar} [H(t), p_n(t)] = -m_n \omega_n^2 x_n(t) + \kappa_n x(t). \tag{3.9}$$

Combining the two last equations, we get a differential equation for the position of the oscillator

$$\ddot{x}_n(t) + \omega_n^2 x_n(t) - \frac{\kappa_n}{m_n} x(t) = 0, \tag{3.10}$$

that can be formally solved

$$x_n(t) = \sqrt{\frac{\hbar}{2m_n \omega_n}} \left(e^{-i\omega_n t} b_n + e^{i\omega_n t} b_n^\dagger \right) + \frac{\kappa_n}{m_n \omega_n} \int_0^t x(s) \sin(\omega_n (t-s)) \, ds, \tag{3.11}$$

where b_n ($b_n^\dagger$) is the annihilation (creation) operator of the n-th oscillator. We can then also combine the equation of motion of the Brownian particle and use the formal solution of the position of the bath oscillators to get the following differential equation

$$\ddot{x}(t) + \left(\omega^2(t) + \sum_n \frac{\kappa_n^2}{mm_n \omega_n^2} \right) x(t) - \sum_n \frac{\kappa_n^2}{mm_n \omega_n} \int_0^t x(s) \sin(\omega_n (t-s)) \, ds = \frac{F(t)}{m}, \tag{3.12}$$

where the operator $F(t) = \sum_n \kappa_n \sqrt{\frac{\hbar}{2m_n \omega_n}} \left(e^{-i\omega_n t} b_n + e^{i\omega_n t} b_n^\dagger \right)$ corresponds to the force

acting on the Brownian particle. The third term in the previous equation corresponds to the dissipation resulting from the interaction between the bath and the Brownian particle. To go further we need to introduce the spectral density function

$$J(\omega) = \sum_n \frac{\kappa_n^2}{2m_n\omega_n}\delta(\omega - \omega_n), \tag{3.13}$$

and the damping kernel

$$\Gamma(t - s) = \frac{2}{m}\int_0^\infty \frac{J(\omega)}{\omega}\cos(\omega(t - s))d\omega, \tag{3.14}$$

that satisfies

$$\frac{d}{dt}\Gamma(t - s) = -\sum_n \frac{\kappa_n^2}{mm_n\omega_n}\sin(\omega_n(t - s)) = -\frac{2}{m}\int_0^\infty J(\omega)\sin(\omega(t - s))d\omega. \tag{3.15}$$

We also have

$$\Gamma(0) = \frac{2}{m}\int_0^\infty \frac{J(\omega)}{\omega}d\omega = \sum_n \frac{\kappa_n^2}{mm_n\omega_n^2}. \tag{3.16}$$

With the damping kernel we can rewrite the dissipative term in Eq. (3.12) as

$$-\sum_n \frac{\kappa_n^2}{mm_n\omega_n}\int_0^t x(s)\sin(\omega_n(t - s))ds = \int_0^t x(s)\frac{d}{dt}\Gamma(t - s)ds$$

$$= \frac{d}{dt}\int_0^t x(s)\Gamma(t - s)ds - \Gamma(0)x(t). \tag{3.17}$$

Note that the term $-\Gamma(0)x(t)$ cancels with the contribution from the counter-term in Eq. (3.12) $\left(\sum_n \frac{\kappa_n^2}{mm_n\omega_n^2}x(t)\right)$, which leads end to the following general quantum Langevin equation

$$\ddot{x}(t) + \omega^2(t)x(t) + \frac{d}{dt}\int_0^t \Gamma(t - s)x(s)ds = \frac{F(t)}{m}, \tag{3.18}$$

Now I will assume that the environment is Markovian and so the spectral density function can be represented by the following Ohmic distribution

$$J(\omega) = \frac{m\gamma}{2\pi}\omega, \tag{3.19}$$

where γ is the damping rate. In that case the damping kernel is given by $\Gamma(t) = \gamma\delta(t)$ and the Langevin equation becomes local in time

$$\ddot{x}(t) + \gamma\dot{x}(t) + \omega^2(t)x(t) = \frac{F(t)}{m}. \tag{3.20}$$

Mapping and effective isolated dynamics

Now that we have the equation of motion of the Brownian particle (3.20), I can proceed to the mapping. For that I got inspired by the the work reported in Ref. [221]. In this work, a mapping between the dissipative dynamics of an unitary Fermi gas described by the Caldirola-Kanai model and the effective dynamics of a dissipationless Fermi gas was derived. The idea consists of starting from the semi-classical equation of motion (in our case the Langevin equation (3.20)) and deriving a Lagrangian $L(\dot{x}(t), x(t), t)$ such that writing down the Euler-Lagrange equation for an isolated system gives us exactly the Langevin equation (3.20). This can be easily found and the corresponding Lagrangian is given by

$$L(\dot{x}(t), x(t), t) = e^{\gamma t}\left(\frac{1}{2}m\dot{x}^2(t) - \frac{1}{2}m\omega^2(t)x^2(t) + F(t)x(t)\right), \qquad (3.21)$$

We can then calculate the corresponding conjugate momentum

$$p = \frac{\partial L}{\partial \dot{x}} = me^{\gamma t}\dot{x}, \qquad (3.22)$$

and thus we can get the corresponding Hamiltonian by calculating the Legendre transform of the Lagrangian. In the end I obtain

$$\tilde{H}(t) = e^{-\gamma t}\frac{p^2}{2m} + \frac{1}{2}m\omega^2(t)e^{\gamma t}x^2 - F(t)e^{\gamma t}x. \qquad (3.23)$$

Some important remarks need to be made about the derivation of the Hamiltonian (3.23). I calculate the effective Lagrangian (3.21) and the corresponding Hamiltonian by assuming the force $F(t)$ is a scalar function, which is of course not true since it contains the ladder operators of the bath oscillators. However this is an acceptable assumption. Indeed, the force is in general a complicated term due to the very large number of oscillators. This is why in classical Brownian motion theory the interaction between the Brownian particle and the environment is usually described with a stochastic force.

Therefore I will proceed to a stochastic treatment of the force $F(t)$ and its statistical properties will depend on the initial state of the environment given by a Gibbs state $\rho_B = \frac{\exp\left(-\frac{H_B}{k_B T}\right)}{Z_B}$ with $Z_B = \text{Tr}_B\left(\exp\left(-\frac{H_B}{k_B T}\right)\right)$ the partition function (T is the temperature of the bath). Since we proceed to a stochastic treatment of the interaction between the Brownian particle and the environment, we can consider a scalar function for the force as long as it preserves the statistical properties of the bath operator.

The statistical properties we need are usually the expectation value and the two-point correlation function of the force. The expectation value is simply

$$\langle F(t)\rangle_T = \frac{1}{m}\text{Tr}_B\left(\rho_B F(t)\right) = 0. \qquad (3.24)$$

From now I will use the bracket $\langle .\rangle_T$ to denote the average calculated with respect to the scalar stochastic force. The two-point correlation function of the stochastic force then

satisfies

$$\langle F(t)F(t')\rangle_T = \frac{1}{2}\operatorname{Tr}_B\left(\rho_B\{F(t),F(t')\}\right)$$
$$= \frac{\hbar}{m^2}\int_0^\infty J(\omega)\coth\left(\frac{\hbar\omega}{2k_BT}\right)\cos(\omega(t-t'))d\omega. \tag{3.25}$$

The statistical properties of the force are therefore characterized by classical numbers and so we can always assume that the force can be mapped to a scalar quantity that reproduces exactly the same properties (average, two-point correlations but also higher order correlations).

Actually this approach is strongly connected to the quantum state diffusion model [222]. Instead of describing an open quantum system with a master equation, one uses a quantum stochastic equation of motion for the wavefunction $|\psi\rangle$. The master equation can be recovered by averaging over all possible trajectories for $|\psi\rangle$ with respect to the stochastic contribution.

In the high temperature limit $k_BT \gg \hbar\omega$, the stochastic force corresponds to Gaussian noise

$$\langle F(t)F(t')\rangle_T \approx \frac{\gamma k_BT}{m}\delta(t-t'). \tag{3.26}$$

Another point to mention is that the Hamiltonian (3.23) that I obtained is very similar to the Caldirola-Kanai (CK) model [218]. The difference is that in the CK Hamiltonian, the stochastic force does not appear and only the position and momentum of the particle are rescaled with the exponential factor to model a damping effect. A couple of studies have been done on the CK model by adding a linear force to the particle [223, 224, 225] however the force is always deterministic, and is not related to the influence of an external environment.

So far no work has been reported where a direct connection between the CK model and the Brownian particle described with an open quantum system model like Eq. (3.1) is established. However a work realized in 1998 by Cavalcanti [226] is connected to the result that I present here. In his case he proposed to define the wave function of a Brownian particle by considering the CK Hamiltonian where the equation of motion of the particle is given by the classical Langevin equation. His work basically corresponds to the high temperature limit of the presented result.

3.1.3   Dynamical invariant and shortcut to equilibration

Dynamical invariant and shortcut to adiabaticity

Now that I have derived the mapping and thus obtained a closed system representation of the QBM with the Hamiltonian (3.23), I can proceed to the STE. For that I will use the dynamical invariant (DI) that I will now briefly explain and show how it can be used for STAs. Let us consider the closed dynamics of a quantum system given by the time-dependent Schrödinger equation

$$i\hbar\frac{\partial}{\partial t}|\Psi(t)\rangle = H(t)|\Psi(t)\rangle. \tag{3.27}$$

A DI is an hermitian operator $I(t)$ that is a constant of the dynamics and thus satisfies

$$\frac{dI(t)}{dt} = \frac{\partial I(t)}{\partial t} + \frac{1}{i\hbar}[I(t), H(t)] = 0. \tag{3.28}$$

An interesting property of the DI is that its eigenstates $\phi_n(t)$ satisfy the time-dependent Schrödinger equation (3.27) [26]. As a consequence, one can show that the general solution of Eq. (3.27) can be expressed as

$$\Psi(t) = \sum_n \langle \phi_n(0)|\Psi(0)\rangle \, e^{i\alpha_n(t)} \phi_n(t), \tag{3.29}$$

where the dynamical phase $\alpha_n(t)$ is given by

$$\alpha_n(t) = \frac{1}{\hbar} \int_0^t \langle \phi_n(t')| \, i\hbar \frac{\partial}{\partial t'} - H(t') \, |\phi_n(t')\rangle \, dt'. \tag{3.30}$$

Calculating a DI can be complicated in general. However in the case of the harmonic oscillator, this is straightforward. Let us consider the following time-dependent Hamiltonian

$$H(t) = \frac{p^2}{2m} + \frac{1}{2}m\omega^2(t)x^2. \tag{3.31}$$

The most common way to obtain a DI is to consider an operator $I(t)$ that has a similar structure to the corresponding Hamiltonian. Since the Hamiltonian of the time-dependent harmonic oscillator is quadratic in position and momentum, one can consider a quadratic ansatz

$$I(t) = \frac{1}{2} \left(\alpha(t)x^2 + \beta(t)p^2 + \delta(t)\{x, p\} \right). \tag{3.32}$$

To get the time-dependent coefficients, we use the condition given by Eq. (3.28). After few calculations, one can show that the invariant can be reduced to

$$I(t) = \frac{1}{2} \left(\frac{m\omega_0^2}{b^2(t)}x^2 + \frac{1}{m} \left(b(t)p - m\dot{b}(t)x \right)^2 \right), \tag{3.33}$$

where $\omega_0 = \omega(0)$ and the scaling function $b(t)$ satisfies the Ermakov equation [26, 219]

$$\ddot{b}(t) + \omega^2(t)b(t) = \frac{\omega_0^2}{b^3(t)}. \tag{3.34}$$

One can notice that the invariant has the structure of a harmonic oscillator with a constant frequency ω_0, a position $x/b(t)$ and momentum $b(t)p - m\dot{b}(t)x$. Thus the eigenstates can be obtained by using the standard ladder operators. In coordinate representation, they are given by

$$\phi_n(x, t) = \frac{1}{\sqrt{2^n n! b(t)}} \exp\left\{ \left(i\frac{m}{2\hbar} \left(\frac{\dot{b}(t)}{b(t)} + \frac{i\omega_0}{b^2(t)} \right) x^2 \right) \right\} H_n \left(\sqrt{\frac{m\omega_0}{\hbar}} \frac{x}{b(t)} \right), \tag{3.35}$$

where $H_n(x)$ are the Hermite polynomials. The dynamical phases take the form

$$\alpha_n(t) = -\omega_0 \left(n + \frac{1}{2}\right) \int_0^t \frac{1}{b^2(\tau)} d\tau. \tag{3.36}$$

For a given protocol $\omega(t)$, one can get the solution to the dynamics by determining the DI. The DI is uniquely determined by the scaling function $b(t)$ that can be calculated with the Ermakov equation (3.34). From that one can then easily get the eigenstates of the invariant, the phases and so the solution.

From the invariant, one can also do reverse engineering for STA [219, 220]. In this situation, we want to change the harmonic frequency from the initial value ω_0 to a final value ω_f at a given time $t = t_f$, such that the particle is in the ground state initially and at $t = t_f$. Since the solution of the dynamics is given by the invariant, we just need to correctly design it to find the shape of $\omega(t)$. In other words, we just need to correctly design the scaling function $b(t)$.

This is actually straightforward. Indeed the solution of the dynamics is given by the eigenstates of the DI, so we just need to ensure that the eigenstates of the Hamiltonian and the DI coincide at $t = 0$ and and $t = t_f$ to make sure that the particle is in the ground state at $t = 0$ and $t = t_f$

$$[H(0), I(0)] = [H(t_f), I(t_f)] = 0. \tag{3.37}$$

The commutation relations are satisfied if we impose the following boundary conditions to the scaling function

$$b(0) = 1, \ \dot{b}(0) = 0, \ \ddot{b}(0) = 0, \ b(t_f) = \sqrt{\frac{\omega_0}{\omega_f}}, \ \dot{b}(t_f) = 0, \ \ddot{b}(t_f) = 0. \tag{3.38}$$

Note that the conditions on the second derivative are not obtained from the commutation relations but from the Ermakov equation (3.34). Since it does not really matters what happens during the dynamics, we can choose any ansatz for $b(t)$ as long as the boundary conditions are satisfied. We have 6 boundary conditions, so we can for example consider a fifth order polynomial function

$$b(t) = 6(b_f - 1)\left(\frac{t}{t_f}\right)^5 - 15(b_f - 1)\left(\frac{t}{t_f}\right)^4 + 10(b_f - 1)\left(\frac{t}{t_f}\right)^3 + 1, \tag{3.39}$$

where $b_f = \sqrt{\frac{\omega_0}{\omega_f}}$. Finally, the profile of the trap frequency $\omega(t)$ can be obtained from the Ermakov equation.

Dynamical invariant of the quantum Brownian motion

Next I explain how I calculate the DI for the effective Hamiltonian 3.23. A way to obtain it could be to use the same method as discussed above for the harmonic oscillator. However I use a different approach based on the method developed in Refs. [227, 225]. The method has the advantage to be more straightforward and elegant. To build the DI, we first derive linear invariants. For that we write down the Heisenberg equations of motion for the Hamiltonian

(3.23)

$$\dot{x}(t) = e^{-\gamma t}\frac{p(t)}{m},$$
$$\dot{p}(t) = -m\omega^2(t)e^{\gamma t}x(t) + F(t)e^{\gamma t}.$$
(3.40)

Now we multiply each equation respectively by two complex functions $\alpha(t)$, $\beta(t)$ and carry out the sum

$$\alpha(t)\dot{x}(t) + \beta(t)\dot{p}(t) = \alpha(t)e^{-\gamma t}\frac{p}{m} - \beta(t)m\omega^2(t)e^{\gamma t}x + \beta(t)F(t)e^{\gamma t}.$$
(3.41)

The previous equation implies the relation

$$\frac{d}{dt}\left(\alpha x + \beta p - \mathcal{F}\right) = \left(\frac{\alpha e^{-\gamma t}}{m} + \dot{\beta}\right)p + \left(\dot{\alpha} - \beta m\omega^2 e^{\gamma t}\right)x,$$
(3.42)

where $\mathcal{F} = \int_0^t \beta(s)F(s)e^{\gamma s}ds$. So if the right hand side of the equation is always equal to zero, this implies

$$\frac{\alpha e^{-\gamma t}}{m} + \dot{\beta} = 0,$$
$$\dot{\alpha} - \beta m\omega^2 e^{\gamma t} = 0,$$
(3.43)

and the operator

$$I_1(t) = \alpha(t)x + \beta(t)p - \mathcal{F}(t)$$
(3.44)

is a linear invariant of the dynamics. The conditions given by (3.43) imply that the linear invariant can be rewritten as

$$I_1(t) = -m\dot{\beta}(t)e^{\gamma t}x + \beta(t)p - \mathcal{F}(t),$$
(3.45)

and the function $\beta(t)$ (which as we will see, corresponds to the scaling function similarly to $b(t)$ in the case of the harmonic oscillator) satisfies the following differential equation

$$\ddot{\beta}(t) + \gamma\dot{\beta}(t) + \omega^2(t)\beta(t) = 0.$$
(3.46)

This is the equation describing a classical harmonic oscillator in the presence of damping. Now if we write $\beta(t)$ as $\beta(t) = \rho(t)e^{i\phi(t)}$, from the previous equation we can easily show that

$$\rho^2(t)\dot{\phi}(t)e^{\gamma t} = c,$$
(3.47)

where c is an arbitrary integration constant, which can be chosen to be equal to the initial frequency $c = \omega(0) = \omega_0$. We can also show that the modulus of the scaling function satisfies the following Ermakov equation

$$\ddot{\rho}(t) + \gamma\dot{\rho}(t) + \omega^2(t)\rho(t) = \frac{e^{-2\gamma t}\omega_0^2}{\rho(t)^3}.$$
(3.48)

Let us remark that in the absence of damping ($\gamma = 0$) we recover the Ermakov equation for the harmonic oscillator (Eq. (3.34)). The linear invariant has interesting algebraic properties. If we calculate the commutator between I_1 and its hermitian conjugate $I_1^\dagger$, we get

$$[I_1(t), I_1^\dagger(t)] = i\hbar m e^{\gamma t} \left(\beta(t)\dot{\beta}^*(t) - \beta^*(t)\dot{\beta}(t) \right) = 2\hbar m \omega_0. \tag{3.49}$$

This commutator gives a real and positive number that I denote $\Omega = 2\hbar m \omega_0$. We can then define the following operators $a = \frac{I_1}{\sqrt{\Omega}}$ and $a^\dagger = \frac{I_1^\dagger}{\sqrt{\Omega}}$ that satisfy the commutation relation

$$[a, a^\dagger] = 1. \tag{3.50}$$

With this, we basically build ladder operators and we can also define the corresponding number operator $\hat{n} = a^\dagger a$ (satisfying the commutation relations $[\hat{n}, a] = -a$ and $[\hat{n}, a^\dagger] = a^\dagger$). Now we can finally build the DI. Indeed any product of I_1 and $I_1^\dagger$ will be an invariant of the dynamics. We consider then the half of the anti-commutator between I_1 and $I_1^\dagger$ for our DI. It can be expressed with the number operator as

$$I(t) = \frac{1}{2}\{I_1(t), I_1^\dagger(t)\} = \Omega \left(\hat{n} + \frac{1}{2} \right). \tag{3.51}$$

In the end, the DI for the QBM is simply a harmonic oscillator. Its expression in terms of the position and momentum of the effective Hamiltonian is

$$I(t) = m^2 e^{2\gamma t} |\dot{\beta}(t)|^2 x^2 + |\beta(t)|^2 p^2 - m e^{\gamma t} \operatorname{Re}\left(\beta^*(t)\dot{\beta}(t) \right) \{x, p\} + 2m e^{\gamma t} \operatorname{Re}\left(\dot{\beta}(t)\mathcal{F}^*(t) \right) x$$
$$- 2\operatorname{Re}\left(\beta(t)\mathcal{F}^*(t) \right) p + \frac{1}{2}|\mathcal{F}(t)|^2. \tag{3.52}$$

The eigenstates can be simply obtained. As in the harmonic oscillator problem, we get the ground state by using the property of the ladder operator $a|0\rangle = 0$. After few lines of calculation, the ground state in coordinate representation is given by

$$\psi_0(x, t) = \left(\frac{\Omega}{2\pi\hbar^2|\beta(t)|^2} \right)^{\frac{1}{4}} \exp\left(\frac{e^{-\gamma t}}{2\hbar m} \left(\operatorname{Im}\left(\frac{\mathcal{F}^2(t)}{\beta(t)\dot{\beta}(t)} \right) - \frac{\operatorname{Im}\left(\frac{\mathcal{F}(t)}{\beta(t)} \right)^2}{\operatorname{Im}\left(\frac{\dot{\beta}(t)}{\beta(t)} \right)} \right) \right)$$
$$\times \exp\left(\frac{im\dot{\beta}(t)e^{\gamma t}}{2\hbar\beta(t)} \left(x + \frac{\mathcal{F}(t)e^{-\gamma t}}{m\dot{\beta}(t)} \right)^2 \right), \tag{3.53}$$

and the excited states are found by induction as

$$\psi_n(x, t) = \frac{1}{\sqrt{2^n n!}} \left(i\sqrt{\frac{\beta^*(t)}{\beta(t)}} \right)^n H_n\left(\sqrt{\frac{\Omega}{2\hbar^2|\beta(t)|^2}} \left(x + \frac{\mathcal{F}(t)e^{-\gamma t}}{m\dot{\beta}^*(t)} \right) \right) \psi_0(x, t). \tag{3.54}$$

Reverse-engineering and shortcut to equilibration

Now that the DI is derived, I can proceed to the shortcut. The protocol that I want to accelerate is the following: the particle is initially at equilibrium with the thermal bath with an initial frequency $\omega(0) = \omega_0$ and thus the state is given by the Gibbs state $\varrho_S(0) = Z_0^{-1} e^{-H_S(0)/k_B T}$. I want to find a protocol such that at the end of it, the particle is in a new equilibrium state with the bath at the final frequency $\omega(t_f) = \omega_f$ i.e $\varrho_S(t_f) = Z_f^{-1} e^{-H_S(t_f)/k_B T}$, where t_f is the duration of the protocol. Unlike the STA protocol, the dynamics here is not unitary and we do not want to keep the occupation populations of the density matrix constant. The method discussed above to do a STA for the harmonic oscillator can thus not be exactly used in the same way here.

The time-evolution operator of the closed dynamics generated by the Hamiltonian (3.23) can be expressed with the eigenstates of the DI [26]

$$U(t) = \sum_n e^{i\alpha_n(t)} |\psi_n(t)\rangle \langle \psi_n(0)|, \qquad (3.55)$$

where the dynamical phase $\alpha_n(t)$ is calculated with Eq. (3.30). Then the evolution of the density matrix of the effective Brownian particle can be obtained

$$\varrho_S(t) = U(t)\varrho_S(0)U^\dagger(t) = \sum_{n,p,q} p_n e^{i(\alpha_p(t) - \alpha_q(t))} \langle \psi_p(0)|\phi_n(0)\rangle \langle \phi_n(0)|\psi_q(0)\rangle |\psi_p(t)\rangle \langle \psi_q(t)|, \qquad (3.56)$$

where $\phi_n(0)$ is the eigenstate of the particle Hamiltonian H_S at $t = 0$, and $p_n = \dfrac{e^{-\frac{\hbar\omega_0\left(n+\frac{1}{2}\right)}{k_B T}}}{Z_0}$ is the corresponding Boltzmann weight. However we need to be careful, as the dynamics is not deterministic but stochastic due to the force $F(t)$. But here, I did the calculation as if solving a deterministic time-dependent Schrödinger equation. The way to interpret these results is the following: the evolution of the density matrix has been obtained for a single realization of the dynamics. Thus I need to average over all possible realizations with respect to the stochastic force in order to get the observed state of the effective particle

$$\varrho_S(t) = \left\langle U(t)\rho_S(0)U^\dagger(t) \right\rangle_T. \qquad (3.57)$$

As for the STA, the protocol is found by ensuring that the state of the particle corresponds to the desired states at $t = 0$ and $t = t_f$. We thus only need to find boundary conditions on the modulus of the scaling function $\rho(t)$ at $t = 0$ and t_f, and we can consider any ansatz for $\rho(t)$ as long as the boundary conditions are satisfied. The profile of the trap frequency is then found by using the damped Ermakov equation (3.48). For $t = 0$ we need to ensure that we start from the Gibbs state of the initial Hamiltonian. We thus need the invariant and the Hamiltonian to commute i.e $[H_S(0), I(0)] = [\tilde{H}(0), I(0)] = 0$ like for the STA. Combined with the damped Ermakov equation, we get exactly the same boundary conditions as for the STA

$$\rho(0) = 1, \; \dot{\rho}(0) = 0, \; \ddot{\rho}(0) = 0. \qquad (3.58)$$

This condition on the commutation relation also allows us to simplify the expression of the

state of the particle

$$\varrho_S(t) = \sum_n p_n \left\langle |\psi_n(t)\rangle \langle \psi_n(t)| \right\rangle_T. \tag{3.59}$$

For $t = t_f$ it becomes more complicated. The most straightforward way to proceed would be to put the state at $t = t_f$ equal to the target state. However calculating explicitly the state with Eq. (3.59) is challenging. Instead, I use the DI to calculate the variance of the position and momentum operators. Since the state of the particle remains Gaussian during the dynamics, we can fully characterize its state with those quantities. They can be calculated by expressing the momentum and position operators with the ladder operators of the DI

$$x = \frac{i\hbar}{\sqrt{\Omega}} \left(\beta^*(t)a - \beta(t)a^\dagger\right) + \frac{2\hbar}{\Omega} \operatorname{Im}\left(\mathcal{F}^*\beta(t)\right),$$
$$p = \frac{i\hbar m e^{\gamma t}}{\sqrt{\Omega}} \left(\dot{\beta}^*(t)a - \dot{\beta}(t)a^\dagger\right) + \frac{2\hbar m e^{\gamma t}}{\Omega} \operatorname{Im}\left(\mathcal{F}^*\dot{\beta}(t)\right). \tag{3.60}$$

I can then calculate the expectation value of x^2 and p^2 with respect to the eigenstates of the invariant

$$\langle\psi_n(t)|\, x^2 \,|\psi_n(t)\rangle = \frac{2\hbar^2}{\Omega}|\beta(t)|^2 \left(n + \frac{1}{2}\right) + \frac{4\hbar^2}{\Omega^2} \operatorname{Im}\left(\mathcal{F}^*\beta(t)\right)^2,$$
$$\langle\psi_n(t)|\, p^2 \,|\psi_n(t)\rangle = \frac{2\hbar^2 m^2 e^{2\gamma t}}{\Omega}|\dot{\beta}(t)|^2 \left(n + \frac{1}{2}\right) + \frac{4\hbar^2 m^2 e^{2\gamma t}}{\Omega^2} \operatorname{Im}\left(\mathcal{F}^*\dot{\beta}(t)\right)^2. \tag{3.61}$$

By putting the variances equal to the desired values, we can obtain boundary conditions for the modulus of the scaling function $\rho(t)$ at $t = t_f$. It is worth remembering that I work with the Hamiltonian from the mapping $\tilde{H}(t)$ (Eq. (3.23)) where p^2 and x^2 are rescaled respectively with the factors $e^{-\gamma t}$ and $e^{\gamma t}$ due to the damping. We also need to average over all the possible trajectories with respect to the stochastic force to get the actual variances of the particle. In the end I get the following conditions

$$\left\langle \sum_n p_n \langle\psi_n(t_f)|\, e^{\gamma t_f} x^2 \,|\psi_n(t_f)\rangle \right\rangle_T = \frac{\hbar|\beta(t_f)|^2 e^{\gamma t_f}}{2m\omega_0} \coth\left(\frac{\hbar\omega_0}{2k_B T}\right) + \frac{e^{\gamma t_f}}{m^2\omega_0^2} \left\langle \operatorname{Im}\left(\mathcal{F}^*(t_f)\beta(t_f)\right)^2 \right\rangle_T$$
$$= \frac{\hbar}{2m\omega_f} \coth\left(\frac{\hbar\omega_f}{2k_B T}\right),$$

$$\left\langle \sum_n p_n \langle\psi_n(t_f)|\, e^{-\gamma t_f} p^2 \,|\psi_n(t_f)\rangle \right\rangle_T = \frac{\hbar m|\dot{\beta}(t_f)|^2 e^{\gamma t_f}}{2\omega_0} \coth\left(\frac{\hbar\omega_0}{2k_B T}\right) + \frac{e^{\gamma t_f}}{\omega_0^2} \left\langle \operatorname{Im}\left(\mathcal{F}^*(t_f)\dot{\beta}(t_f)\right)^2 \right\rangle_T$$
$$= \frac{\hbar m\omega_f}{2} \coth\left(\frac{\hbar\omega_f}{2k_B T}\right) \tag{3.62}$$

The last terms of the two previous equations correspond to the variances of the target state. Note that the condition on x^2 and p^2 give respectively a condition for the scaling function and its first derivative at $t = t_f$. A condition on the second derivative can be obtained from the damped Ermakov equation.

Now we need to take care of the terms that contain the stochastic force. If we replace the Ohmic spectral density function $J(\omega)$ by its expression (Eq. (3.19)) in Eq. (3.25), the two-point correlation of the force is given by

$$\langle F(t)F(t')\rangle_T = \frac{\hbar\gamma}{2\pi m} \int_0^\infty \omega \coth\left(\frac{\hbar\omega}{2k_BT}\right) \cos\left(\omega(t-t')\right) d\omega. \tag{3.63}$$

One can notice that for a finite temperature, the integral in the above expression diverges. This is because I assumed that the particle is coupled to a thermal bath of infinite modes with a diverging cut-off. A way to fix this issue is to consider a finite cut-off Ω_c in the upper bound of the integral. However this will still give a large contribution to the energy of the particle, that scales as $\ln(\Omega_c/\gamma)$, coming from the interaction between the particle and the vacuum fluctuations with the highest modes of the bath [29].

This singular behavior is due to the assumption that the particle and the bath are initially not correlated. The only way to rigorously prevent this nonphysical behavior, is to restrict the study to the high temperature limit. The two-points correlation function is then given by Eq. (3.26) and the correlation function for $\mathcal{F}(t) = \int_0^t \beta(s)F(s)e^{\gamma s}$ is given by

$$\langle \mathcal{F}(t)\mathcal{F}(t')\rangle_T = \frac{\gamma k_BT}{m} \int_0^{\min(t,t')} \beta^2(s)e^{2\gamma s}ds,$$
$$\langle \mathcal{F}(t)\mathcal{F}^*(t')\rangle_T = \frac{\gamma k_BT}{m} \int_0^{\min(t,t')} |\beta(s)|^2 e^{2\gamma s}ds. \tag{3.64}$$

In the high temperature limit, the boundary conditions then become

$$\langle x^2(t_f)\rangle_T = \frac{|\beta(t_f)|^2 e^{\gamma t_f} k_BT}{m\omega_0^2} + \frac{e^{\gamma t_f} k_BT\gamma}{4m^3\omega_0^2}\left(|\beta(t_f)|^2 \int_0^{t_f} |\beta(s)|^2 e^{2\gamma s}ds\right.$$
$$\left. - \operatorname{Re}\left(\beta^2(t_f)\int_0^{t_f}(\beta^2(s))^*e^{2\gamma s}ds\right)\right)$$
$$= \frac{k_BT}{m\omega_f^2},$$
$$\langle p^2(t_f)\rangle_T = \frac{mk_BT|\dot\beta(t_f)|^2 e^{\gamma t_f}}{\omega_0^2} + \frac{e^{\gamma t_f} k_BT\gamma}{4m\omega_0^2}\left(|\dot\beta(t_f)|^2 \int_0^{t_f} |\beta(s)|^2 e^{2\gamma s}ds\right.$$
$$\left. - \operatorname{Re}\left(\dot\beta^2(t_f)\int_0^{t_f}(\beta^2(s))^*e^{2\gamma s}ds\right)\right)$$
$$= mk_BT. \tag{3.65}$$

From those boundary conditions, we actually recover the equipartition theorem

$$\frac{1}{2}m\omega_f^2 \left\langle x^2(t_f)\right\rangle_T = \frac{\langle p^2(t_f)\rangle_T}{2m} = \frac{k_BT}{2}. \tag{3.66}$$

By using the equipartition theorem and the boundary conditions Eq.(3.65), we can deduce that they are both satisfied if $\omega_f^2\beta(t_f)^2 = \dot\beta(t_f)^2$. From that I deduce that $\dot\rho(t_f) = 0$ and $\omega_f^2 = -\dot\phi(t_f)$. However the last equality cannot be satisfied since $\dot\phi(t_f) = \omega_0 e^{-\gamma t_f}/\rho(t_f)^2 > 0$ (see

Eq. (3.47)). Another condition can be considered to ensure that the boundary conditions and the equipartition theorem are satisfied which is $\omega_f^2|\beta(t_f)|^2 = |\dot{\beta}(t_f)|^2$ with the additional condition

$$\text{Im}\,(\beta(t_f)) = 0 \implies \phi(t_f) = 2k\pi,\ k \in \mathbf{N}^* \tag{3.67}$$

or

$$\text{Im}\left(\int_0^{t_f}\beta(s)^2 e^{2\gamma s}ds\right) = 0 \implies \int_0^{t_f}\rho(s)^2\sin(2\phi(s))e^{2\gamma s}ds = 0 \tag{3.68}$$

I have so far only explored the first boundary condition given by Eq. (3.67) with $k = 1$. For that, I consider a 5th order polynomial as an ansatz for the modulus of the scaling function $\rho(t) = \sum_{n=0}^{5}a_n t^n$, like for the STA of the harmonic oscillator. The coefficients a_0, a_1 and a_2 can be simply found by using the boundary conditions at $t = 0$ while the coefficients a_3, a_4 and a_5 need to be calculated with numerical methods from the boundary conditions at $t = t_f$.

Unfortunately, I was not able to find solutions for those coefficients, even by changing the damping coefficient γ and the duration of the protocol t_f. This strongly suggests that no solution and thus no protocol can be found by this way. However I still need to explore the other boundary condition given by Eq. (3.68).

3.1.4 Conclusion and perspectives

In this research project, I have tried to use the powerful toolbox provided by STA techniques and apply it in the case of STE protocols in open quantum systems. I have considered the specific case of the QBM. To do that, I proposed to describe the dynamics of the Brownian particle by mapping the total Hamiltonian of the model to an effective Hamiltonian of a single particle in Harmonic trap with the presence of a stochastic force representing the effect of the interaction with the bath. The position and momentum of the effective Hamiltonian are also rescaled due to the presence of the damping.

The mathematical derivation of the effective Hamiltonian is consistent with the quantum Langevin equation describing the dynamics of the Brownian particle. Actually the proposed description is very similar to the quantum state diffusion approach where the dynamics is also described with a stochastic dynamics of the wavefunction. Once the mapping is established, I constructed a DI of the effective Hamiltonian. This can be done straightforwardly since the Hamiltonian is a quadratic operator. While the Hamiltonian is stochastic, the construction of the DI seems to be still possible at the level of a single trajectory.

The shortcut was then formulated by reverse-engineering the dynamics with the DI. By using the prior knowledge on the initial and final state of the particle during the protocol, I was able to chose boundary conditions for the scaling function $\beta(t)$ that uniquely define the DI. From that, I could infer the profile of the trap frequency. Unfortunately the boundary conditions that I obtained at the end of the protocol can not be satisfied. I still need to explore one more possibility for the boundary condition (Eq. (3.68)). If it still does not work, then it means that there is a mistake in the interpretation and construction of the DI. It is likely that the use of the DI for quantum stochastic dynamics is not as straightforward as in the deterministic case, and there is a subtle point that is missing for now.

Nevertheless, this project still strongly suggests that the dynamics of driven open quantum system and STE protocols could be solved by using STA techniques combined with

a quantum stochastic dynamics approach. More generally an interesting direction to take in the future, would be to figure out how STA techniques like the DI but also others (e.g the counter-diabatic driving [216]) can be extended to quantum stochastic dynamics. This could contribute to the improvement of techniques for controlling open quantum systems for various kind of applications.

3.2 Dynamical invariant based shortcut to equilibration

3.2.1 Motivation and introduction of the research project

This section presents a different method to realize the same STE protocol discussed in the previous section. The shortcut is realized by overcoming the mathematical challenges of deriving a time-dependent quantum master. Indeed, their derivation can be a very difficult task for an underlying general time-dependent Hamiltonian.

For example a shortcut to equilibration (STE) in Refs. [147, 149] was realized by deriving a non-adiabatic time-dependent master equation in the inertial limit [160, 228], which assumes small variations of the adiabatic parameter of the system. While this allows to obtain the Lindblad operators explicitly, the resulting driving protocol can be restricted.

In this work, I propose a STE protocol by using this time the DI to derive a time-dependent master equation. The master equation can be derived in a very comprehensive way, and it has the advantage to not restrict the driving protocol timescale like the inertial limit. Also the DI gives a clear picture of the influence of the driving protocol on the dissipative effects [161]. Once I obtain the time-dependent master equation, I find the shortcut between the equilibrium state of the initial and final Hamiltonian by reverse engineering it.

To show the power of this approach, I apply this technique to the damped harmonic oscillator (DHO). I also compare the shortcut to simpler, non-optimized protocols, showing that the approach can achieve enhanced performance on shorter timescales. I also discuss physical insights into the strategy adopted by the method.

3.2.2 Dynamical invariant based time-dependent master equation

First I briefly present how one can derive the master equation for a driven open quantum system by using the DI. Let us start from the general Hamiltonian of a driven open quantum system

$$H(t) = H_S(t) + H_B + H_I, \tag{3.69}$$

The interaction term is written as $H_I = \sum_k A_k \otimes B_k$, where A_k act on the system and B_k act on the bath. In order to derive a tractable master equation, I use the Born and Markov approximations. After tracing out the bath, we can then obtain a Redfield master equation in the interaction picture of the form (see Sec. 1.3 for more details)

$$\frac{d\tilde{\rho}_S(t)}{dt} = -\frac{1}{\hbar^2} \sum_{k,l} \int_0^\infty B_{kl}(\tau) \left[\tilde{A}_k(t), \tilde{A}_l(t-\tau)\tilde{\rho}_S(t) \right]$$
$$-B_{lk}(-\tau) \left[\tilde{A}_k(t), \tilde{\rho}_S(t)\tilde{A}_l(t-\tau) \right] d\tau, \tag{3.70}$$

where $B_{kl}(\tau) = \text{Tr}_B\left(\tilde{B}_k(\tau)B_l\rho_B\right)$ is the two-point correlation function of the bath and the tilde indicates operators in the interaction picture. In the presence of a time-dependent system Hamiltonian, the evaluation of $\tilde{A}_k(t)$ can be challenging since there is no general procedure that allows to calculate the time evolution operator of the system $U_S(t) = T_{\leftarrow}\exp\left(-\frac{i}{\hbar}\int_0^t H_S(\tau)d\tau\right)$ (where $T_{\leftarrow}$ is the time-ordering operator).

However, this problem can be solved by using the DI. We already saw in the previous section that the time-evolution operator of the system can be obtained from the eigenstates of the DI (Eq. (3.55)). We can therefore use them to calculate the operators acting on the system in the interaction picture as [161]

$$\tilde{A}_k(t) = \sum_{n,m} e^{i(\alpha_n(t)-\alpha_m(t))} \langle\psi_m(t)| A_k |\psi_n(t)\rangle F_{mn}, \qquad (3.71)$$

with $F_{mn} = |\psi_m(0)\rangle\langle\psi_n(0)|$. The operators can therefore be written as products of time-dependent scalar functions that contain the information on the driving protocol, and time-independent operators F_{mn}. Those operators are jump operators constructed with the DI eigenstate suggesting that the dissipative part of the open dynamics will involve transitions of the system between those states.

3.2.3 Time-dependent master equation for the damped harmonic oscillator

From now I focus on the time-dependent damped harmonic oscillator and I will show below the derivation of the master equation. The particle is coupled to a thermal bath of harmonic oscillators with an interaction term given by Eq. (1.98). Let us start from the Redfield equation given by Eq. (3.70) applied to the damped harmonic oscillator

$$\frac{d\tilde{\rho}_S(t)}{dt} = -\frac{1}{\hbar^2}\int_0^\infty B_{12}(\tau)\left[\tilde{a}^\dagger(t), \tilde{a}(t-\tau)\tilde{\rho}_S(t)\right] - B_{21}(-\tau)\left[\tilde{a}^\dagger(t), \tilde{\rho}_S(t)\tilde{a}(t-\tau)\right]$$
$$+ B_{21}(\tau)\left[\tilde{a}(t), \tilde{a}^\dagger(t-\tau)\tilde{\rho}_S(t)\right] - B_{12}(-\tau)\left[\tilde{a}(t), \tilde{\rho}_S(t)\tilde{a}^\dagger(t-\tau)\right]d\tau, \qquad (3.72)$$

with the bath two-point correlation functions given by

$$B_{12}(\tau) = \sum_n g_n^2 \text{Tr}_B(\tilde{b}_n(\tau)b_n^\dagger\rho_B) = \sum_n e^{-i\omega_n\tau}g_n^2(1+n(\omega_n))$$
$$= \int_0^\infty e^{-i\omega\tau}J(\omega)(1+n(\omega))d\omega,$$
$$B_{21}(\tau) = \sum_n g_n^2 \text{Tr}_B(\tilde{b}_n^\dagger(\tau)b_n\rho_B) = \sum_n e^{i\omega_n\tau}g_n^2 n(\omega_n) \qquad (3.73)$$
$$= \int_0^\infty e^{i\omega\tau}J(\omega)n(\omega)d\omega,$$

where I have introduced the spectral density function of the bath $J(\omega) \sum_n g_n^2\delta(\omega - \omega_n)$ and the Planck distribution $n(\omega) = (e^{\frac{\hbar\omega}{k_BT}}-1)^{-1}$. Now I need to evaluate the ladder operators

of the particle in the interaction picture. Since they are conjugate, we can just focus on the annihilation operator, which we can write with the position and momentum operators in the interaction picture as

$$\tilde{a}(t) = \sqrt{\frac{m\omega_0}{2\hbar}}\left(\tilde{x}(t) + i\frac{\tilde{p}(t)}{m\omega_0}\right). \tag{3.74}$$

I now use the invariant of the harmonic oscillator (Eq. (3.33)) to evaluate the operator in the interaction picture. Since the invariant is a harmonic oscillator with a position $x/b(t)$ and momentum $\Pi = b(t)p - m\dot{b}(t)x$, one can express the position and momentum of the particle in terms of the instantaneous ladder operators of the invariant that are denoted by a_{I_t} and $a_{I_t}^\dagger$

$$
\begin{aligned}
x &= b(t)\sqrt{\frac{\hbar}{2m\omega_0}}(a_{I_t} + a_{I_t}^\dagger), \\
p &= \frac{\Pi}{b(t)} + m\dot{b}(t)\frac{x}{b(t)} = \sqrt{\frac{\hbar m\omega_0}{2}}\left(C(t)a_{I_t} + C^*(t)a_{I_t}^\dagger\right),
\end{aligned}
\tag{3.75}
$$

with the complex function

$$C(t) = \frac{\dot{b}(t)}{\omega_0} - \frac{i}{b(t)}. \tag{3.76}$$

One can deduce that the annihilation operator of the harmonic oscillator in the Schrödinger picture is related to the ladder operators of the invariant through the following Bogoliubov transformation

$$a = \frac{1}{2}\left(D_1(t)a_{I_t} + D_2^*(t)a_{I_t}^\dagger\right), \tag{3.77}$$

where

$$D_{1,2}(t) = b(t) \pm \frac{1}{b(t)} \pm i\frac{\dot{b}(t)}{\omega_0}. \tag{3.78}$$

I now need to calculate the ladder operators of the invariant in the interaction picture. This is easily done by using the time-evolution operator written with the eigenstates of the invariant (Eq. (3.55)) and using the expression of the dynamical phase for the harmonic oscillator $\alpha_n(t) = -\omega_0(n+1/2)\int_0^t 1/b(\tau)^2 d\tau$

$$
\begin{aligned}
\tilde{a}_{I_t}(t) &= \sum_{n,m} e^{i(\alpha_m(t)-\alpha_n(t))}|\phi_n(0)\rangle\langle\phi_n(t)|\,a_{I_t}\,|\phi_m(t)\rangle\langle\phi_m(0)| \\
&= \sum_{n,m} e^{i(\alpha_m(t)-\alpha_n(t))}\sqrt{m}\delta_{n,m-1}|\phi_n(0)\rangle\langle\phi_m(0)| \\
&= e^{-i\varphi(t)}\sum_n \sqrt{n+1}|\phi_n(0)\rangle\langle\phi_{n+1}(0)| = e^{-i\varphi(t)}a_{I_0},
\end{aligned}
\tag{3.79}
$$

where the phase φ is given by

$$\varphi(t) = \int_0^t \frac{\omega_0}{b(\tau)^2}d\tau = \int_0^t \tilde{\omega}(\tau)d\tau. \tag{3.80}$$

Next I will use a_I $(a_I^\dagger)$ instead of a_{I_0} $(a_{I_0}^\dagger)$ to denote the ladder operators of the invariant at $t = 0$. Through this, I can obtain an explicit expression of the annihilation operator of the

particle in the interaction picture

$$\tilde{a}(t) = \frac{1}{2} \left(D_1(t) e^{-i\varphi(t)} a_I + D_2^*(t) e^{i\varphi(t)} a_I^\dagger \right). \tag{3.81}$$

I can then insert Eq. (3.81) in the Redfield equation (3.72), but only explicitly write it down for the first commutator in the right-hand side of Eq.(3.72) since the same treatment can be straightforwardly done for the other terms. After expanding the commutator, one obtains

$$\begin{aligned}
[\tilde{a}^\dagger(t), \tilde{a}(t-\tau)\tilde{\rho}_S(t)] = \frac{1}{4} \Big(& e^{-i(\varphi(t)-\varphi(t-\tau))} D_2(t) D_2^*(t-\tau) [a_I, a_I^\dagger \tilde{\rho}_S(t)] \\
& + e^{-i(\varphi(t)+\varphi(t-\tau))} D_2(t) D_1(t-\tau) [a_I, a_I \tilde{\rho}_S(t)] \\
& + e^{i(\varphi(t)+\varphi(t-\tau))} D_1^*(t) D_2^*(t-\tau) [a_I^\dagger, a_I^\dagger \tilde{\rho}_S(t)] \\
& + e^{i(\varphi(t)-\varphi(t-\tau))} D_1^*(t) D_1(t-\tau) [a_I^\dagger, a_I \tilde{\rho}_S(t)] \Big).
\end{aligned} \tag{3.82}$$

The integral in the Redfield equation is dominated by the bath two-point correlation function that rapidly decays with a characteristic time τ_B. The decay time is given by the cut-off of the bath $\tau_B \sim \Lambda^{-1}$. Based on the Markov approximation, the decay time must be much smaller than the typical timescale of the system given by $\omega(t)^{-1}$ i.e. $\tau_B \ll \omega(t)^{-1}$. One can thus use the first order approximation of the phase in the integral $\varphi(t-\tau) \approx \varphi(t) - \tilde{\omega}(t)\tau$. I also make the zero-th order approximation $D_i(t-\tau) \approx D_i(t)$ meaning that the variations of the scaling function $b(t)$ and its derivative are negligible in the time window $[0, \tau_B]$. Formally, it implies $\tau_B \ll \left| \frac{D_i(t)}{\dot{D}_i(t)} \right|$. This approximation can be reformulated as $\tau_B \ll \tau_D$ where a driving timescale $\tau_D = \min_{i,t} \left| \frac{D_i(t)}{\dot{D}_i(t)} \right|$ is introduced [160]. I would like to emphasize that this approximation is not necessary to derive the master equation, however it allows to simplify the reverse-engineering for the shortcut.

The last approximation I will use is the secular approximation. The non-secular terms are neglected, in order to derive a master equation in Lindblad form and ensure that the state of the system remains physical. This means that the non-secular contributions contain fast oscillating terms that average to zero. This implies $\varphi(t) + \varphi(t-\tau) \gg \varphi(t) - \varphi(t-\tau)$. By using a first order expansion and the Markov approximation, I obtain $\varphi(t) \gg \tilde{\omega}(t)\tau_B$ i.e $\int_0^t \tilde{\omega}(\tau)d\tau \gg \tilde{\omega}(t)\tau_B$.

Taking account of the different approximations in Eq. (3.82), I obtain

$$\begin{aligned}
\int_0^\infty B_{12}(\tau) \left[\tilde{a}^\dagger(t), \tilde{a}(t-\tau)\tilde{\rho}_S(t) \right] d\tau \approx & \frac{|D_2(t)|^2}{4} \int_0^\infty B_{12}(\tau) e^{-i\tilde{\omega}(t)\tau} d\tau [a_I, a_I^\dagger \tilde{\rho}_S(t)] \\
& + \frac{|D_1(t)|^2}{4} \int_0^\infty B_{12}(\tau) e^{i\tilde{\omega}(t)\tau} d\tau [a_I^\dagger, a_I \tilde{\rho}_S(t)].
\end{aligned} \tag{3.83}$$

As mentioned in Sec. 1.3, the integrals can be calculated by using the well known result $\int_0^\infty e^{i\omega\tau} d\tau = \pi\delta(\omega) + iP(1/\omega)$ where P denotes the principal value. After combining the

different terms and a few lines of algebra, I obtain the time-dependent master equation for the damped harmonic oscillator in the interaction picture

$$
\frac{d\tilde{\rho}_S(t)}{dt} = -\frac{i}{\hbar}\left[\tilde{H}_{LS}(t), \tilde{\rho}_S(t)\right] + \frac{|D(t)|^2}{2\hbar^2}\gamma_+(\tilde{\omega}(t))\left(a_I\tilde{\rho}_S(t)a_I^\dagger - \frac{1}{2}\{a_I^\dagger a_I, \tilde{\rho}_S(t)\}\right)
$$
$$
+ \frac{|D(t)|^2}{2\hbar^2}\gamma(\tilde{\omega}(t))\left(a_I^\dagger\tilde{\rho}_S(t)a_I - \frac{1}{2}\{a_I a_I^\dagger, \tilde{\rho}_S(t)\}\right),
$$

(3.84)

where $\tilde{H}_{LS}(t)$ is a time-dependent Lamb shift in the interaction picture

$$
\tilde{H}_{LS}(t) = \frac{\hbar}{4}\left(|D_1(t)|^2 P \int_0^\infty \frac{J(\omega)}{\tilde{\omega}(t) - \omega}d\omega - |D_2(t)|^2 P \int_0^\infty \frac{J(\omega)}{\tilde{\omega}(t) + \omega}d\omega\right),
$$

(3.85)

and $D(t) = D_1(t)$. The time-dependent decay rates characterizing the emission and absorption are given by $\gamma_+(\tilde{\omega}(t)) = \pi J(\tilde{\omega}(t))(1 + n(\tilde{\omega}(t)))$ and $\gamma(\tilde{\omega}(t)) = \gamma_+(\tilde{\omega}(t))e^{-\frac{\hbar\tilde{\omega}(t)}{k_B T}}$. One can notice that the dissipative part of the dynamics occurs at a time-dependent Bohr frequency given by $\tilde{\omega}(t) = \omega_0/b(t)^2$ which gives a new physical interpretation of the scaling function $b(t)$ in the context of open quantum systems theory. Also the Lindblad operators in the interaction picture are the ladder operators of the invariant at $t = 0$, however if one considers a driving protocol with a continuous start from the initial Hamiltonian $[H_S(0), I(0)] = 0$, one can recover the creation and annihilation operators of the particle, $a_I = a$ ($a_I^\dagger = a^\dagger$).

3.2.4 Shortcut to equilibration

Formulation of the shortcut protocol and reverse engineering

The STE protocols is the same as in the previous section. The particle is driven from an equilibrium state with an initial frequency $\omega(0) = \omega_0$ toward a new equilibrium state at the frequency $\omega(t_f) = \omega_f$. Here I focus on the compression stroke $\omega_f > \omega_0$ but the expansion can also be done in the same way.

The state of the particle will be Gaussian during the dynamics and thus can be fully determined by the expectation values $\langle a^\dagger a\rangle(t) = \mathrm{Tr}(a^\dagger a\rho_S(t))$ and $\langle a^2\rangle(t) = \mathrm{Tr}(a^2\rho_S(t))$ characterizing the excitation and the squeezing of the particle. The equations describing their evolution during the driving protocol are obtained in the interaction picture from the master equation (3.84) as

$$
\frac{d\langle\tilde{a}^\dagger\tilde{a}\rangle}{dt} = \frac{\pi}{2\hbar^2}|D(t)|^2 J(\tilde{\omega}(t))\left(n(\tilde{\omega}(t)) - \langle\tilde{a}^\dagger\tilde{a}\rangle\right),
$$

(3.86)

$$
\frac{d\langle\tilde{a}^2\rangle}{dt} = -\frac{\pi}{2\hbar^2}|D(t)|^2 J(\tilde{\omega}(t))\langle\tilde{a}^2\rangle.
$$

(3.87)

Since the particle is initially in a Gibbs state with $\langle\tilde{a}^2\rangle(0) = 0$, it follows from Eq. (3.87) that $\langle\tilde{a}^2\rangle = 0$ at any time during the dynamics. Thus, the protocol is described by the differential equation (3.86) alone. Furthermore, the initial and target states are equilibrium states which

implies $\langle \tilde{a}^\dagger \tilde{a} \rangle (0) = (e^{\frac{\hbar \omega_0}{k_B T}} - 1)^{-1}$, $\langle \tilde{a}^\dagger \tilde{a} \rangle (t_f) = (e^{\frac{\hbar \omega_f}{k_B T}} - 1)^{-1}$ and $\frac{d\langle \tilde{a}^\dagger \tilde{a} \rangle(0)}{dt} = \frac{d\langle \tilde{a}^\dagger \tilde{a} \rangle(t_f)}{dt} = 0$. In addition to these boundary conditions, I impose $\frac{d^2 \langle \tilde{a}^\dagger \tilde{a} \rangle(0)}{dt^2} = \frac{d^2 \langle \tilde{a}^\dagger \tilde{a} \rangle(t_f)}{dt^2} = 0$ to ensure a smooth evolution of the system between the initial state and the target state.

The protocol can now be found by reverse-engineering Eq. (3.86) to obtain the scaling function $b(t)$, which in turn allows one to obtain the trap frequency from the Ermakov equation (3.34). The boundary conditions on $\langle \tilde{a}^\dagger \tilde{a} \rangle$ combined with Eq. (3.86) imply $b(0) = 1$, $b(t_f) = \sqrt{\omega_0/\omega_f}$ and $\dot{b}(0) = \dot{b}(t_f) = 0$. We also obtain additional boundary conditions from the Ermakov equation $\ddot{b}(0) = \ddot{b}(t_f) = 0$.

Those boundary conditions are the same as the STA case. I can thus consider a 6-th order polynomial ansatz for the scaling function $b(t) = \sum_{n=0}^{6} a_n (t/t_f)^n$, in which the first 6 coefficients allow to satisfy the above boundary conditions. The 6-th order term can then ensure that the scaling function connects the initial state and the target state through Eq. (3.86). The coefficient a_6 is simply found by maximizing the fidelity between the target state and the state of the particle at the end of the protocol.

Properties of the shortcut

To quantify the performance of the shortcut, I calculate the fidelity between the target state ρ_T and the state of the particle at the end of the protocol

$$F(\rho_S(t_f), \rho_T) = \text{Tr}\left(\sqrt{\sqrt{\rho_T} \rho_S(t_f) \sqrt{\rho_T}} \right)^2. \qquad (3.88)$$

Since the total Hamiltonian (3.69) is quadratic for the DHO, the states of the particle and the bath remain Gaussian. I can thus numerically track the dynamics without approximation by time-evolving the covariance matrix of the particle as discussed in Sec. 1.3.2. This allows to see when the validity of the master equation actually breaks down for a given set of bath parameters (number of particles, spectral density function) and when the shortcut therefore does not work anymore.

To demonstrate the benefit of the shortcut, I compare it to two simple protocols: the sudden quench $\omega_q(t > 0) = \omega_f$ and a reference ramp described by a polynomial function $\omega_r(t) = \omega_0 + 10\Delta\omega(t/t_f)^3 - 15\Delta\omega(t/t_f)^4 + 6\Delta\omega(t/t_f)^5$ with $\Delta\omega = \omega_f - \omega_0$. For the DHO, the quench protocol is characterized by an asymptotic exponential convergence of the fidelity to one as $F \approx 1 - e^{-t_f/\tau_q}$ where τ_q is a characteristic time related to the decay rates [147]. The physical parameters I choose are the following: the final compression is $\omega_f = 3\omega_0$, the bath temperature $T = \hbar\omega_0/k_B$ and for for the spectral density function, I consider an Ohmic distribution with an abrupt cut-off $J(\omega) = \gamma\omega\Theta(\Lambda - \omega)$ with $\gamma = \hbar^2/500$ and $\Lambda = 100\omega_0$. The number of particles in the bath is $N = 600$.

The fidelity as a function of t_f is shown in Fig. 3.1(a). The STE outperforms the sudden quench and the reference ramp that also shows an asymptotic exponential behavior but with a longer characteristic time than the sudden quench. However, one can see that for short durations, the fidelity for the STE protocol collapses because at shorter times the description provided by the master equation indeed deviates from the exact dynamics. The fidelity reaches approximately the value 0.999 around $t_f \approx 16/\omega_0$ and then keeps increasing to one.

In order to obtain physical insights on the STE protocol the profile of the trap frequency $\omega(t)$ is shown in Fig. 3.1(b) for different protocol durations t_f and compared to the reference

ramp (black dashed line). We see that the profiles are quite different: while for the reference ramp the frequency increases monotonically toward ω_f, in the STE protocol the particle is driven to large trap frequency values at intermediate times before decreasing to reach the final frequency at $t = t_f$. Notably, for faster protocols the particle is driven to higher frequency values. Inversely, for larger t_f, the amplitude of the trap frequency decreases and we observe that the STE protocol actually gets closer to the reference ramp when t_f approaches the adiabatic limit.

Such a trap frequency profile necessarily implies non-equilibrium features in the dynamics. To quantify them, I calculate the coherence in the system during the STE, which has been suggested to play a key role in the control of open quantum systems [150]. We define it as the change of entropy between the diagonal part of the state and the full density matrix in the instantaneous eigenenergy basis [229]

$$C(t) = S\left(\rho_{diag}(t)\right) - S(\rho_S(t)), \tag{3.89}$$

where $S(\rho) = -\operatorname{Tr}(\rho \log(\rho))$ is the von Neumann entropy. The coherence is shown in Fig. 3.1(c). One can see that its profile reflects the results I have shown before: coherence is generated in the system when the trap frequency is changing. It vanishes when the maximum value is reached, and increases again when the trap frequency decreases toward the final value. There is no coherence remaining in the system at the end of the protocol and the amount generated during the dynamics increases for faster protocols.

This also allows to explain why the quench protocol works better than the reference ramp. Indeed, coherence causes transitions of the particle between its eigenstates and can be used as a catalysis that helps to accelerate the thermalization of an open quantum system. A right manipulation of coherence allows to reach the new equilibrium state and this is what the STE shows. Even though this is not the optimal protocol and it does not reach the target state, the sudden quench will thus always work better than a smooth ramp that generates much less non-adiabatic excitations. This is in contrast with STA [25].

Finally I characterized the dynamics of the STE by calculating the effective temperature of the system. During the dynamics, the state of the particle can be written in the interaction picture as $\tilde{\rho}_S(t) = Z(t)^{-1} \sum_n e^{-\epsilon(t)n} |\phi_n(0)\rangle \langle\phi_n(0)|$ with

$$\langle \tilde{a}^\dagger \tilde{a} \rangle(t) = (e^{\epsilon(t)} - 1)^{-1}, \tag{3.90}$$

and the effective partition function is given by $Z(t) = (1 - e^{-\epsilon(t)})^{-1}$. Thus, back to the Schrödinger picture the Hamiltonian is always diagonal in the instantaneous eigenbasis of the DI $\rho_S(t) = Z(t)^{-1} \sum_n e^{-\epsilon(t)n} |\phi_n(t)\rangle \langle\phi_n(t)|$, which shows that similarly to the closed dynamics, the eigenstates of the DI give us the states that the system will explore for a given protocol. We then simply define the effective temperature of the system as

$$T_{\text{eff}}(t) = \frac{\hbar\omega(t)}{k_B \epsilon(t)}. \tag{3.91}$$

The effective temperature of the particle during the STE is shown in Fig. 3.1(d). It deviates significantly from the bath temperature before returning to it at the end of the protocol. More interestingly, the particle is driven to states that are effectively hotter, and the faster the shortcut is, the hotter the state of the particle is. While the shortcut is designed for an
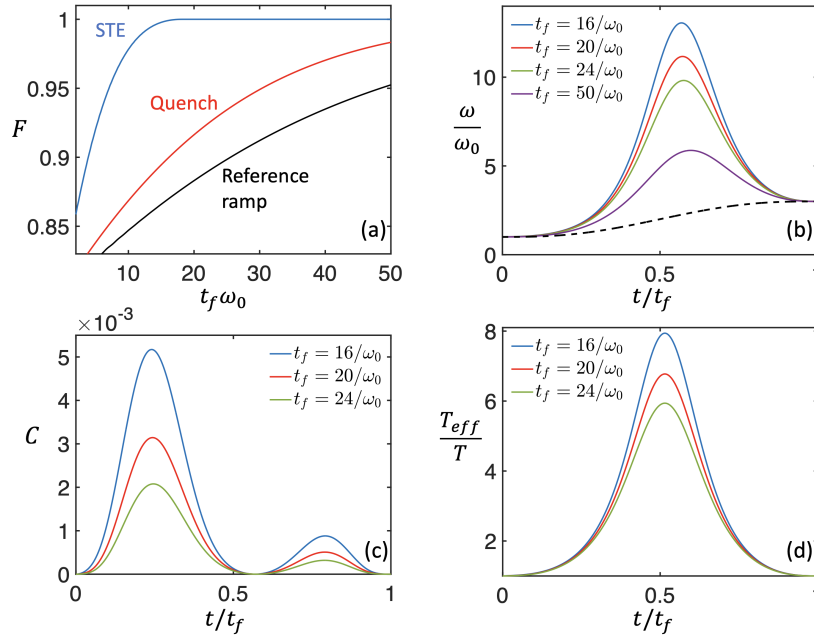
Figure 3.1: (a) Fidelity between the final state and the target state as a function of t_f. (b) Profile of the trap frequency for the STE protocol as a function of time for different protocol durations. The black dashed line shows the reference ramp. (c) Coherence generated during the dynamics of the STE as a function of time. (d) Effective temperature of the particle during the STE protocol as a function of time.

isothermal compression, which corresponds to a cooling process, the strategy adopted by the STE actually consists of warming up the particle in order to cool it down faster.

This is reminiscent of the Mpemba effect [230], an empirical phenomenon where a hot liquid can freeze faster than a cold liquid. Recently, the Mpemba effect has been discussed and predicted for a quantum dot coupled to two reservoirs [231]. Here, we observe a similar feature to the thermal Mpemba effect in the context of driven open quantum systems.

3.2.5 Conclusion and perspectives

In this part of the work, some remarkable results have been obtained that pave the way for improving the control of driven open quantum system and the performance of quantum heat engines in the future. The dynamical invariant has proven to be a powerful framework for describing and accelerating the equilibration for a well known model, without additional restrictions on the timescale of the dynamics beside the Born-Markov approximation.

This work also brings new physical interpretations of the dynamical invariant. Indeed the scaling function $b(t)$, that fully characterizes the invariant, sets both the driving protocol and the decay rates. This allows to derive protocols that modify simultaneously both the unitary part and the dissipative part of the dynamics. Also the eigenstates of the invariant can give access to the states that the particle goes through like in the closed dynamics case.

I was able to show that the STE protocol is characterized by a manipulation of the coherence that drives the particle to hotter states in the case of the isothermal compression. This observation resonates with the thermal Mpemba effect and a rigorous formulation of this phenomenon in the context of driven open quantum systems would be an interesting

direction to take in the future.

However while the progress made are significant, they are still questions that are needed to be addressed. They concerns the irreversibility during the shortcut protocol and the energy cost of realizing such process at finite time. Indeed as the dynamics is non-unitary it will lead to an entropy production [232]. Moreover when the duration of the shortcut protocol decreases, it will cause an increase of the entropy production and being able to quantify it in the future is necessary to rigorously define the performance of a quantum engine assisted by the STE. In particular we saw that the STE is characterized by a large generation of coherence, that is actually genuinely associated to an additional entropy production [233]. The energy cost of the STE also needs to be investigated in the future to evaluate the resources needed to realize such a task [234, 235, 128, 147].

Therefore it would be also very interesting in the future to design shortcuts by minimizing the dissipated work and address the question whether the geometric bound [236, 237, 238] can be reached. While I only considered the isothermal stroke in this work, one can consider different strokes, or start from non-equilibrium states. It would be also possible to design shortcuts for applications other than thermodynamics. For example, the method could be used to design fast and robust protocols for quantum gates [214, 239]. Also recently, a similar approach has been used to rapidly generate entangled states in a double two-level system [240].

Finally, an important extension would be to go beyond the single particle problem and optimize the equilibration of interacting many-body states. While not an easy task, two possible directions are within reach: two particles with short-range interactions [48] and the hardcore Tonks–Girardeau limit [55]. Beside having well-known analytical results, both systems have showed enhanced performances compared to non-interacting quantum engines [193, 197, 1], paving the way for fully-optimized many-body quantum heat engines.

3.3 Optimal control and thermalization of open quantum systems at the speed limit

3.3.1 Motivation and introduction of the research project

While the project presented in the two previous section concerns the control of driven open quantum system for accelerating isothermal strokes, in this project I am interested in the acceleration of the isochoric thermal stroke, that is relevant for optimizing engines described by e.g. the Otto cycle or the Stirling cycle. In that case, the Hamiltonian of the system of interest is constant and the thermalization process is accelerated by finding an appropriate manipulation of the interaction strength between the system and the bath.

Actually only one work so far has been reported in that direction, done by Das and Mukherjee [151]. They considered an Otto cycle with a two-level system as the working medium (WM) and the ioschoric strokes were accelerated by periodically switching on and off the coupling between the WM and the bath. This results in a non-Markovian anti-Zeno effect that reduces the thermalization time. The work is remarkable since they showed that a boost of the engine performance can be achieved with a pure quantum effect. However the proposed protocol is not optimized and finding one that could achieve faster thermalization strokes is definitely within reach.

In this research project, I propose to use well known approaches from optimal control theory [241] to optimize the isochoric stroke. In particular, I use bang-bang type protocols that are a very efficient technique for controlling quantum systems to realize e.g. STA protocols [242, 243], or to prepare a quantum many-body system in a critical ground state [244] and also to design coherent control in order to enhance quantum information processing tasks [245, 246, 247]. I also use the so called chopped random basis (CRAB) algorithm that has been originally developed for optimizing time-dependent density matrix renormalization group simulations [248]. However in the past decade, the algorithm was shown to be a very efficient and powerful technique to use for general quantum optimization tasks [249, 250].

To demonstrate the efficiency of those methods to accelerate the thermalization of an open quantum system, I apply it to the case of a quantum Brownian motion (QBM) whose dynamics can be described without any approximation (see Sec. 1.3.2). Thus non-Markovianity, strong coupling regimes and finite size effects of the bath can be explored.

I also propose a quantum speed limit (QSL) to predict the time below which the optimization fails to converge. The QSL is a fundamental concept that has been developed to characterize the minimum time at which a quantum state can reach a specific target state for a given Hamiltonian, by deriving a bound on the time that is related to the energy of the system [251]. The QSL has been extended to the case of open quantum systems with many different bounds [252, 253, 254, 255]. However most of the works that have been reported fail to actually fulfill the original role of QSL and (maybe worse than that), they can be hard to physically interpret. I will present the derivation of the QSL that I consider and compare it to the results from the optimization for the QBM case.

3.3.2 Model and dynamics

I consider the QBM described by the Caldeira-Leggett model (CL) with a time-dependent coupling between the particle and the bath. The Hamiltonian of the total system is then given by

$$H(t) = H_S + H_B + H_I(t) + H_c(t), \tag{3.92}$$

where the Hamiltonian of the system in a fixed harmonic trap is

$$H_S = \frac{p^2}{2m} + \frac{1}{2}m\omega_S^2 x^2, \tag{3.93}$$

As in the previous projects, the bath consists of a large number of non-interacting harmonic oscillators described by the Hamiltonian

$$H_B = \sum_{n=0}^{N} \left(\frac{p_n^2}{2m_n} + \frac{1}{2}m_n\omega_n^2 \right), \tag{3.94}$$

The interaction between the Brownian particle and the bath is

$$H_I(t) = -g(t)x \sum_{n=0}^{N} \kappa_n x_n, \tag{3.95}$$

where I assume that coupling strength can be manipulated with a scalar function $g(t)$. Finally the counter term is given by

$$H_c(t) = g(t)^2 x^2 \sum_{n=0}^{N} \frac{\kappa_n^2}{2m_n \omega_n^2}. \tag{3.96}$$

Let us note that the counter-term has to scale as $g(t)^2$ to cancel out the divergent renormalization of the Brownian particle. To describe the dynamics of the system, I time evolve the covariance matrix of the particle by using the Heisenberg equation of motion as discussed in Sec. 1.3.2.

3.3.3 Optimal control for finite-time thermalization

Formulation of the problem

The problem is the following: initially the particle is isolated and uncoupled to any environment, denoted by $\rho_S(0)$. The aim is to couple the particle to a bath with an appropriate manipulation of the interaction strength $g(t)$ such that after a given duration of the protocol t_f, the particle is at equilibrium with the bath i.e $\rho_S(t_f) = \rho_T$ where $\rho_T = Z^{-1} e^{-H_S/k_B T}$ is the target Gibbs state with T being the temperature of the bath. Optimal control problems are formulated by minimizing or maximizing a given cost function. Since I want the particle to reach a specific state at a given fixed time t_f, the cost function I consider is simply the fidelity between the final state of the particle and the target state

$$F(\rho_S(t_f), \rho_T) = \text{Tr} \left(\sqrt{\sqrt{\rho_S(t_f)} \rho_T \sqrt{\rho_S(t_f)}} \right)^2. \tag{3.97}$$

We can again take advantage of the fact that for Gaussian states, the fidelity can be simply calculated with the knowledge of covariance matrix only [256, 257]

$$F(\rho_S(t_f), \rho_T) = \frac{2}{\sqrt{\Lambda + \Phi} - \sqrt{\Phi}}. \tag{3.98}$$

where

$$\begin{aligned} \Lambda &= \frac{\det\left(C_S(t_f) + C_T\right)}{\hbar^2}, \\ \Phi &= \left(\frac{\det C_S(t_f)}{\hbar^2} - 1\right)\left(\frac{\det C_T}{\hbar^2} - 1\right), \end{aligned} \tag{3.99}$$

with $C_S(t_f)$ the covariance matrix of the the Brownian particle at the end of the protocol and C_T is the covariance matrix of the target state given by

$$
C_T = \begin{bmatrix} \frac{\hbar}{m\omega_S} \left(1 + \frac{2}{\exp\left(\frac{\hbar\omega_S}{k_B T}\right) - 1}\right) & 0 \\ 0 & \hbar m\omega_S \left(1 + \frac{2}{\exp\left(\frac{\hbar\omega_S}{k_B T}\right) - 1}\right) \end{bmatrix}, \tag{3.100}
$$

The success of speeding up the thermalization will then be ensured by minimizing the infidelity between the final state and the target state

$$
\min_{g(t)} 1 - F(\rho_S(t_f), \rho_T). \tag{3.101}
$$

At first glance, the optimization problem seems challenging. Indeed, the solution is in the set of real functions which is in principle infinitely large and thus could have any type of shape. To find the protocol for such a problem, gradient based methods are commonly used [258]. However, calculating numerically the gradient of a functional can be computationally expensive. This is particularly true when one does not have an analytical expression for the gradient (which is the case here). To solve this issue I decided to use bang-bang type protocols and the CRAB algorithm that have the advantage to simplify the problem by considering a specific ansatz for the coupling strength $g(t)$ and thus reduce the dimension of the solutions space.

Bang–bang type protocols

The bang-bang protocol is defined as

$$
g_{BB}(t) = \begin{cases} g_1 & \text{if } 0 \leq t \leq t_s \\ g_2 & \text{if } t_s < t < t_f. \end{cases} \tag{3.102}
$$

The coupling strength is basically turned on and kept constant at the value g_1 then at $t = t_s$ it suddenly switches to the value g_2, and at $t = t_f$ the Brownian particle is uncoupled from the bath. In that case, the protocol is found by minimizing the infidelity over the coupling strengths g_1, g_2 but also over the time at which the coupling strength changes t_s i.e. only three real parameters, showing the computational advantage of this method. The bang-bang protocol can be generalized to a multi-bang protocol

$$
g_{MB}(t) = \sum_{n=1}^{N_b} g_n \chi_{[t_n, t_{n+1}]}(t), \tag{3.103}
$$

where $\chi_I(t)$ is the characteristic function of the interval I i.e $X_I(t) = 1$ if $t \in I$ and 0 otherwise. The multi-bang protocol allows to explore more complex dynamics than the double-bang and thus potentially obtains a better convergence to the minimum. The optimization is done over $(g_1, g_2, ..., g_{N_b}, t_2, ..., t_{N_b})$ (here $t_1 = 0$ and $t_{N_b+1} = t_f$) i.e. $2N_b - 1$ real parameters.

Chopped random basis algorithm

The CRAB algorithm consists of using a time-dependent protocol that is written as a modulation of a linear or polynomial function that connects the initial and final values that one specifically chooses. The function is modulated by using trigonometric functions. The ansatz is thus given by

$$g_{CRAB}(t) = g_0(t) \left(1 + \sum_{n=1}^{N_c} a_n \cos\left(2\pi f_n t\right) + b_n \sin\left(2\pi f_n t\right) \right), \tag{3.104}$$

where $g_0(t)$ is a polynomial function that I choose to be given by

$$g_0(t) = 16 \left(\frac{t}{t_f}\right)^2 - 32 \left(\frac{t}{t_f}\right)^3 + 16 \left(\frac{t}{t_f}\right)^4. \tag{3.105}$$

The polynomial function is such that $g_0(0) = g_0(t_f) = 0$ and the maximum is reached at the middle of the protocol $g_0(\frac{t_f}{2}) = 1$. I choose this ansatz such that the interaction is smoothly turned on at the beginning of the protocol and smoothly turned off at the end of it. The frequencies are randomly sampled around the harmonics

$$f_n = \frac{n}{t_f}(1 + \xi_n), \tag{3.106}$$

where $\xi_n = U\left(-\frac{1}{2}, \frac{1}{2}\right)$ is a random and uniformly distributed function. The use of random frequencies allows to break the orthogonality of the harmonic basis and it has been shown that it can enhance the performance of the algorithm [249]. The optimization is done over the amplitudes $(a_n, b_n)_{1 \leq n \leq N_c}$ i.e $2N_c$ real parameters where N_c is a cut-off on the number of modes that are initially set. The CRAB algorithm thus woks as follows: I initialize the frequencies $(f_n)_{1 \leq n \leq N_c}$, then I optimize the cost function given by the infidelity Eq. (3.101) over $(a_n, b_n)_{1 \leq n \leq N_c}$. Once the optimization is finished I choose a new set of random frequencies and repeat the procedure. After this is done for several times, I choose the set of frequencies and amplitudes that gives the best result.

Results and comparison between the two methods

For my simulations, I consider the following physical parameters for the bath: I assume that the frequencies of the modes of the bath are linearly distributed $\omega_n = \frac{n}{N}(\omega_N - \omega_0) + \omega_0$, with $\omega_0 = \frac{\omega}{N}$ and $\omega_N = 2\omega_s$. For the spectral density function $J(\omega) = \sum_{n=0}^{N} \frac{\kappa_n^2}{2m_n \omega_n} \delta(\omega - \omega_n)$, I consider an Ohmic distribution with an abrupt cutoff

$$\lim_{N \to \infty} J(\omega) = \frac{m\omega}{\pi} \Theta\left(|\omega| - \omega_N\right), \tag{3.107}$$

where $\Theta(\omega)$ is the Heaviside function. This implies that the constant coupling strength of each mode has to be defined as $\kappa_n = m_n \omega_n \sqrt{\frac{2\omega_N}{\pi N}}$. For the size of the bath, I choose $N = 350$. Those parameters allow to run the dynamics and do the optimization in a reasonable amount of time but more importantly, it allows to study the thermalization of an open
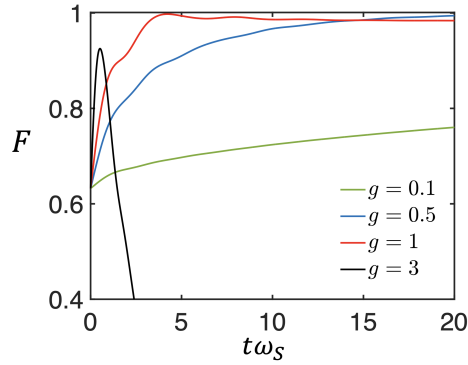
Figure 3.2: Fidelity between the instantaneous state of the Brownian particle $\rho_S(t)$ and the target state ρ_T as a function of time for the case of the sudden quench, and for different interaction strengths.

quantum system in a more realistic set-up. Indeed an ideal Markovian bath is in principle impossible to experimentally create in a quantum platform. Usually the bath will contain a mesoscopic number of particles and the cut-off is not necessarily very large compared the frequency of the particle of interest. For simplicity, I assume that the particle is initially at the ground state $\rho_S(0) = |\psi_0\rangle \langle\psi_0|$ and for the bath temperature, I choose $T = \hbar\omega_S/k_B$.

To benchmark my results, I have also considered the simple case where the Brownian particle is coupled with a constant coupling strength $g(t) = g$, which basically corresponds to the sudden quench and can be seen as a non optimized single-bang protocol. Figure 3.2 shows the fidelity between the instantaneous state of the particle and the target i.e. $F(\rho_S(t), \rho_T)$ as a function of times during the dynamics. I have looked at the dynamics for different interaction strengths between the particle and the bath, which allows to show the different possible behaviors that can occur.

For $g = 0.1$ (green line in Fig. 3.2), the fidelity slowly increases to one showing that the particle is relaxing to equilibrium. For $g = 0.5$ (blue line in Fig. 3.2) the particle also relaxes toward equilibrium but at a significantly faster speed. Indeed for both of those interaction strengths, the dynamics is within the scope of the Born-Markov approximation and thus the particle goes to a stationary state given by the Gibbs state. In this case, the relaxation time is given by the interaction strength and this is why the particle equilibrates faster for stronger interactions.

However for $g = 1$ the behavior starts to differ from the previous cases. The interaction strength is sufficiently high that the bath is also affected by the interaction. Correlations are created and information back-flow starts to occur. The Born-Markov approximation starts to break down and this is why we see that the particle goes away from the equilibrium state even though it gets very close at $t\omega_S = 4.22$ and then oscillates nearby. At $g = 3$ the interaction strength becomes large enough to significantly influence the bath. Strong non-Markovian effects occur leading to a more complex dynamics of the system where the particle goes far away from the Gibbs state.

Figure 3.3 shows the fidelity between the final state of the particle $\rho(t_f)$ and the target state as a function of the duration of the protocol t_f, obtained from both optimal control schemes. The convergence criteria that I choose for both cases is $1 - F(\rho_S(t_f), \rho_T) \leq 10^{-6}$. The panel Fig. 3.3(a) shows the results for the bang-bang method where I consider the single-bang (blue circles), the double-bang (red crosses) and the triple-bang (green diamonds). One can see that for the three cases, the optimal control allows to reach the target state at finite
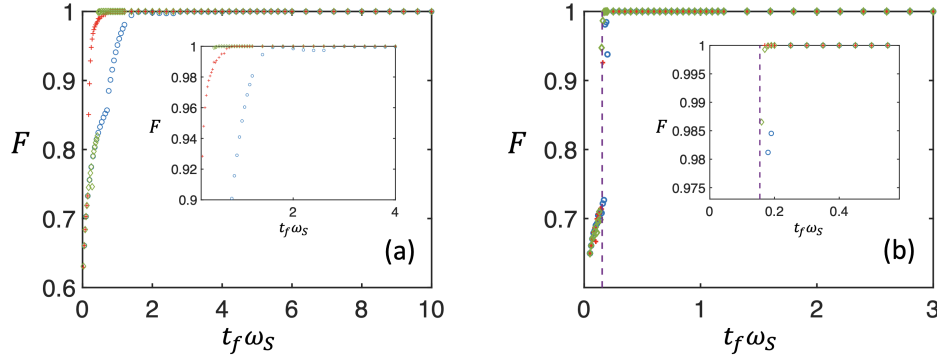
Figure 3.3: (a) Fidelity between the final state $\rho_S(t_f)$ and the target state sate ρ_T of the Brownian particle as a function of the duration of the protocol t_f, obtained with bang-bang type protocols. The blue circle correspond to the single-bang optimal protocol, the red crosses to the double-bang and the green diamonds correspond to the triple-bang. The panel (b) shows the same results obtained with the CRAB algorithm. The blue circles correspond to $N_c = 3$, the green diamonds to $N_c = 4$ and the red crosses to $N_c = 5$. The vertical purple dashed line shows the QSL time.

time and for a timescale significantly better than the relaxation time shown in Fig. 3.2.

However we can also see that for all the three cases, the optimal control fails to converge below a certain time. Another interesting feature is that for an increasing number of bangs, this time decreases, but eventually at some point, the optimization can not converge anymore. For the triple-bang, the fidelity fails to converge to one for $t_f\omega_S \lesssim 0.55$

The panel Fig. 3.3(b) shows the results obtained for the CRAB algorithm where they are plotted in a smaller timescale than the bang-bang method. One can see that the CRAB works better than the bang-bang protocol. This is expected since the ansatz for the CRAB allows to explore more diverse profiles for the interaction strength $g(t)$. However we observe the same feature i.e. the algorithm fails to converge below a certain time, and this time is lower than in the bang-bang case. We can also observe an improvement from $N_c = 3$ (blue circles in Fig. 3.3(b)) to $N_c = 4$ (green diamonds). Nonetheless, both results for $N_c = 4$ and $N_c = 5$ show a very similar performance, suggesting that keeping increasing the cut-off does not improve anymore the optimization. For $N_c = 5$ the optimization fails to converge for $t_f\omega_S \lesssim 0.17$.

We have seen that both optimal control schemes allow to significantly speed up the thermalization of the particle. However both have also the common point that they fail below a certain time. Moreover we see that the fidelity drops drastically. Those results seem to suggest that a fundamental limit on the duration of the protocol exists, that optimal control can not pass beyond. The existence of a quantum speed limit for the thermalization could explain and predict all these observations.

3.3.4 Quantum speed limit for the thermalization of an open quantum system

The concept of quantum speed limit (QSL) as we know it now, was established first by Mandelstam and Tamm [259]. They showed that during the closed dynamics of a quantum system, the time at which the system evolves toward an orthogonal state is bound by the QSL

time

$$\tau_{QSL}^{MT} = \frac{\hbar\pi}{2\Delta H}, \tag{3.108}$$

where ΔH is the variance calculated with respect to the initial state of the system. Later, an alternative expression was derived by Margolus and Levitin [260] based on the expectation value instead of the variance

$$\tau_{QSL}^{ML} = \frac{\hbar\pi}{2\langle H\rangle}. \tag{3.109}$$

They also later showed that the unified bound

$$\tau_{QSL} = \max\left(\frac{\hbar\pi}{2\Delta H}, \frac{\hbar\pi}{2\langle H\rangle}\right), \tag{3.110}$$

is actually tight to predict the orthogonalisation time of a given closed quantum system [261]. The bound has been extended to the case where the final state and the initial state are not orthogonal and separated by an arbitrary angle [262]. It has also been generalized to a large class of metrics by using an information geometric approach [263]. Moreover the QSL is strongly connected to optimal control and sets a fundamental limit for the time at which a quantum system can evolve toward a specific state even if the protocol is optimized.

Indeed, in a remarkable work by Caneva *et. al.* [264], they showed that optimal control applied to the Landau-Zener model fails to work below a time that is predicted by the Mandelstam-Tamm bound. With this result in mind, the existence of a QSL time that also puts a fundamental limit on the time at which the Brownian particle can thermalize is very likely, and this could predict and explain the results that I obtained.

The QSL time has been extended to the case of open quantum system dynamics. Even though various bounds have been derived [252, 253, 254, 255], they unfortunately can not be used in the context of optimal control for open quantum systems and more generally, it is hard to get a physical interpretation for them.

The main reason is due to the mathematical procedure to derive them. Usually one first considers a metric to distinguish the initial quantum state to a time-evolved state (for example the fidelity). Then a bound is derived on the time-derivative of the metric by using inequalities like the Cauchy-Schwartz inequality and the properties of the equation that governs the dynamics (usually a master equation). After integrating the obtained inequality, one can isolate the time and get a bound for it.

However the QSL time will involve time-averaged quantities and thus the QSL time will explicitly depend on the time of the dynamics. In that case it seems very difficult to understand the physical meaning of such a bound and to connect it the original idea of QSL. This is even more true if one considers driving and optimal control protocols. Indeed how can a bound that depends on the actual time protocol tell us when the optimal control protocol will fail?

Derivation of a quantum speed limit time for the thermalization

For the reasons mentioned above, I propose to derive an alternative QSL time as a characteristic time that only depends on the intrinsic properties of the considered open quantum system and predicts a fundamental limit that optimal control can not go beyond as in Ref. [264].

The bound that I derived is inspired by a work done recently by Il'in and Lychkovskiy [265], where they derived a bound for an isolated quantum system that is initially prepared in the Gibbs state.

To derive the bound, I consider the state of the particle plus the bath as an isolated system denoted by the density matrix ρ. Considering the total system can be an interesting approach to use techniques similar to ones in the closed dynamics case. Initially, the total state is given by the product state $\rho(0) = \rho_S(0) \otimes \rho_B$ with the Hamiltonian $H_S + H_B = H_0$ and I assume that it gets perturbed by an interaction term H_I. The dynamics is then dictated by the von Neumann equation

$$i\hbar \frac{d\rho(t)}{dt} = [H_0 + H_I, \rho(t)].$$
(3.111)

Let me remark that I assume the interaction term to be time-independent. This allows to simplify the derivation and to ensure that the bound will only depend on intrinsic properties of the system. Moreover, the same approach has been considered for the Mandelstam-Tamm bound that has been derived originally for a quench, and this same bound has been used by Caneva *et. al.* [264]. Now I need to choose a metric that measures the distance between two quantum states. As in Ref. [265], I use the quantum Hellinger distance defined as [266]

$$D(\rho_1, \rho_2) = 1 - \text{Tr}(\sqrt{\rho_1}\sqrt{\rho_2}).$$
(3.112)

The quantum Hellinger distance can be related to the fidelity through the following inequality with the Bures angle [267]

$$L(\rho_1, \rho_2) \leq \arcsin\left(\sqrt{2D(\rho_1, \rho_2)}\right),$$
(3.113)

where

$$L(\rho_1, \rho_2) = \arccos\left(\sqrt{F(\rho_1, \rho_2)}\right)$$
(3.114)

Now that I have chosen a metric that characterizes the distance between the initial state of the system $\rho(0)$ and the instantaneous state during the dynamics $\rho(t)$, I can define an instantaneous speed which is simply given by the time derivative of the quantum Hellinger distance $\frac{dD(\rho(0),\rho(t))}{dt}$. An expression of the speed can be obtained by using the fact that the square root of the total density matrix $\sqrt{\rho}$ also satisfies the von Neumann equation

$$i\hbar \frac{d\sqrt{\rho(t)}}{dt} = \left[H_0 + H_I, \sqrt{\rho(t)}\right].$$
(3.115)

By assuming that $[H_0, \rho(0)] = 0$, one can show that the instantaneous speed is given by

$$\frac{dD}{dt} = \frac{i}{\hbar} \text{Tr}\left(\left[\sqrt{\rho(0)}, H_I\right]\sqrt{\rho(t)}\right).$$
(3.116)

Now I can upper bound the speed by using the Cauchy-Schwartz inequality for the trace

$$\left|\frac{dD}{dt}\right| \leq \frac{1}{\hbar}\sqrt{\text{Tr}\left(\left[\sqrt{\rho(0)}, H_I\right]^2\right)}\sqrt{\text{Tr}(\rho(t))} = \frac{\sqrt{\text{Tr}\left(\left[\sqrt{\rho(0)}, H_I\right]^2\right)}}{\hbar}.$$
(3.117)

The quantum Hellinger distance between the initial state and the instantaneous state can then be upper bound by integrating the above inequality

$$|D(\rho(0), \rho(t))| \leq \int_0^t \left| \frac{dD}{d\tau} d\tau \right| \leq t \frac{\sqrt{\mathrm{Tr}\left(\left[\sqrt{\rho(0)}, H_I \right]^2 \right)}}{\hbar}. \tag{3.118}$$

Next I assume the instantaneous state is given by a product of the target state of the Brownian particle and the bath $\rho(t) = \rho_T \otimes \rho_B$. This gives the following bound on the time evolution

$$t \geq \frac{\hbar |D(\rho(0), \rho_T)|}{\sqrt{\mathrm{Tr}\left(\left[\sqrt{\rho_S(0)} \otimes \sqrt{\rho_B}, H_I \right]^2 \right)}}. \tag{3.119}$$

The bound is based on the quantum Hellinger distance, but one can go back to the fidelity through the Bures angle by using the inequality (3.113) and get

$$t \geq \frac{\hbar \sin^2 \left(L \left(\rho_S(0), \rho_T \right) \right)}{2 \sqrt{\mathrm{Tr}\left(\left[\sqrt{\rho_S(0)} \otimes \sqrt{\rho_B}, H_I \right]^2 \right)}} = \tau_{QSL}. \tag{3.120}$$

The bound obtained using the Bures angle is more consistent with the fact that I use the fidelity as a cost function to find the optimal protocol. By using the well known relation $\sin(\arccos(x)) = \sqrt{1 - x^2}$, the QSL time can be rewritten as

$$\tau_{QSL} = \frac{\hbar \left(1 - F(\rho_S(0), \rho_T) \right)}{2 \sqrt{\mathrm{Tr}\left(\left[\sqrt{\rho_S(0)} \otimes \sqrt{\rho_B}, H_I \right]^2 \right)}}. \tag{3.121}$$

Applied to my case with $\rho(0) = |\psi_0\rangle \langle \psi_0|$, $\rho_T = Z^{-1} e^{-\frac{H_S}{k_B T}}$ and $H_I = -x \sum_{n=0}^{n=N} \kappa_n x_n$, I obtain the following QSL time for the thermalization of the quantum Brownian motion

$$\tau_{QSL} = \frac{\sqrt{m\omega_S} e^{-\frac{\hbar\omega_S}{k_B T}}}{2\sqrt{\sum_{n=0}^N \frac{\kappa_n^2}{2m_n\omega_n} \coth\left(\frac{\hbar\omega_n}{2k_B T} \right)}} = \frac{\sqrt{m\omega_S} e^{-\frac{\hbar\omega_S}{k_B T}}}{2\sqrt{\int_0^{\omega_N} J(\omega) \coth\left(\frac{\hbar\omega}{2k_B T} \right) d\omega}}. \tag{3.122}$$

The obtained QSL time seems to satisfy the main desired criteria i.e an explicit dependency on the intrinsic properties of the system. In particular, the influence of the bath can be written in terms of the spectral density function. Let us remark that for an Ohmic spectral density function, the integral in the denominator tends to infinity when the cut-off ω_N goes to infinity and thus the bound tends to zero. It implies that for an ideal Markovian bath, there is no limit on how fast the particle can thermalize.

The result is in accordance with relaxation processes and the result I show for the quench case (Fig. 3.2). Indeed a particle in contact with a Markovian bath will always relax to
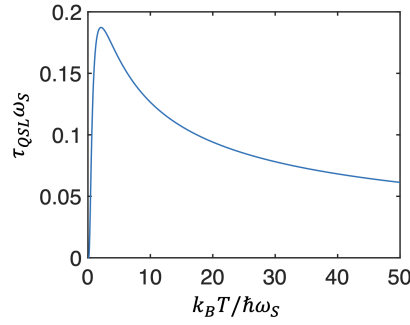
Figure 3.4: Quantum speed limit for the thermalization of the Brownian particle particle as a function of the bath temperature.

equilibrium and the stronger the interaction is, the faster the process is. In conclusion, if the particle is in a contact with an ideal Markovian bath, then one can always keep increasing the interaction strength to accelerate the thermalization.

Besides the spectral density function, the bound is also strongly influenced by the temperature. Figure 3.4 shows the bound as a function of the bath temperature. We see that the QSL time increases with increasing temperature which can be explained by the fact that when the temperatures increases, the initial state and the target state become distant. However we can see that the QSL time starts to decrease after some temperature and reach a plateau. This suggests that when the temperature increases, the average speed of the evolution of the particle increases due to an increase of the energy of the bath, and at some point, it increases faster than the distance between the initial state and the target state.

With the parameters that I consider for the optimal control, the numerical application of the bound gives $\tau_{QSL}\omega_S \approx 0.1547$ while the optimal control by using the CRAB algorithm fails below $t_f\omega_S \approx 0.17$ (see the vertical purple dashed line in Fig. 3.3), showing that the proposed bound seems to be promising for predicting timescales of physical processes in open quantum systems.

3.3.5   Conclusion and perspectives

In this research project, I have shown that tools from optimal control theory can be successfully used to accelerate the thermalization of an open quantum system by considering the QBM. I have used bang-bang protocols and the CRAB algorithm that have the advantage to simplify the optimization scheme, and as in previous works on quantum control, they both proved to work very well. Indeed, even though thermalization is in principle a very slow process, both methods allow to reach the equilibrium state in a finite time and over timescales that are much shorter than the relaxation time for a simple quench. The CRAB algorithm gives better results as it allows to explore more complicated profile of the interaction strength during the protocol.

We have also seen that in both cases, the optimal control scheme fails to converge below a certain time even if the number of parameters is increased. This strongly suggests that the optimal control can not work at an arbitrary time because of the existence of a QSL as in Ref. [264]. I thus derived a QSL time that could explain and predict this observation. The QSL was derived by considering the time-evolution of the square root of the density matrix of the Brownian particle plus the bath. This also allows to get rid of the time dependency of

the state and obtain a bound that only depends on the intrinsic properties of the system.

The QSL bound strongly depends on the properties of the bath through the spectral density function and the temperature. The bound that I have obtained is in agreement with the results from the optimal control. This suggests that it could be eventually used in other applications that involve open quantum system dynamics.

However, even though major results have been obtained, the project remains unfinished before considering an eventual publication of it in the future. To complete this project, I also want to do the optimization for different values of the cut-off of the bath ω_N and for different numbers particles N. I want to see how this affects the optimization performance and if the QSL time can still match the results. In particular I want to see how non-Markovianity affects the speed of evolution during the optimal control [268].

For that, I plan to only focus on the CRAB algorithm since it works better than the ban-bang approach, and I also want to take $N_c = 6$ to see if the optimization gets even closer to the bound. I also plan to consider different initial states. In particular I want see if non-equilibrium states and more generally the presence of non-diagonal terms in the density matrix can influence the performance of the optimization. And again I want to see if this can also be predicted with the QSL time.

After that, several other interesting directions can be considered from this work. The most straightforward one is to apply the approach to realize an optimized quantum Otto cycle, where the adiabatic stokes could be optimized with STA techniques. Another interesting direction to consider, would be to do the optimization by also minimizing the energetic cost of the control protocol. The QSL could be also applied to scale the power output of quantum heat engines [126, 269]. But it could also potentially be used for different applications like in quantum gates e.g. to give a fundamental limit on the speed of quantum information processing task by taking account of the environment [213, 215].

Conclusion

In this thesis, I have explored the quantum properties of quantum heat engines by considering the great versatility of cold atomic systems as an experimental platform. To do that, I first exploited the physical properties of interacting few-body systems, and proposed original ways to design heat engines for cooling and work extraction processes. Then I proposed techniques for realizing fast thermalization protocols in open quantum systems to boost the performance of quantum heat engines. The models that I considered describe physical systems that are realistic to be studied in cold atoms laboratories. Therefore all the results that I have shown emphasize the determinant role of cold atomic systems in the exploration and development of quantum engines.

The first part of my work explored processes and phenomena with no classical counterparts. Indeed the study of the anomalous heat flow in Section 2.1 can be only observed and measured with quantum correlations while classical correlations only lead to effects too small to be measurable. The quantum heat engine enhanced by the interaction in Section 2.2 can only be realized by considering atomic systems that interact at the quantum level.

In the second part of my work, I explored new approaches but also well known established techniques to control open quantum systems. The use of STA techniques combined with a stochastic description of open quantum systems in Section 3.1 has not been studied so far for designing STE protocols. The use of the dynamical invariant to derive a time-dependent quantum master equation is a very recent approach, and I am the first to propose to use it for STEs in open quantum systems. Finally bang-bang protocols and the CRAB algorithm are well known methods for optimal control theory, and I exploited their effectiveness in the specific case of quantum isochoric strokes in Section 3.3. The last two projects showed to be efficient to realize fast equilibration protocols and improve the performance of quantum heat engines, while for the first project, further investigations are needed in the future.

I also showed with my work that while quantum heat engines exploit quantum properties with no classical equivalences, this does not necessarily means that one can obtain an advantage in terms of performance. We saw in Section 2.1 that quantum correlations can allow us to realize cooling process and in Section 3.2 that coherence allows us to speed-up the thermalization of an open quantum system. However we also saw in Section 2.2 that quantum statistics can actually limit the performance of quantum heat engines and distinguishable particles are a better choice for an interacting working medium. Moreover the same coherence that improves thermalization strokes also decreases the performance of a quantum heat engine when the adiabatic strokes are realized at finite time.

My work resulted in one publication in a peer reviewed journal [1] and another preprint manuscript that is now under review [2]. Moreover, I emphasized in the thesis various inter-

esting directions that can be taken in the future in the continuity of this work. For example a generalization of the project presented in Section 2.2 to larger systems with the Lieb-Liniger model is now investigated by another PhD student in my research group.

In the future experimental implementations of my work are also definitely within reach. Indeed experimental cold atomic quantum heat engines involving a change of the trapping potential and the scattering length have been recently reported [23, 24] and therefore the quantum heat engine that I proposed could also be implemented with a large number of particles. Also a single particle cold atomic engine with controlled collisions with the bath has been experimentally realized [21] and could be a great platform to implement the control protocols that I developed in the second part of my PhD. Finally while the shortcut technique that I propose and the optimal control schemes that I apply can definitely improve the performance of quantum engines, they can also have applications beyond quantum thermodynamics as they target the general problem of preparing quantum states in the presence of an environment.

Bibliography

[1] M. Boubakour, T. Fogarty, and T. Busch, *Interaction-enhanced quantum heat engine*, Phys. Rev. Res. **5**, 013088 (2023).

[2] M. Boubakour, S. Endo, T. Fogarty, and T. Busch, *Dynamical invariant based shortcut to equilibration*, arXiv **2401.11659** (2024).

[3] D. Kondepudi and I. Prigogine, *Modern Thermodynamics*, John Wiley and Sons, Ltd (2014).

[4] R. Landauer, *Information is Physical*, Physics Today **44**, 23–29 (1991).

[5] J. M. R. Parrondo, J. M. Horowitz, and T. Sagawa, *Thermodynamics of information*, Nature Physics **8**, 131–139 (2015).

[6] U. Seifert, *Stochastic thermodynamics, fluctuation theorems and molecular machines*, Reports on Progress in Physics **75**, 126001 (2012).

[7] S. Vinjanampathy and J. Anders, *Quantum thermodynamics*, Contemporary Physics **57**, 545–579 (2016).

[8] F. Binder, L. A. Correa, C. Gogolin, J. Anders, and G. Adresso, *Thermodynamics in the Quantum Regime*, Springer (2018).

[9] R. Alicki and R. Kosloff. *Introduction to Quantum Thermodynamics: History and Prospects*, pages 1–33. Springer International Publishing, Cham, (2018).

[10] R. Kosloff and A. Levy, *Quantum Heat Engines and Refrigerators: Continuous Devices*, Annual Review of Physical Chemistry **65**, 365–393 (2014).

[11] J. Roßnagel, S. T. Dawkins, K. N. Tolazzi, O. Abah, E. Lutz, F. Schmidt-Kaler, and K. Singer, *A single-atom heat engine*, Science **352**, 325–329 (2016).

[12] O. Abah, J. Roßnagel, G. Jacob, S. Deffner, F. Schmidt-Kaler, K. Singer, and E. Lutz, *Single-Ion Heat Engine at Maximum Power*, Phys. Rev. Lett. **109**, 203006 (2012).

[13] J. P. S. Peterson, T. B. Batalhão, M. Herrera, A. M. Souza, R. S. Sarthour, I. S. Oliveira, and R. M. Serra, *Experimental Characterization of a Spin Quantum Heat Engine*, Phys. Rev. Lett. **123**, 240601 (2019).

[14] M. H. Anderson, J. R. Ensher, M. R. Matthews, C. E. Wieman, and E. A. Cornell, *Observation of Bose-Einstein Condensation in a Dilute Atomic Vapor*, Science **269**, 198–201 (1995).

[15] K. B. Davis, M. O. Mewes, M. R. Andrews, N. J. van Druten, D. S. Durfee, D. M. Kurn, and W. Ketterle, *Bose-Einstein Condensation in a Gas of Sodium Atoms*, Phys. Rev. Lett. **75**, 3969–3973 (1995).

[16] H. Feshbach, *Unified theory of nuclear reactions*, Annals of Physics **5**, 357–390 (1958).

[17] S. Inouye, M. R. Andrews, J. Stenger, H.-J. Miesner, D. M. Stamper-Kurn, and W. Ketterle, *Observation of Feshbach resonances in a Bose-Einstein condensate*, Nature **392**, 151–154 (1998).

[18] P. Courteille, R. S. Freeland, D. J. Heinzen, F. A. van Abeelen, and B. J. Verhaar, *Observation of a Feshbach Resonance in Cold Atom Scattering*, Phys. Rev. Lett. **81**, 69–72 (1998).

[19] D. Barredo, V. Lienhard, S. de Léséleuc, T. Lahaye, and A. Browaeys, *Synthetic three-dimensional atomic structures assembled atom by atom*, Nature **561**, 79–82 (2018).

[20] Y. Zou, Y. Jiang, Y. Mei, X. Guo, and S. Du, *Quantum Heat Engine Using Electromagnetically Induced Transparency*, Phys. Rev. Lett. **119**, 050602 (2017).

[21] Q. Bouton, J. Nettersheim, S. Burgardt, D. Adam, E. Lutz, and A. Widera, *A quantum heat engine driven by atomic collisions*, Nature Communications **12**, 2063 (2021).

[22] J. Nettersheim, S. Burgardt, Q. Bouton, D. Adam, E. Lutz, and A. Widera, *Power of a Quasispin Quantum Otto Engine at Negative Effective Spin Temperature*, PRX Quantum **3**, 040334 (2022).

[23] J. Koch, K. Menon, E. Cuestas, S. Barbosa, E. Lutz, T. Fogarty, T. Busch, and A. Widera, *A quantum engine in the BEC-BCS crossover*, Nature **621**, 723–727 (2023).

[24] E. Q. Simmons, R. Sajjad, K. Keithley, H. Mas, J. L. Tanlimco, E. Nolasco-Martinez, Y. Bai, G. H. Fredrickson, and D. M. Weld, *Thermodynamic engine with a quantum degenerate working fluid*, Phys. Rev. Res. **5**, L042009 (2023).

[25] D. Guéry-Odelin, A. Ruschhaupt, A. Kiely, E. Torrontegui, S. Martínez-Garaot, and J. G. Muga, *Shortcuts to adiabaticity: Concepts, methods, and applications*, Rev. Mod. Phys. **91**, 045001 (2019).

[26] H. R. Lewis and W. B. Riesenfeld, *An Exact Quantum Theory of the Time-Dependent Harmonic Oscillator and of a Charged Particle in a Time-Dependent Electromagnetic Field*, J. Math. Phys. **10**, 1458–1473 (1969).

[27] A. O. Caldeira and A. J. Leggett, *Influence of Dissipation on Quantum Tunneling in Macroscopic Systems*, Phys. Rev. Lett. **46**, 211–214 (1981).

[28] A. Caldeira and A. Leggett, *Path integral approach to quantum Brownian motion*, Physica A: Statistical Mechanics and its Applications **121**, 587–616 (1983).

[29] H.-P. Breuer and F. Petruccione, *The theory of Open Quantum Systems*, Oxford University Press (2002).

[30] A. Rivas, A. D. K. Plato, S. F. Huelga, and M. B. Plenio, *Markovian master equations: a critical study*, New Journal of Physics **12**, 113032 (2010).

[31] S. N. Bose, *Plancks Gesetz und Lichtquantenhypothese*, Zeitschrift für Physik **26**, 178–181 (1924).

[32] L. Pitaevskii and S. Stringari, *Bose-Einstein Condensation and Superfluidity*, Oxford University Press (2016).

[33] T.-L. Ho, *Spinor Bose Condensates in Optical Traps*, Phys. Rev. Lett. **81**, 742–745 (1998).

[34] M. R. Andrews, C. G. Townsend, H.-J. Miesner, D. S. Durfee, D. M. Kurn, and W. Ketterle, *Observation of Interference Between Two Bose Condensates*, Science **275**, 637–641 (1997).

[35] M. Greiner, O. Mandel, T. Esslinger, T. W. Hänsch, and I. Bloch, *Quantum phase transition from a superfluid to a Mott insulator in a gas of ultracold atoms*, Nature **415**, 39–44 (2002).

[36] P. A. M. Dirac, *On the theory of quantum mechanics*, Proceedings of the Royal Society of London. Series A , 661–677 (1926).

[37] L. H. Hoddeson, G. Baym, and N. F. Mott, *The development of the quantum mechanical electron theory of metals: 1900-28*, Proceedings of the Royal Society of London. A. Mathematical and Physical Sciences **371**, 8–23 (1980).

[38] R. H. Fowler, *On Dense Matter*, Monthly Notices of the Royal Astronomical Society **87**, 114–122 (1926).

[39] B. DeMarco and D. S. Jin, *Onset of Fermi Degeneracy in a Trapped Atomic Gas*, Science **285**, 1703–1706 (1999).

[40] F. Schreck, L. Khaykovich, K. L. Corwin, G. Ferrari, T. Bourdel, J. Cubizolles, and C. Salomon, *Quasipure Bose-Einstein Condensate Immersed in a Fermi Sea*, Phys. Rev. Lett. **87**, 080403 (2001).

[41] H. Bethe, *Zur Theorie der Metalle*, Zeitschrift für Physik **71**, 205–226 (1931).

[42] M. A. Cazalilla, R. Citro, T. Giamarchi, E. Orignac, and M. Rigol, *One dimensional bosons: From condensed matter systems to ultracold gases*, Rev. Mod. Phys. **83**, 1405–1466 (2011).

[43] J. M. Zhang and R. X. Dong, *Exact diagonalization: the Bose-Hubbard model as an example*, European Journal of Physics **31**, 591 (2010).

[44] J.-H. Jung and J. D. Noh, *Guide to Exact Diagonalization Study of Quantum Thermalization*, Journal of the Korean Physical Society **76**, 670 (2020).

[45] S. Dettmer, D. Hellweg, P. Ryytty, J. J. Arlt, W. Ertmer, K. Sengstock, D. S. Petrov, G. V. Shlyapnikov, H. Kreutzmann, L. Santos, and M. Lewenstein, *Observation of Phase Fluctuations in Elongated Bose-Einstein Condensates*, Phys. Rev. Lett. **87**, 160406 (2001).

[46] A. Görlitz, J. M. Vogels, A. E. Leanhardt, C. Raman, T. L. Gustavson, J. R. Abo-Shaeer, A. P. Chikkatur, S. Gupta, S. Inouye, T. Rosenband, and W. Ketterle, *Realization of Bose-Einstein Condensates in Lower Dimensions*, Phys. Rev. Lett. **87**, 130402 (2001).

[47] E. H. Lieb and W. Liniger, *Exact Analysis of an Interacting Bose Gas. I. The General Solution and the Ground State*, Phys. Rev. **130**, 1605–1616 (1963).

[48] T. Busch, B.-G. Englert, K. Rzażewski, and M. Wilkens, *Two Cold Atoms in a Harmonic Trap*, Foundations of Physics **28**, 549–559 (1998).

[49] C. J. Pethick and H. Smith. *Interactions between atoms*, pages 109–158. Cambridge University Press, 2 edition, (2008).

[50] P. O. Fedichev, Y. Kagan, G. V. Shlyapnikov, and J. T. M. Walraven, *Influence of Nearly Resonant Light on the Scattering Length in Low-Temperature Atomic Gases*, Phys. Rev. Lett. **77**, 2913–2916 (1996).

[51] K. M. Jones, E. Tiesinga, P. D. Lett, and P. S. Julienne, *Ultracold photoassociation spectroscopy: Long-range molecules and atomic scattering*, Rev. Mod. Phys. **78**, 483–535 (2006).

[52] C. Chin, R. Grimm, P. Julienne, and E. Tiesinga, *Feshbach resonances in ultracold gases*, Rev. Mod. Phys. **82**, 1225–1286 (2010).

[53] M. Olshanii, *Atomic Scattering in the Presence of an External Confinement and a Gas of Impenetrable Bosons*, Phys. Rev. Lett. **81**, 938–941 (1998).

[54] M. D. Girardeau, E. M. Wright, and J. M. Triscari, *Ground-state properties of a one-dimensional system of hard-core bosons in a harmonic trap*, Phys. Rev. A **63**, 033601 (2001).

[55] M. Girardeau, *Relationship between Systems of Impenetrable Bosons and Fermions in One Dimension*, Journal of Mathematical Physics **1**, 516–523 (1960).

[56] B. Paredes, A. Widera, V. Murg, O. Mandel, S. Fölling, I. Cirac, G. V. Shlyapnikov, T. W. Hänsch, and I. Bloch, *Tonks-Girardeau gas of ultracold atoms in an optical lattice*, Nature **429**, 277–281 (2004).

[57] T. Kinoshita, T. Wenger, and D. S. Weiss, *Observation of a One-Dimensional Tonks-Girardeau Gas*, Science **305**, 1125–1128 (2004).

[58] S. Deffner and S. Campbell, *Quantum Thermodynamics: An introduction to the thermodynamics of quantum information*, arXiv:1907.01596v1 (2020).

[59] R. Clausius, *Uber eine veranderte Form des zweiten Hauptsatzes der mechanischen Warmetheorien*, Annalen der Physik und Chemie **93:481** (1854).

[60] L. Landau and E. Lifshitz. *Chapter II - Thermodynamic Quantities*. In L. Landau and E. Lifshitz, editors, *Statistical Physics (Third Edition)*, pages 34 − 78. Butterworth-Heinemann, Oxford, third edition edition, (1980).

[61] S. Vinjanampathy and J. Anders, *Quantum thermodynamics*, Contemporary Physics **57**, 545–579 (2016).

[62] R. Kosloff and A. Levy, *Quantum Heat Engines and Refrigerators: Continuous Devices*, Annual Review of Physical Chemistry **65**, 365–393 (2014).

[63] J. Klatzow, J. N. Becker, P. M. Ledingham, C. Weinzetl, K. T. Kaczmarek, D. J. Saunders, J. Nunn, I. A. Walmsley, R. Uzdin, and E. Poem, *Experimental Demonstration of Quantum Effects in the Operation of Microscopic Heat Engines*, Phys. Rev. Lett. **122**, 110601 (2019).

[64] W. Niedenzu, V. Mukherjee, A. Ghosh, A. G. Kofman, and G. Kurizki, *Quantum engine efficiency bound beyond the second law of thermodynamics*, Nature Communications **9**, 165 (2018).

[65] F. Brandao, M. Horodecki, N. Ng, J. Oppenheim, and S. Wehner, *The second laws of quantum thermodynamics*, Proceedings of the National Academy of Sciences **112**, 3275–3279 (2015).

[66] P. Strasberg and A. Winter, *First and Second Law of Quantum Thermodynamics: A Consistent Derivation Based on a Microscopic Definition of Entropy*, PRX Quantum **2**, 030202 (2021).

[67] L. Buffoni, S. Gherardini, E. Zambrini Cruzeiro, and Y. Omar, *Third Law of Thermodynamics and the Scaling of Quantum Computers*, Phys. Rev. Lett. **129**, 150602 (2022).

[68] M. Lobejko, *The tight Second Law inequality for coherent quantum systems and finite-size heat baths*, Nature Communications **12**, 918 (2021).

[69] L. d. Rio, J. Åberg, R. Renner, O. Dahlsten, and V. Vedral, *The thermodynamic meaning of negative entropy*, Nature **474**, 61–63 (2011).

[70] Y. Guryanova, S. Popescu, A. J. Short, R. Silva, and P. Skrzypczyk, *Thermodynamics of quantum systems with multiple conserved quantities*, Nature Communications **7**, 12049 (2016).

[71] M. Horodecki and J. Oppenheim, *Fundamental limitations for quantum and nanoscale thermodynamics*, Nature Communications **4**, 2059 (2013).

[72] M. Lostaglio, D. Jennings, and T. Rudolph, *Description of quantum coherence in thermodynamic processes requires constraints beyond free energy*, Nature Communications **6**, 7383 (2016).

[73] P. Skrzypczyk, A. J. Short, and S. Popescu, *Work extraction and thermodynamics for individual quantum systems*, Nature Communications **5**, 4185 (2014).

[74] R. Kosloff, *Quantum Thermodynamics: A Dynamical Viewpoint*, Entropy **15**, 2100–2128 (2013).

[75] A. Levy and R. Kosloff, *The local approach to quantum transport may violate the second law of thermodynamics*, Europhysics Letters **107**, 20004 (2014).

[76] R. Dann and R. Kosloff, *Unification of the first law of quantum thermodynamics*, New Journal of Physics **25**, 043019 (2023).

[77] B. Gardas and S. Deffner, *Thermodynamic universality of quantum Carnot engines*, Phys. Rev. E **92**, 042126 (2015).

[78] D. A. Lidar, *Lecture Notes on the Theory of Open Quantum Systems*, arXiv:1902.00967v2 (2019).

[79] M. F. Gelin and M. Thoss, *Thermodynamics of a subensemble of a canonical ensemble*, Phys. Rev. E **79**, 051121 (2009).

[80] H. Peter, I. Gert-Ludwig, and T. Peter, *Finite quantum dissipation: the challenge of obtaining specific heat*, New Journal of Physics **10**, 115008 (2008).

[81] B. L. Hu, J. P. Paz, and Y. Zhang, *Quantum Brownian motion in a general environment: Exact master equation with nonlocal dissipation and colored noise*, Phys. Rev. D **45**, 2843–2861 (1992).

[82] C. Hörhammer and H. Büttner, *Information and Entropy in Quantum Brownian Motion*, J. Stat. Phys **133**, 1161–1174 (2008).

[83] M. N. Bera, A. Riera, M. Lewenstein, and A. Winter, *Generalized laws of thermodynamics in the presence of correlations*, Nature Communications **8**, 2180 (2017).

[84] V. Vedral, *The role of relative entropy in quantum information theory*, Rev. Mod. Phys. **74**, 197–234 (2002).

[85] R. Landauer, *Information is Physical*, Phys. Tod. **44**, 23 (1991).

[86] S. Lloyd, *Use of mutual information to decrease entropy: Implications for the second law of thermodynamics*, Phys. Rev. A **39**, 5378–5386 (1989).

[87] V. Vedral. *The Arrow of Time and Correlations in Quantum Physics*, (2016).

[88] L. Maccone, *Quantum Solution to the Arrow-of-Time Dilemma*, Phys. Rev. Lett. **103**, 080401 (2009).

[89] M. H. Partovi, *Entanglement versus Stosszahlansatz: Disappearance of the thermodynamic arrow in a high-correlation environment*, Phys. Rev. E **77**, 021110 (2008).

[90] D. Jennings and T. Rudolph, *Entanglement and the thermodynamic arrow of time*, Physical Review E **81** (2010).

[91] I. Henao and R. M. Serra, *Role of quantum coherence in the thermodynamics of energy transfer*, Phys. Rev. E **97**, 062105 (2018).

[92] K. Micadei, J. P. S. Peterson, A. M. Souza, R. S. Sarthour, I. S. Oliveira, G. T. Landi, T. B. Batalhão, R. M. Serra, and E. Lutz, *Reversing the direction of heat flow using quantum correlations*, Nat. Commun. **10**, 2456 (2019).

[93] R. S. of Edinburgh., *Transactions of the Royal Society of Edinburgh*, Edinburgh, Royal Society of Edinburgh, (1850). https://www.biodiversitylibrary.org/bibliography/2290.

[94] S. Carnot, *Réflexions sur la puissance motrice du feu et sur les machines propres à développer cette puissance*, Paris: Bachelier (1824).

[95] H. T. Quan, Y.-x. Liu, C. P. Sun, and F. Nori, *Quantum thermodynamic cycles and quantum heat engines*, Phys. Rev. E **76**, 031105 (2007).

[96] F. L. Curzon and B. Ahlborn, *Efficiency of a Carnot engine at maximum power output*, American Journal of Physics **43**, 22–24 (1975).

[97] H. S. Leff, *Thermal efficiency at maximum work output: New results for old heat engines*, American Journal of Physics **55**, 602–610 (1987).

[98] C. Van den Broeck, *Thermodynamic Efficiency at Maximum Power*, Phys. Rev. Lett. **95**, 190602 (2005).

[99] M. Esposito, K. Lindenberg, and C. Van den Broeck, *Universality of Efficiency at Maximum Power*, Phys. Rev. Lett. **102**, 130602 (2009).

[100] M. Esposito, R. Kawai, K. Lindenberg, and C. Van den Broeck, *Efficiency at Maximum Power of Low-Dissipation Carnot Engines*, Phys. Rev. Lett. **105**, 150603 (2010).

[101] C. Van den Broeck, N. Kumar, and K. Lindenberg, *Efficiency of Isothermal Molecular Machines at Maximum Power*, Phys. Rev. Lett. **108**, 210602 (2012).

[102] A. E. Allahverdyan, R. S. Johal, and G. Mahler, *Work extremum principle: Structure and function of quantum heat engines*, Phys. Rev. E **77**, 041118 (2008).

[103] Y. Izumida and K. Okuda, *Molecular kinetic analysis of a finite-time Carnot cycle*, Europhysics Letters **83**, 60003 (2008).

[104] T. Schmiedl and U. Seifert, *Efficiency at maximum power: An analytically solvable model for stochastic heat engines*, Europhysics Letters **81**, 20003 (2007).

[105] M. Esposito, K. Lindenberg, and C. V. den Broeck, *Thermoelectric efficiency at maximum power in a quantum dot*, Europhysics Letters **85**, 60010 (2009).

[106] M. Esposito, N. Kumar, K. Lindenberg, and C. Van den Broeck, *Stochastically driven single-level quantum dot: A nanoscale finite-time thermodynamic machine and its various operational modes*, Phys. Rev. E **85**, 031117 (2012).

[107] R. Wang, J. Wang, J. He, and Y. Ma, *Efficiency at maximum power of a heat engine working with a two-level atomic system*, Phys. Rev. E **87**, 042119 (2013).

[108] J.-F. Chen, C.-P. Sun, and H. Dong, *Achieve higher efficiency at maximum power with finite-time quantum Otto cycle*, Phys. Rev. E **100**, 062140 (2019).

[109] M. L. Bera, S. Julià-Farré, M. Lewenstein, and M. N. Bera, *Quantum heat engines with Carnot efficiency at maximum power*, Phys. Rev. Res. **4**, 013157 (2022).

[110] J. Lira, L. Sanz, and A. Alcalde, *Photovoltaic efficiency at maximum power of a quantum dot molecule*, Physics Letters A **442**, 128179 (2022).

[111] K. E. Dorfman, D. Xu, and J. Cao, *Efficiency at maximum power of a laser quantum heat engine enhanced by noise-induced coherence*, Phys. Rev. E **97**, 042120 (2018).

[112] S. Deffner, *Efficiency of Harmonic Quantum Otto Engines at Maximal Power*, Entropy **20** (2018).

[113] P. A. Erdman, V. Cavina, R. Fazio, F. Taddei, and V. Giovannetti, *Maximum power and corresponding efficiency for two-level heat engines and refrigerators: optimality of fast cycles*, New Journal of Physics **21**, 103049 (2019).

[114] F. J. Peña, N. M. Myers, D. Órdenes, F. Albarrán-Arriagada, and P. Vargas, *Enhanced Efficiency at Maximum Power in a Fock-Darwin Model Quantum Dot Engine*, Entropy **25** (2023).

[115] Y. Rezek and R. Kosloff, *Irreversible performance of a quantum harmonic heat engine*, New J. Phys. **8**, 83–83 (2006).

[116] A. Alecce, F. Galve, N. L. Gullo, L. Dell'Anna, F. Plastina, and R. Zambrini, *Quantum Otto cycle with inner friction: finite-time and disorder effects*, New J. Phys. **17**, 075007 (2015).

[117] T. Feldmann and R. Kosloff, *Performance of discrete heat engines and heat pumps in finite time*, Phys. Rev. E **61**, 4774–4790 (2000).

[118] T. Feldmann and R. Kosloff, *Quantum four-stroke heat engine: Thermodynamic observables in a model with intrinsic friction*, Phys. Rev. E **68**, 016101 (2003).

[119] S. Çakmak, F. Altintas, A. Gençten, and O. E. Müstecaplıoğlu, *Irreversible work and internal friction in a quantum Otto cycle of a single arbitrary spin*, The European Physical Journal D **71**, 016101 (2017).

[120] M. Esposito, R. Kawai, K. Lindenberg, and C. Van den Broeck, *Efficiency at Maximum Power of Low-Dissipation Carnot Engines*, Phys. Rev. Lett. **105**, 150603 (2010).

[121] B. Andresen, *Current Trends in Finite-Time Thermodynamics*, Angewandte Chemie International Edition **50**, 2690–2704 (2011).

[122] R. S. Whitney, *Most Efficient Quantum Thermoelectric at Finite Power Output*, Phys. Rev. Lett. **112**, 130601 (2014).

[123] N. Shiraishi, K. Saito, and H. Tasaki, *Universal Trade-Off Relation between Power and Efficiency for Heat Engines*, Phys. Rev. Lett. **117**, 190601 (2016).

[124] B. Lin and J. Chen, *Performance analysis of an irreversible quantum heat engine working with harmonic oscillators*, Phys. Rev. E **67**, 046105 (2003).

[125] O. Abah and E. Lutz, *Optimal performance of a quantum Otto refrigerator*, EPL (Europhysics Letters) **113**, 60002 (2016).

[126] A. d. Campo, J. Goold, and M. Paternostro, *More bang for your buck: Super-adiabatic quantum engines*, Scientific Reports **4**, 6208 (2014).

[127] O. Abah and M. Paternostro, *Shortcut-to-adiabaticity Otto engine: A twist to finite-time thermodynamics*, Phys. Rev. E **99**, 022110 (2019).

[128] O. Abah, R. Puebla, A. Kiely, G. D. Chiara, M. Paternostro, and S. Campbell, *Energetic cost of quantum control protocols*, New J. Phys. **21**, 103048 (2019).

[129] O. Abah, M. Paternostro, and E. Lutz, *Shortcut-to-adiabaticity quantum Otto refrigerator*, Phys. Rev. Res. **2**, 023120 (2020).

[130] J. Deng, Q.-h. Wang, Z. Liu, P. Hänggi, and J. Gong, *Boosting work characteristics and overall heat-engine performance via shortcuts to adiabaticity: Quantum and classical systems*, Phys. Rev. E **88**, 062122 (2013).

[131] Z. C. Tu, *Stochastic heat engine with the consideration of inertial effects and shortcuts to adiabaticity*, Phys. Rev. E **89**, 052148 (2014).

[132] S. Çakmak and O. E. Müstecaplıoğlu, *Spin quantum heat engines with shortcuts to adiabaticity*, Phys. Rev. E **99**, 032108 (2019).

[133] T. Keller, T. Fogarty, J. Li, and T. Busch, *Feshbach engine in the Thomas-Fermi regime*, Phys. Rev. Research **2**, 033335 (2020).

[134] A. Hartmann, V. Mukherjee, W. Niedenzu, and W. Lechner, *Many-body quantum heat engines with shortcuts to adiabaticity*, Phys. Rev. Research **2**, 023145 (2020).

[135] M. Beau, J. Jaramillo, and A. Del Campo, *Scaling-Up Quantum Heat Engines Efficiently via Shortcuts to Adiabaticity*, Entropy **18**, 168 (2016).

[136] R. Kosloff and Y. Rezek, *The Quantum Harmonic Otto Cycle*, Entropy **19**, 136 (2017).

[137] A. Hartmann, V. Mukherjee, W. Niedenzu, and W. Lechner, *Many-body quantum heat engines with shortcuts to adiabaticity*, Phys. Rev. Res. **2**, 023145 (2020).

[138] S. Deng, A. Chenu, P. Diao, F. Li, S. Yu, I. Coulamy, A. del Campo, and H. Wu, *Superadiabatic quantum friction suppression in finite-time thermodynamics*, Science Advances **4**, 5909 (2018).

[139] A. Pedram, S. C. Kadıoğlu, A. Kabakçıoğlu, and O. E. Müstecaplıoğlu, *A Quantum Otto Engine with Shortcuts to Thermalization and Adiabaticity*, arXiv **2306.14847** (2023).

[140] V. Mukherjee, A. Carlini, A. Mari, T. Caneva, S. Montangero, T. Calarco, R. Fazio, and V. Giovannetti, *Speeding up and slowing down the relaxation of a qubit by optimal control*, Phys. Rev. A **88**, 062326 (2013).

[141] N. Suri, F. C. Binder, B. Muralidharan, and S. Vinjampathy, *Speeding up thermalisation via open quantum systems variational optimisation*, Eur. Phys. J. Spec. Top. **227**, 203–216 (2018).

[142] V. Cavina, A. Mari, A. Carlini, and V. Giovannetti, *Optimal thermodynamic control in open quantum systems*, Phys. Rev. A **98**, 012139 (2018).

[143] R. Xu, *Reinforcement learning approach to shortcuts between thermodynamic states with minimum entropy production*, Phys. Rev. E **105**, 054123 (2022).

[144] N. Pancotti, M. Scandi, M. T. Mitchison, and M. Perarnau-Llobet, *Speed-Ups to Isothermality: Enhanced Quantum Thermal Machines through Control of the System-Bath Coupling*, Phys. Rev. X **10**, 031015 (2020).

[145] T. Villazon, A. Polkovnikov, and A. Chandran, *Swift heat transfer by fast-forward driving in open quantum systems*, Phys. Rev. A **100**, 012126 (2019).

[146] S. Alipour, A. Chenu, A. T. Rezakhani, and A. del Campo, *Shortcuts to Adiabaticity in Driven Open Quantum Systems: Balanced Gain and Loss and Non-Markovian Evolution*, Quantum **4**, 336 (2020).

[147] R. Dann, A. Tobalina, and R. Kosloff, *Shortcut to Equilibration of an Open Quantum System*, Phys. Rev. Lett. **122**, 250402 (2019).

[148] L. Dupays, I. L. Egusquiza, A. del Campo, and A. Chenu, *Superadiabatic thermalization of a quantum oscillator by engineered dephasing*, Phys. Rev. Res. **2**, 033178 (2020).

[149] R. Dann, A. Tobalina, and R. Kosloff, *Fast route to equilibration*, Phys. Rev. A **101**, 052102 (2020).

[150] R. Dann and R. Kosloff, *Quantum signatures in the quantum Carnot cycle*, New J. Phys. **22**, 013055 (2020).

[151] A. Das and V. Mukherjee, *Quantum-enhanced finite-time Otto cycle*, Phys. Rev. Research **2**, 033083 (2020).

[152] M. Schlosshauer, editor, *Decoherence and the Quantum-To-Classical Transition*, Springer Berlin, Heidelberg (2007).

[153] R. Alicki, *The quantum open system as a model of the heat engine*, Journal of Physics A: Mathematical and General **12**, L103 (1979).

[154] D. F. Walls and J. Gerard, *Quantum Optics 2nd Edition*, Springer, 2 edition (2008).

[155] T. c. v. Prosen, *Open XXZ Spin Chain: Nonequilibrium Steady State and a Strict Bound on Ballistic Transport*, Phys. Rev. Lett. **106**, 217206 (2011).

[156] D. Manzano, M. Tiersch, A. Asadian, and H. J. Briegel, *Quantum transport efficiency and Fourier's law*, Phys. Rev. E **86**, 061118 (2012).

[157] D. Manzano, C. Chuang, and J. Cao, *Quantum transport ind-dimensional lattices*, New Journal of Physics **18**, 043044 (2016).

[158] H.-P. Breuer, E.-M. Laine, J. Piilo, and B. Vacchini, *Colloquium: Non-Markovian dynamics in open quantum systems*, Rev. Mod. Phys. **88**, 021002 (2016).

[159] I. de Vega and D. Alonso, *Dynamics of non-Markovian open quantum systems*, Rev. Mod. Phys. **89**, 015001 (2017).

[160] R. Dann, A. Levy, and R. Kosloff, *Time-dependent Markovian quantum master equation*, Phys. Rev. A **98**, 052129 (2018).

[161] S. L. Wu, X. L. Huang, and X. X. Yi, *Driven Markovian master equation based on the Lewis-Riesenfeld-invariant theory*, Phys. Rev. A **106**, 052217 (2022).

[162] A. Redfield. *The Theory of Relaxation Processes*. In J. S. Waugh, editor, *Advances in Magnetic Resonance*, volume 1 of *Advances in Magnetic and Optical Resonance*, pages 1–32. Academic Press, (1965).

[163] C. P. Poole and H. A. Farach. *Chapter 8 - The Redfield Theories*. In *Relaxation in Magnetic Resonance*, pages 106–123. Academic Press, (1971).

[164] P. Gaspard and M. Nagaoka, *Slippage of initial conditions for the Redfield master equation*, The Journal of Chemical Physics **111**, 5668–5675 (1999).

[165] R. S. Whitney, *Staying positive: going beyond Lindblad with perturbative master equations*, Journal of Physics A: Mathematical and Theoretical **41**, 175304 (2008).

[166] A. Kossakowski, *On quantum statistical mechanics of non-Hamiltonian systems*, Reports on Mathematical Physics **3**, 247–274 (1972).

[167] G. Lindblad, *On the generators of quantum dynamical semigroups*, Communications in Mathematical Physics **48**, 119 – 130 (1976).

[168] V. Gorini, A. Kossakowski, and E. C. G. Sudarshan, *Completely positive dynamical semigroups of N-level systems*, Journal of Mathematical Physics **17**, 821–825 (1976).

[169] W. A. Majewski and R. F. Streater, *Detailed balance and quantum dynamical maps*, Journal of Physics A: Mathematical and General **31**, 7981 (1998).

[170] J. Eisert and M. B. Plenio, *Introduction to the basics of entanglement theory in continuous-variable systems*, International Journal of Quantum Information **01**, 479–506 (2003).

[171] G. Adesso, S. Ragy, and A. R. Lee, *Continuous Variable Quantum Information: Gaussian States and Beyond*, Open Systems and Information Dynamics **21**, 1440001 (2014).

[172] V. Blickle and C. Bechinger, *Realization of a micrometre-sized stochastic heat engine*, Nature Physics **8**, 143–146 (2012).

[173] B. L. Hu, J. P. Paz, and Y. Zhang, *Quantum Brownian motion in a general environment: Exact master equation with nonlocal dissipation and colored noise*, Phys. Rev. D **45**, 2843–2861 (1992).

[174] A. Lampo, S. H. Lim, M. Á. García-March, and M. Lewenstein, *Bose polaron as an instance of quantum Brownian motion*, Quantum **1**, 30 (2017).

[175] A. Lampo, M. A. García-March, and M. Lewenstein, editors, *Quantum Brownian Motion Revisited*, Springer Cham (2019).

[176] C. Charalambous, M. A. Garcia-March, M. Mehboudi, and M. Lewenstein, *Heat current control in trapped Bose-Einstein Condensates*, New J. Phys. **21**, 083037 (2019).

[177] L. A. Correa, M. Mehboudi, G. Adesso, and A. Sanpera, *Individual Quantum Probes for Optimal Thermometry*, Phys. Rev. Lett. **114**, 220405 (2015).

[178] M. Mehboudi, A. Lampo, C. Charalambous, L. A. Correa, M. A. García-March, and M. Lewenstein, *Using Polarons for sub-nK Quantum Nondemolition Thermometry in a Bose-Einstein Condensate*, Phys. Rev. Lett. **122**, 030403 (2019).

[179] C. L. Latune, I. Sinayskiy, and F. Petruccione, *Heat flow reversals without reversing the arrow of time: The role of internal quantum coherences and correlations*, Phys. Rev. Research **1**, 033097 (2019).

[180] P. U. Medina González, I. Ramos-Prieto, and B. M. Rodríguez-Lara, *Heat-flow reversal in a trapped-ion simulator*, Phys. Rev. A **101**, 062108 (2020).

[181] J. Du, T. Fu, J. Chen, S. Su, and J. Chen, *The reverse flow and amplification of heat in quantum-dot systems*, Physica A: Statistical Mechanics and its Applications **615**, 128560 (2023).

[182] M. Na and F. Marsiglio, *Two and three particles interacting in a one-dimensional trap*, American Journal of Physics **85**, 769–782 (2017).

[183] A. P. Luca D'Alessio, Yariv Kafri and M. Rigol, *From quantum chaos and eigenstate thermalization to statistical mechanics and thermodynamics*, Advances in Physics **65**, 239–362 (2016).

[184] T. Fogarty, L. Ruks, J. Li, and T. Busch, *Fast control of interactions in an ultracold two atom system: Managing correlations and irreversibility*, SciPost Phys. **6**, 21 (2019).

[185] H. E. D. Scovil and E. O. Schulz-DuBois, *Three-Level Masers as Heat Engines*, Phys. Rev. Lett. **2**, 262–263 (1959).

[186] L. A. Correa, J. P. Palao, D. Alonso, and G. Adesso, *Quantum-enhanced absorption refrigerators*, Scientific Reports **4**, 3949 (2014).

[187] E. Geva and R. Kosloff, *A quantum-mechanical heat engine operating in finite time. A model consisting of spin-1/2 systems as the working fluid*, The Journal of Chemical Physics **96**, 3054–3067 (1992).

[188] T. E. Humphrey, R. Newbury, R. P. Taylor, and H. Linke, *Reversible Quantum Brownian Heat Engines for Electrons*, Phys. Rev. Lett. **89**, 116801 (2002).

[189] T. Hugel, N. B. Holland, A. Cattani, L. Moroder, M. Seitz, and H. E. Gaub, *Single-Molecule Optomechanical Cycle*, Science **296**, 1103–1106 (2002).

[190] H. P. Goswami and U. Harbola, *Thermodynamics of quantum heat engines*, Phys. Rev. A **88**, 013842 (2013).

[191] D. Newman, F. Mintert, and A. Nazir, *Performance of a quantum heat engine at strong reservoir coupling*, Phys. Rev. E **95**, 032139 (2017).

[192] K. Ono, S. N. Shevchenko, T. Mori, S. Moriyama, and F. Nori, *Analog of a Quantum Heat Engine Using a Single-Spin Qubit*, Phys. Rev. Lett. **125**, 166802 (2020).

[193] J. Jaramillo, M. Beau, and A. del Campo, *Quantum supremacy of many-particle thermal machines*, New J. Phys. **18**, 075019 (2016).

[194] Y.-Y. Chen, G. Watanabe, Y.-C. Yu, X.-W. Guan, and A. del Campo, *An interaction-driven many-particle quantum heat engine and its universal behavior*, npj Quantum Inf **5**, 88 (2019).

[195] F. Carollo, F. M. Gambetta, K. Brandner, J. P. Garrahan, and I. Lesanovsky, *Nonequilibrium Quantum Many-Body Rydberg Atom Engine*, Phys. Rev. Lett. **124**, 170602 (2020).

[196] N. M. Myers, J. McCready, and S. Deffner, *Quantum Heat Engines with Singular Interactions*, Symmetry **13** (2021).

[197] T. Fogarty and T. Busch, *A many-body heat engine at criticality*, Quantum Science and Technology **6**, 015003 (2020).

[198] N. Yunger Halpern, C. D. White, S. Gopalakrishnan, and G. Refael, *Quantum engine based on many-body localization*, Phys. Rev. B **99**, 024203 (2019).

[199] R. Uzdin, *Coherence-Induced Reversibility and Collective Operation of Quantum Heat Machines via Coherence Recycling*, Phys. Rev. Applied **6**, 024004 (2016).

[200] H. Vroylandt, M. Esposito, and G. Verley, *Collective effects enhancing power and efficiency*, EPL (Europhysics Letters) **120**, 30009 (2017).

[201] W. Niedenzu and G. Kurizki, *Cooperative many-body enhancement of quantum thermal machine power*, New J. Phys. **20**, 113038 (2018).

[202] N. M. Myers, O. Abah, and S. Deffner, *Quantum thermodynamic devices: From theoretical proposals to experimental reality*, AVS Quantum Science **4**, 027101 (2022).

[203] J. Chen, H. Dong, and C.-P. Sun, *Bose-Fermi duality in a quantum Otto heat engine with trapped repulsive bosons*, Phys. Rev. E **98**, 062119 (2018).

[204] T. Keller, T. Fogarty, J. Li, and T. Busch, *Feshbach engine in the Thomas-Fermi regime*, Phys. Rev. Res. **2**, 033335 (2020).

[205] J. Li, T. Fogarty, S. Campbell, X. Chen, and T. Busch, *An efficient nonlinear Feshbach engine*, New J. Phys. **20**, 015005 (2018).

[206] M. Mikkelsen, T. Fogarty, and T. Busch, *Connecting Scrambling and Work Statistics for Short-Range Interactions in the Harmonic Oscillator*, Phys. Rev. Lett. **128**, 070605 (2022).

[207] A. Weiße and H. Fehske. *Exact Diagonalization Techniques*, pages 529–544. Springer Berlin Heidelberg, Berlin, Heidelberg, (2008).

[208] T. R. de Oliveira and D. Jonathan, *Efficiency gain and bidirectional operation of quantum engines with decoupled internal levels*, Phys. Rev. E **104**, 044133 (2021).

[209] S. Deffner and E. Lutz, *Generalized Clausius Inequality for Nonequilibrium Quantum Processes*, Phys. Rev. Lett. **105**, 170402 (2010).

[210] F. Plastina, A. Alecce, T. J. G. Apollaro, G. Falcone, G. Francica, F. Galve, N. Lo Gullo, and R. Zambrini, *Irreversible Work and Inner Friction in Quantum Thermodynamic Processes*, Phys. Rev. Lett. **113**, 260601 (2014).

[211] M. Beau, S. M. Pittman, G. E. Astrakharchik, and A. del Campo, *Exactly Solvable System of One-Dimensional Trapped Bosons with Short- and Long-Range Interactions*, Phys. Rev. Lett. **125**, 220602 (2020).

[212] C. Brif, R. Chakrabarti, and H. Rabitz, *Control of quantum phenomena: past, present and future*, New J. Phys. **12**, 075008 (2010).

[213] C. P. Koch, *Controlling open quantum systems: tools, achievements, and limitations*, Journal of Physics: Condensed Matter **28**, 213001 (2016).

[214] S. Kallush, R. Dann, and R. Kosloff, *Controlling the uncontrollable: Quantum control of open-system dynamics*, Science Advances **8**, eadd0828 (2022).

[215] Koch, Christiane P., Boscain, Ugo, Calarco, Tommaso, Dirr, Gunther, Filipp, Stefan, Glaser, Steffen J., Kosloff, Ronnie, Montangero, Simone, Schulte-Herbrüggen, Thomas, Sugny, Dominique, and Wilhelm, Frank K., *Quantum optimal control in quantum technologies. Strategic report on current status, visions and goals for research in Europe*, EPJ Quantum Technol. **9**, 19 (2022).

[216] M. V. Berry, *Transitionless quantum driving*, Journal of Physics A: Mathematical and Theoretical **42**, 365303 (2009).

[217] P. Hänggi and G.-L. Ingold, *Fundamental aspects of quantum Brownian motion*, Chaos: An Interdisciplinary Journal of Nonlinear Science **15**, 026105 (2005).

[218] E. Kanai, *On the Quantization of the Dissipative Systems**, Progress of Theoretical Physics **3**, 440–442 (1948).

[219] X. Chen, A. Ruschhaupt, S. Schmidt, A. del Campo, D. Guéry-Odelin, and J. G. Muga, *Fast Optimal Frictionless Atom Cooling in Harmonic Traps: Shortcut to Adiabaticity*, Phys. Rev. Lett. **104**, 063002 (2010).

[220] X. Chen and J. G. Muga, *Transient energy excitation in shortcuts to adiabaticity for the time-dependent harmonic oscillator*, Phys. Rev. A **82**, 053403 (2010).

[221] M. Tokieda and S. Endo, *Equivalence of Dissipative and Dissipationless Dynamics of Interacting Quantum Systems With Its Application to the Unitary Fermi Gas*, Frontiers in Physics **9** (2021).

[222] N. Gisin and I. C. Percival, *The quantum-state diffusion model applied to open systems*, Journal of Physics A: Mathematical and General **25**, 5677 (1992).

[223] C.-I. Um, K.-H. Yeon, and T. F. George, *The quantum damped harmonic oscillator*, Physics Reports **362**, 63–192 (2002).

[224] Å. A. Büyükaşık, *Squeezing and resonance in a generalized Caldirola-Kanai type quantum parametric oscillator*, Journal of Mathematical Physics **59**, 082104 (2018).

[225] M. C. Bertin, J. R. B. Peleteiro, B. M. Pimentel, and J. A. Ramirez, *Dynamical Invariants and Quantization of the One-Dimensional Time-Dependent, Damped, and Driven Harmonic Oscillator*, Brazilian Journal of Physics **50**, 534–540 (2020).

[226] R. M. Cavalcanti, *Wave function of a Brownian particle*, Phys. Rev. E **58**, 6807–6809 (1998).

[227] M. C. Bertin, B. M. Pimentel, and J. A. Ramirez, *Construction of time-dependent dynamical invariants: A new approach*, Journal of Mathematical Physics **53**, 042104 (2012).

[228] R. Dann and R. Kosloff, *Inertial Theorem: Overcoming the quantum adiabatic limit*, Phys. Rev. Res. **3**, 013064 (2021).

[229] T. Baumgratz, M. Cramer, and M. B. Plenio, *Quantifying Coherence*, Phys. Rev. Lett. **113**, 140401 (2014).

[230] E. B. Mpemba and D. G. Osborne, *Cool?*, Physics Education **4**, 172 (1969).

[231] A. K. Chatterjee, S. Takada, and H. Hayakawa, *Quantum Mpemba Effect in a Quantum Dot with Reservoirs*, Phys. Rev. Lett. **131**, 080402 (2023).

[232] G. T. Landi and M. Paternostro, *Irreversible entropy production: From classical to quantum*, Rev. Mod. Phys. **93**, 035008 (2021).

[233] J. P. Santos, L. C. CÃľleri, G. T. Landi, and M. Paternostro, *The role of quantum coherence in non-equilibrium entropy production*, npj Quantum Information **5**, 23 (2019).

[234] S. Campbell and S. Deffner, *Trade-Off Between Speed and Cost in Shortcuts to Adiabaticity*, Phys. Rev. Lett. **118**, 100601 (2017).

[235] E. Torrontegui, I. Lizuain, S. González-Resines, A. Tobalina, A. Ruschhaupt, R. Kosloff, and J. G. Muga, *Energy consumption for shortcuts to adiabaticity*, Phys. Rev. A **96**, 022133 (2017).

[236] P. Salamon and R. S. Berry, *Thermodynamic Length and Dissipated Availability*, Phys. Rev. Lett. **51**, 1127–1130 (1983).

[237] M. Scandi and M. Perarnau-Llobet, *Thermodynamic length in open quantum systems*, Quantum **3**, 197 (2019).

[238] G. Li, J.-F. Chen, C. P. Sun, and H. Dong, *Geodesic Path for the Minimal Energy Cost in Shortcuts to Isothermality*, Phys. Rev. Lett. **128**, 230603 (2022).

[239] D. Turyansky, O. Ovdat, R. Dann, Z. Aqua, R. Kosloff, B. Dayan, and A. Pick. *Inertial geometric quantum logic gates*, (2023).

[240] W. Ma, X. L. Huang, and S. L. Wu, *Dynamics of a driven open double two-level system and its entanglement generation*, Phys. Rev. A **107**, 032409 (2023).

[241] V. F. Krotov. *Global Methods in Optimal Control Theory*, pages 74–121. Birkhäuser Boston, Boston, MA, (1993).

[242] J. Cohn, A. Safavi-Naini, R. J. Lewis-Swan, J. G. Bohnet, M. Gärttner, K. A. Gilmore, J. E. Jordan, A. M. Rey, J. J. Bollinger, and J. K. Freericks, *Bang-bang shortcut to adiabaticity in the Dicke model as realized in a Penning trap experiment*, New Journal of Physics **20**, 055013 (2018).

[243] S. Balasubramanian, S. Han, B. T. Yoshimura, and J. K. Freericks, *Bang-bang shortcut to adiabaticity in trapped-ion quantum simulators*, Phys. Rev. A **97**, 022313 (2018).

[244] L. Innocenti, G. D. Chiara, M. Paternostro, and R. Puebla, *Ultrafast critical ground state preparation via bang–bang protocols*, New Journal of Physics **22**, 093050 (2020).

[245] L. Viola and S. Lloyd, *Dynamical suppression of decoherence in two-state quantum systems*, Phys. Rev. A **58**, 2733–2744 (1998).

[246] J. J. L. Morton, A. M. Tyryshkin, A. Ardavan, S. C. Benjamin, K. Porfyrakis, S. A. Lyon, and G. A. D. Briggs, *Bang-bang control of fullerene qubits using ultrafast phase gates*, Nature Phys **2**, 40–43 (2006).

[247] J. Alonso, Z. U. Solèr, M. Fadel, M. Marinelli, B. C. Keitch, V. Negnevitsky, and H. J. P, *Generation of large coherent states by bang-bang control of a trapped-ion oscillator*, Nat Commun **7**, 11243 (2016).

[248] P. Doria, T. Calarco, and S. Montangero, *Optimal Control Technique for Many-Body Quantum Dynamics*, Phys. Rev. Lett. **106**, 190501 (2011).

[249] T. Caneva, T. Calarco, and S. Montangero, *Chopped random-basis quantum optimization*, Phys. Rev. A **84**, 022326 (2011).

[250] M. M. Müller, R. S. Said, F. Jelezko, T. Calarco, and S. Montangero, *One decade of quantum optimal control in the chopped random basis*, Reports on Progress in Physics **85**, 076001 (2022).

[251] S. Deffner and S. Campbell, *Quantum speed limits: from Heisenberg's uncertainty principle to optimal quantum control*, Journal of Physics A: Mathematical and Theoretical **50**, 453001 (2017).

[252] S. Deffner and E. Lutz, *Quantum Speed Limit for Non-Markovian Dynamics*, Phys. Rev. Lett. **111**, 010402 (2013).

[253] Z. Sun, J. Liu, J. Ma, and X. Wang, *Quantum speed limits in open systems: Non-Markovian dynamics without rotating-wave approximation*, Scientific Reports **5**, 8444 (2015).

[254] K. Funo, N. Shiraishi, and K. Saito, *Speed limit for open quantum systems*, New Journal of Physics **21**, 013006 (2019).

[255] N. Shiraishi and K. Saito, *Speed limit for open systems coupled to general environments*, Phys. Rev. Res. **3**, 023074 (2021).

[256] H. Scutaru, *Fidelity for displaced squeezed thermal states and the oscillator semigroup*, Journal of Physics A: Mathematical and General **31**, 3659–3663 (1998).

[257] G.-S. Paraoanu and H. Scutaru, *Fidelity for multimode thermal squeezed states*, Phys. Rev. A **61**, 022306 (2000).

[258] J. Nocedal and S. Wright, *Numericla Optimization*, Springer, New York, NY, 2 edition (2006).

[259] L. Mandelstam and I. Tamm. *The Uncertainty Relation Between Energy and Time in Non-relativistic Quantum Mechanics*, pages 115–123. Springer Berlin Heidelberg, Berlin, Heidelberg, (1991).

[260] N. Margolus and L. B. Levitin, *The maximum speed of dynamical evolution*, Physica D: Nonlinear Phenomena **120**, 188–195 (1998).

[261] L. B. Levitin and T. Toffoli, *Fundamental Limit on the Rate of Quantum Dynamics: The Unified Bound Is Tight*, Phys. Rev. Lett. **103**, 160502 (2009).

[262] K. Bhattacharyya, *Quantum decay and the Mandelstam-Tamm-energy inequality*, Journal of Physics A: Mathematical and General **16**, 2993 (1983).

[263] D. P. Pires, M. Cianciaruso, L. C. Céleri, G. Adesso, and D. O. Soares-Pinto, *Generalized Geometric Quantum Speed Limits*, Phys. Rev. X **6**, 021031 (2016).

[264] T. Caneva, M. Murphy, T. Calarco, R. Fazio, S. Montangero, V. Giovannetti, and G. E. Santoro, *Optimal Control at the Quantum Speed Limit*, Phys. Rev. Lett. **103**, 240501 (2009).

[265] N. Il'in and O. Lychkovskiy, *Quantum speed limit for thermal states*, Phys. Rev. A **103**, 062204 (2021).

[266] S. Luo and Q. Zhang, *Informational distance on quantum-state space*, Phys. Rev. A **69**, 032106 (2004).

[267] K. M. R. Audenaert. *Comparisons between quantum state distinguishability measures*, (2013).

[268] M. Cianciaruso, S. Maniscalco, and G. Adesso, *Role of non-Markovianity and backflow of information in the speed of quantum evolution*, Phys. Rev. A **96**, 012105 (2017).

[269] O. Abah and E. Lutz, *Energy efficient quantum machines*, Europhysics Letters **118**, 40005 (2017).